LEVEL II

ARL-TR-79-5

Copy No. 50

DEVELOPMENT AND EVALUATION OF AN EXPERIMENTAL PARAMETRIC ACOUSTIC RECEIVING ARRAY (PARRAY)

Final Report under Contract N00039-76-C-0231

Tommy G. Goldsberry et al.

APPLIED RESEARCH LABORATORIES
THE UNIVERSITY OF TEXAS AT AUSTIN
POST OFFICE BOX 8029, AUSTIN, TEXAS 78712

16 February 1979

Final Report

5 May 1976 - 31 January 1978

Approved for public release;
distribution unlimited.

Prepared for:

DEFENSE ADVANCED RESEARCH PROJECTS AGENCY
1400 WILSON BLVD.
ARLINGTON, VA 22209

NAVAL ELECTRONIC SYSTEMS COMMAND
DEPARTMENT OF THE NAVY
WASHINGTON, DC 20360

UNCLASSIFIED

SECURITY CLASSIFICATION OF THIS PAGE (When Data Entered)

REPORT DOCUMENTATION PAGE

READ INSTRUCTIONS BEFORE COMPLETING FORM

1. REPORT NUMBER

2. GOVT ACCESSION NO.

3. RECIPIENT'S CATALOG NUMBER

4. TITLE (and Subtitle)
DEVELOPMENT AND EVALUATION OF AN EXPERIMENTAL PARAMETRIC ACOUSTIC RECEIVING ARRAY (PARRAY).

5. TYPE OF REPORT & PERIOD COVERED
Final Technical Report
5 May 1976 — 31 Jan 1978

6. PERFORMING ORG. REPORT NUMBER
ARL-TR-79-5

7. AUTHOR(s)
Tommy G. Goldsberry
C. Richard Reeves
David F. Rohde
M. Ward Widener
Robert A. Lamb
Voldi E. Maki, Jr.
Wiley S. Olsen

8. CONTRACT OR GRANT NUMBER(s)
N00039-76-C-0231

9. PERFORMING ORGANIZATION NAME AND ADDRESS
Applied Research Laboratories
The University of Texas at Austin
Austin, Texas 78712

10. PROGRAM ELEMENT, PROJECT, TASK AREA & WORK UNIT NUMBERS
DARPA Order 2910
Program Code 5010

11. CONTROLLING OFFICE NAME AND ADDRESS
Defense Advanced Research Projects Agency
1400 Wilson Boulevard
Arlington, VA 22209

12. REPORT DATE
16 February 1979

13. NUMBER OF PAGES
144

14. MONITORING AGENCY NAME & ADDRESS (if different from Controlling Office)
Naval Electronic Systems Command
Department of the Navy
Washington, DC 20360

15. SECURITY CLASS. (of this report)
UNCLASSIFIED

15a. DECLASSIFICATION/DOWNGRADING SCHEDULE
N/A

16. DISTRIBUTION STATEMENT (of this Report)

Approved for public release; distribution unlimited.

17. DISTRIBUTION STATEMENT (of the abstract entered in Block 20, if different from Report)

18. SUPPLEMENTARY NOTES

19. KEY WORDS (Continue on reverse side if necessary and identify by block number)

PARRAY
nonlinear acoustics
parametric receiver
end-fire array
crystal oscillator
sideband detector
transducers

20. ABSTRACT (Continue on reverse side if necessary and identify by block number)

(U) The development, test, and evaluation of an experimental parametric acoustic receiving array (PARRAY) with a pump-hydrophone separation of 340 m are described in this report. Tests in Lake Travis, Texas, demonstrated a greater than 40 dB reduction in the self-noise floor of the experimental PARRAY compared to any previous parametric acoustic receiver. This reduction in the self-noise floor was achieved through state-of-the-art advances in four major hardware subsystems employed in the experimental PARRAY: high spectral purity pump signal generation; commensurate power amplification;

DD FORM 1 JAN 73 1473 EDITION OF 1 NOV 65 IS OBSOLETE

404 434

UNCLASSIFIED

SECURITY CLASSIFICATION OF THIS PAGE (When Data Entered)

20. (Cont'd)

(U) high efficiency, high power transducer element and array design; and detection of sideband signals with very small modulation indices. Design and test results are presented for a crystal controlled oscillator with spectrum level single sideband phase noise less than -170 dB referenced to the carrier level. The design of a band elimination receiver preprocessor capable of detecting sideband signals approaching 180 dB below the carrier is presented and discussed. Test results are presented for simple, high efficiency transducer elements and arrays. Tests and experiments that were performed to evaluate the experimental 340 m PARRAY are described. Results of these measurements show that the experimental 340 m PARRAY was ambient noise limited over the frequency range 35 to 800 Hz under the quietest conditions encountered in Lake Travis during the tests. These conditions were approximately equivalent to light shipping and sea state 2. The spatial processing gain and front-to-back ratio were in agreement with predictions from the directional response function of the PARRAY. Temporal and phase stability of signals received by the PARRAY was demonstrated for filter bandwidths of 0.01 Hz. The effect of transducer motion on the PARRAY was investigated analytically and experimentally. Analytical expressions developed to predict the output of the PARRAY from measurements of the axial accelerations of the pump and hydrophone were verified by the experiments.

TABLE OF CONTENTS

TABLE OF CONTENTS (Cont'd)

LIST OF FIGURES

LIST OF FIGURES (Cont'd)

LIST OF FIGURES (Cont'd)

LIST OF TABLES

I. INTRODUCTION

The parametric acoustic receiving array (PARRAY) exploits the inherent nonlinearity in the pressure density relationship of water to achieve directional reception of low frequency acoustic waves. It can be characterized as a volumetric, virtual array synthesized in the water column between two small high frequency transducers called the pump and the hydrophone. The directional response characteristics of the PARRAY are similar to those of a continuous end-fire array of length equivalent to the distance between the pump and hydrophone. The maximum response axis (MRA) of the synthesized array lies along the directed line segment from the hydrophone to the pump.

The parametric reception concept was first proposed by Westervelt and shortly thereafter it was demonstrated experimentally by Berktay.[1,2] There followed a number of theoretical and experimental investigations, most of which emphasized demonstrating the existence of the phenomenon and developing and validating mathematical models to describe the basic physics of the process.[3-12] Beam patterns were obtained and the acoustic pressures of the interaction components were measured. Typical of basic measurements that use available laboratory equipment, the incoming low frequency signals were relatively high amplitude signals to assure adequate signal-to-noise ratios for reliable measurement.

It was recognized, however, that if the PARRAY were to progress from the status of an academic novelty to a useful tool in underwater acoustics, systematic methods would have to be developed to select optimal parameters within the constraints of existing engineering technology. Studies conducted at Applied Research Laboratories, The University of Texas at Austin (ARL:UT), addressed this problem and identified several areas of technology where there was significant technical risk.[13-16] Under sponsorship of Defense Advanced Research

Projects Agency (DARPA), ARL:UT undertook development of the technology to reduce the risk.

The program to develop an experimental, large aperture PARRAY at ARL:UT was structured as an integrated program of analysis, experiments, hardware design, fabrication, lake testing, and sea testing to be conducted in three sequential stages. The first phase of the program was accomplished in 1975 under Contract N00039-75-C-0207 with Naval Electronic Systems Command (NAVELEX) as technical agents for DARPA. During this exploratory phase, mission analysis and system definition studies were performed, subsystem requirements were developed, and technical risk areas were investigated.[17] Objectives of the first phase of the program were achieved on schedule and, consequently, the scope of the program was expanded to encompass the second phase of detailed design, fabrication, installation, and tests of the system at Lake Travis Test Station (LTTS), ARL:UT. This report summarizes the results of the second phase of the development program. Additional information is contained in quarterly progress reports, technical reports, and papers presented at scientific and technical meetings.[18-31]

A brief description of the parametric reception process and some of the more important properties of the PARRAY are presented in section II.

A number of experiments were performed at LTTS with a long baseline 340 m PARRAY and two short baseline 5 m and 11 m PARRAYs. These experiments are described and the results obtained are presented in section III.

State-of-the art advances were made in four major hardware areas: high spectral purity pump signal generation; commensurate power amplification; high efficiency, high power transducer element and array design; and detection of sideband signals with very small modulation indices. These hardware developments are described in section IV.

Several analyses and design support studies were performed during the course of this work. Three of these are reviewed in section V.

The report is summarized and major conclusions are presented in section VI.

II. DESCRIPTION OF THE PARRAY

The PARRAY can be characterized as a volumetric, virtual array that is synthesized in the water column between two high frequency transducers. The operation of the PARRAY is illustrated schematically in Fig. 1. A continuous, high frequency acoustic wave, symbolized by the closely spaced, concentric arcs, is projected from one of the transducers (pump) to the second transducer (hydrophone), which is located a distance L from the pump. A low frequency acoustic wave, represented by the widely spaced diagonal lines, propagates through the area and interacts nonlinearly with the pump wave to generate modulation sidebands of the pump signal. The phasing of this interaction process is such that a continuous, end-fire array of length L is synthesized in the interaction volume between the pump and hydrophone. The maximum response of the synthesized end-fire array is in the direction of a line extending from the hydrophone through the pump. It is this end-fire array effect that provides the directivity of the PARRAY and hence its ability to discriminate against the low frequency ambient noise that otherwise masks the signal wave.

Ideally, the pump signal is a pure sinusoid of frequency f_p; however, in practice, the characteristic spectrum of the pump signal is similar to that shown in the box at the upper left. The level of the sideband noise is dependent on the quality of the signal generation equipment, i.e., on the spectral purity of the pump electronics. As a result of the nonlinear mixing in the water, the pump signal spectrum is modulated by the signal frequency spectrum and contains the signal frequency information as the upper and lower sidebands ($f_p \pm f_s$), illustrated in the box at the lower right of Fig. 1.

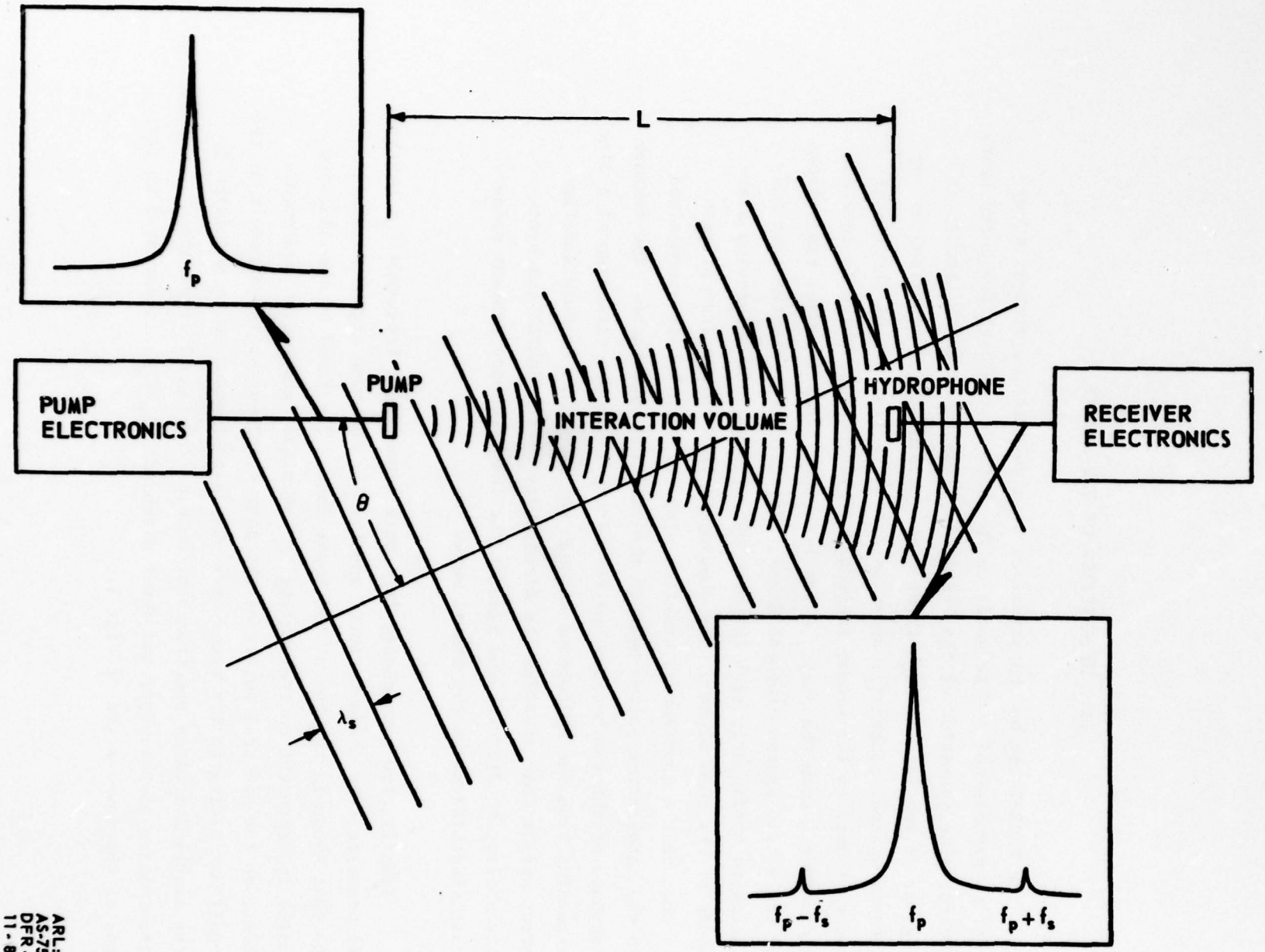

FIGURE 1
PARRAY FUNCTIONAL DIAGRAM

ARL:UT
AS-75-1846-S
DFR-GA
11-8-78

The directional response of the PARRAY, which is similar to that of a continuous, end-fire array of length L, is given by[5]

$$D(\theta) = \frac{\beta - (1-\cos\theta)}{\beta} \frac{\sin[(kL/2)(1-\cos\theta)]}{(kL/2)(1-\cos\theta)} \quad , \tag{1}$$

where

θ is the plane angle measured from the line joining the pump and hydrophone,

k is the acoustic wave number of the signal to be detected,

L is the pump-hydrophone separation, and

β is the coefficient of nonlinearity of the medium, approximately equal to 3.5 in sea water.

The value of β is approximately 8% less in fresh water than in sea water.[32,33]

The directional response of the PARRAY is symmetric about the line joining the pump and hydrophone, i.e., the PARRAY has a conical beam pattern. The half-power beamwidth of the PARRAY, in degrees, is given approximately by

$$\theta = 105 \sqrt{\lambda/L} \quad , \tag{2}$$

where λ is the acoustic wavelength of the signal to be detected. These characteristics are illustrated in Fig. 2, which shows the directional response of the PARRAY for a kL of 33π. This would correspond, for example, to a frequency of 50 Hz and a pump-hydrophone separation of 500 m, or to a frequency of 500 Hz and a pump-hydrophone separation of 50 m. Since the directional response of the PARRAY is symmetric about the line joining the pump and hydrophone, the beam pattern is the same in both the vertical and horizontal planes.

The detection of low frequency signals from a distant source is closely related to the ability of the acoustic sensor to discriminate against low frequency ambient noise and thus to improve the signal-to-noise ratio (S/N) compared to a simple, omnidirectional sensor. One

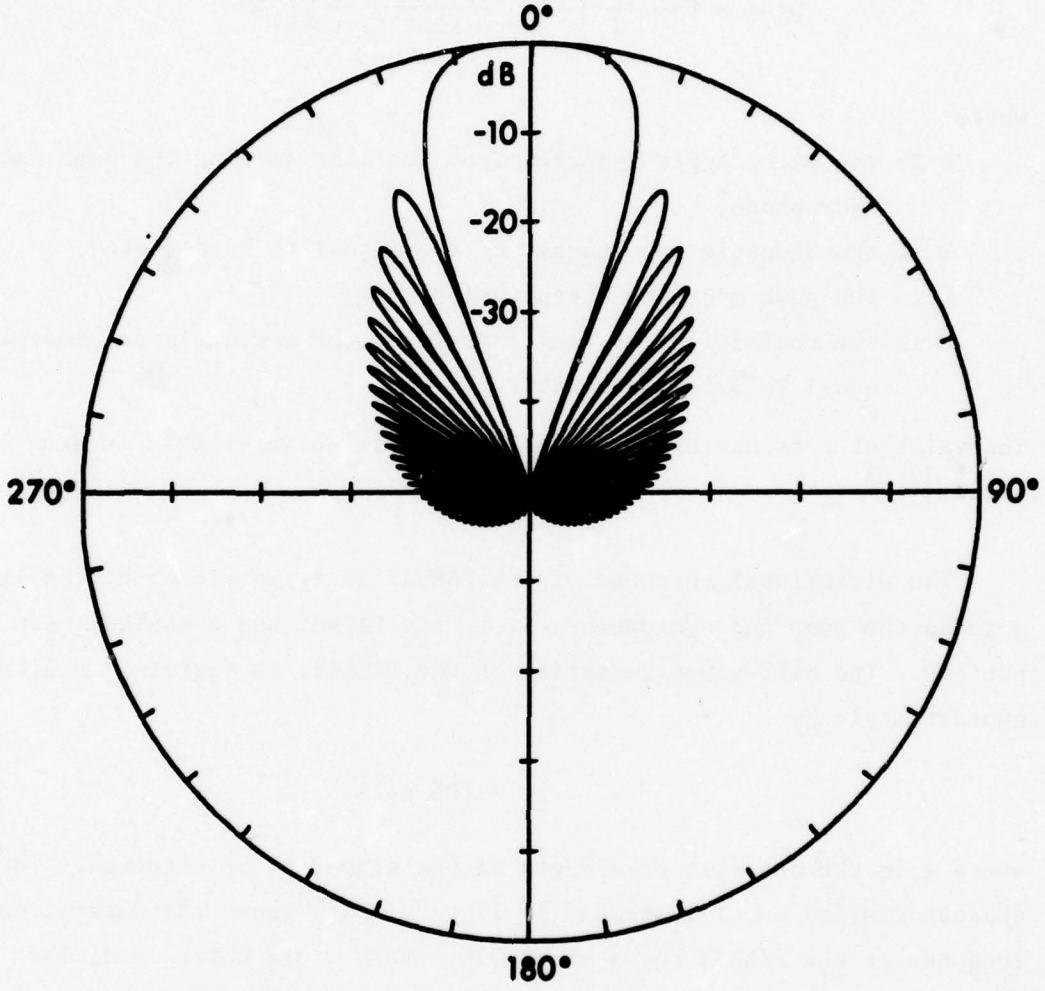

FIGURE 2
DIRECTIONAL RESPONSE FUNCTION OF PARRAY
kL = 33 π

ARL:UT
AS-78-1698-S
DFR-GA
11-8-78

measure of the S/N improvement of an acoustic sensor is spatial processing gain (SPG). The SPG of an acoustic sensor is given by

$$SPG = \frac{\int_{4\pi} N(\theta,\phi)d\Omega}{\int_{4\pi} b(\theta,\phi)\, N(\theta,\phi)d\Omega} \quad , \tag{3}$$

where $b(\theta,\phi)$ is the directional response function of the acoustic sensor, $N(\theta,\phi)$ is the noise power per unit solid angle, and the integral is over 4π steradians. If $N(\theta,\phi)$ is a constant, i.e., if the noise is isotropic, Eq. (3) reduces to the familiar expression for the DI of the acoustic sensor,

$$DI = 10 \log \frac{4\pi}{\int_{4\pi} b(\theta,\phi)d\Omega} \quad . \tag{4}$$

Although the ambient noise field is rarely isotropic, the DI is a convenient and useful measure for first order comparisons of different acoustic sensors. The DI of the PARRAY is given by

$$DI = 10 \log[1.86 + 4L/\lambda] \quad . \tag{5}$$

The lower curve in Fig. 3 shows the DI of the PARRAY as a function of the pump-hydrophone separation in wavelengths. For example, a pump-hydrophone separation of 500 m is 10λ at a signal frequency of 30 Hz, which yields a DI of 16 dB.

The front-to-back ratio (F/B) of the PARRAY is also a function of the acoustic aperture. For $kL>1$, the ratio of the maximum response of the PARRAY to the envelope of the back lobes is given by (in decibels)

$$F/B_{dB} = 20 \log(7kL/3) \quad . \tag{6}$$

The F/B of the PARRAY is shown in the upper curve in Fig. 3. It should be noted that both the DI and the F/B of the PARRAY are functions of the acoustic aperture and hence do not depend upon the pump frequency.

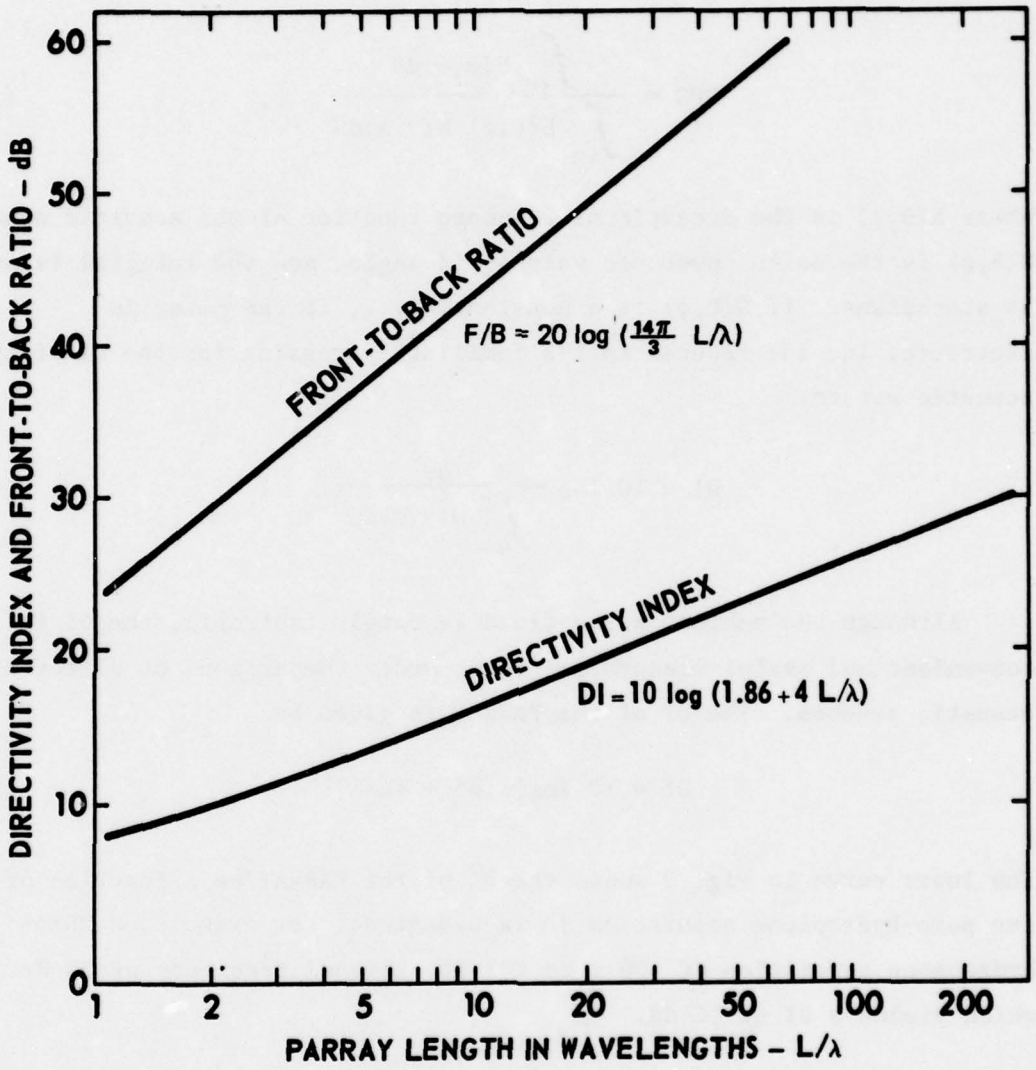

FIGURE 3
DIRECTIVITY INDEX AND FRONT-TO-BACK RATIO OF THE PARRAY AS A FUNCTION OF ACOUSTIC APERTURE IN WAVELENGTHS (L/λ)

ARL:UT
AS-77-2296-S
DFR-GA
11-8-78

Summarized below are several desirable characteristics that derive from the fact that the PARRAY is essentially a continuous, end-fire array synthesized in the water.

- Vertical Directivity - Since the directional response is symmetric about the line joining the pump and hydrophone, the PARRAY provides vertical as well as horizontal discrimination against noise.
- No Grating Lobes - Grating lobes are not generated as the signal frequency increases because the PARRAY is a continuous end-fire array.
- Good Sidelobe Behavior - The sidelobes are well behaved and decrease monotonically to a minimum on the back side of the PARRAY.
- High Front-to-Back Ratio - The PARRAY is relatively insensitive to signals arriving from the back side.
- Wide Bandwidth - The PARRAY is inherently wideband because the heterodyne process translates the absolute bandwidth of the high frequency transducers to the low frequency signal region.
- Minimum Number of Transducers - Two relatively small high frequency transducers are required to form the PARRAY because the nonlinearity of the water is exploited to synthesize the array in the region between the transducers.

III. MEASUREMENTS ON PARRAY AT LAKE TRAVIS

Using both newly developed hardware and refurbished equipment, extremely good data were obtained from PARRAY experiments at LTTS. Experiments were performed on a long baseline (340 m) and two short baseline (5 m and 11 m) PARRAY systems utilizing a pump frequency of 65 kHz.

A. Measurements With 340 m PARRAY

Experiments were performed on a 340 m PARRAY at LTTS yielding results that agreed with performance predictions and indicating that a PARRAY system could be built to provide a successful ocean demonstration. The 340 m PARRAY system was described in detail in previous documentation;[18-22] basically it consisted of a pump and hydrophone, located at middepth in approximately 46 m of water and connected by cables to the PARRAY electronics located on a nearby barge. The transducers were attached to two underwater towers separated by a distance of 340 m. The signal source was located approximately 1500 m from the PARRAY at middepth of a fairly constant depth contour of an old river channel of Lake Travis. The signal source consisted of a stable source driving a Naval Research Laboratory/Underwater Sound Reference Division (NRL/USRD) Type J9 transducer which was suspended from a small boat anchored in the water. The PARRAY pump was driven with a 65 kHz pump signal at a source level of 218 dB re 1 μPa at 1 m.

A brief description and a summary of the results of each of the more significant experiments are included in this report.

1. Lake Test Fixtures

The geometry of the experiment is shown in Fig. 4, which is a topographic map of the lower portion of Lake Travis. Lake Travis is formed by Mansfield Dam, a large concrete structure containing a hydroelectric plant. Three turbine generators are located at the site labeled "Powerhouse" on the map. The elevation contours are labeled in feet above mean sea level and, as noted on the figure, normal lake level is 681 ft (207.6 m). Lake level at the time of the experiment was constant at 207.3 m. The PARRAY transducers are located on two towers, denoted "West Tower" and "East Tower" in Fig. 4, separated by 340 m. The transducers are cabled back to the PARRAY electronics console located on the NAVSEA Barge.

In these experiments, the PARRAY pump was located on the east tower and the PARRAY hydrophone was mounted on the west tower. Thus, the MRA of the PARRAY was along the dashed line, denoted "PARRAY Axis," from the west tower to the east tower at a bearing of 068° magnetic. The towers are set in approximately 46 m of water with the PARRAY transducers located 21 m below the water surface, or near middepth at those points. Figure 5 shows the means of attaching the transducer and control mechanism to the tower. The small cables from the control units run to a junction box, where they are attached to a large cable stretching along the lake floor to the NAVSEA Barge where the PARRAY electronic equipment is housed and the experiments are conducted.

Figure 6 is a closeup view of the transducer and control mechanism. Each of the control units contains a control motor and a position indicator to allow the transducer to be pointed for precise alignment. The control is an open loop servo system; once the alignment is made, no further adjustment of the transducers should be necessary for the tests at this depth. The 21 m depth was chosen to minimize possible interferences from the bottom and the lake surface.

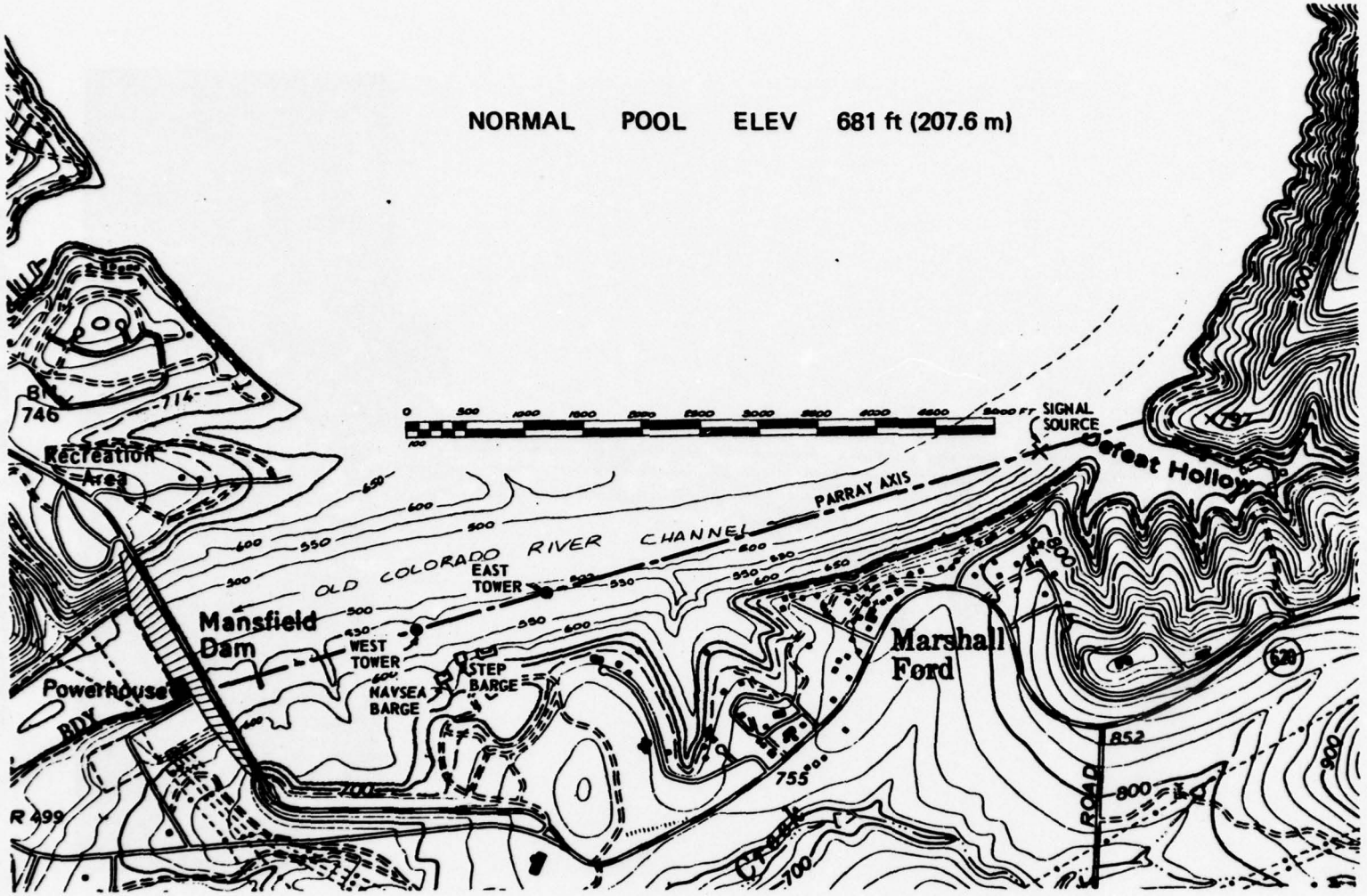

FIGURE 4
TOPOGRAPHY OF LAKE TRAVIS TEST STATION

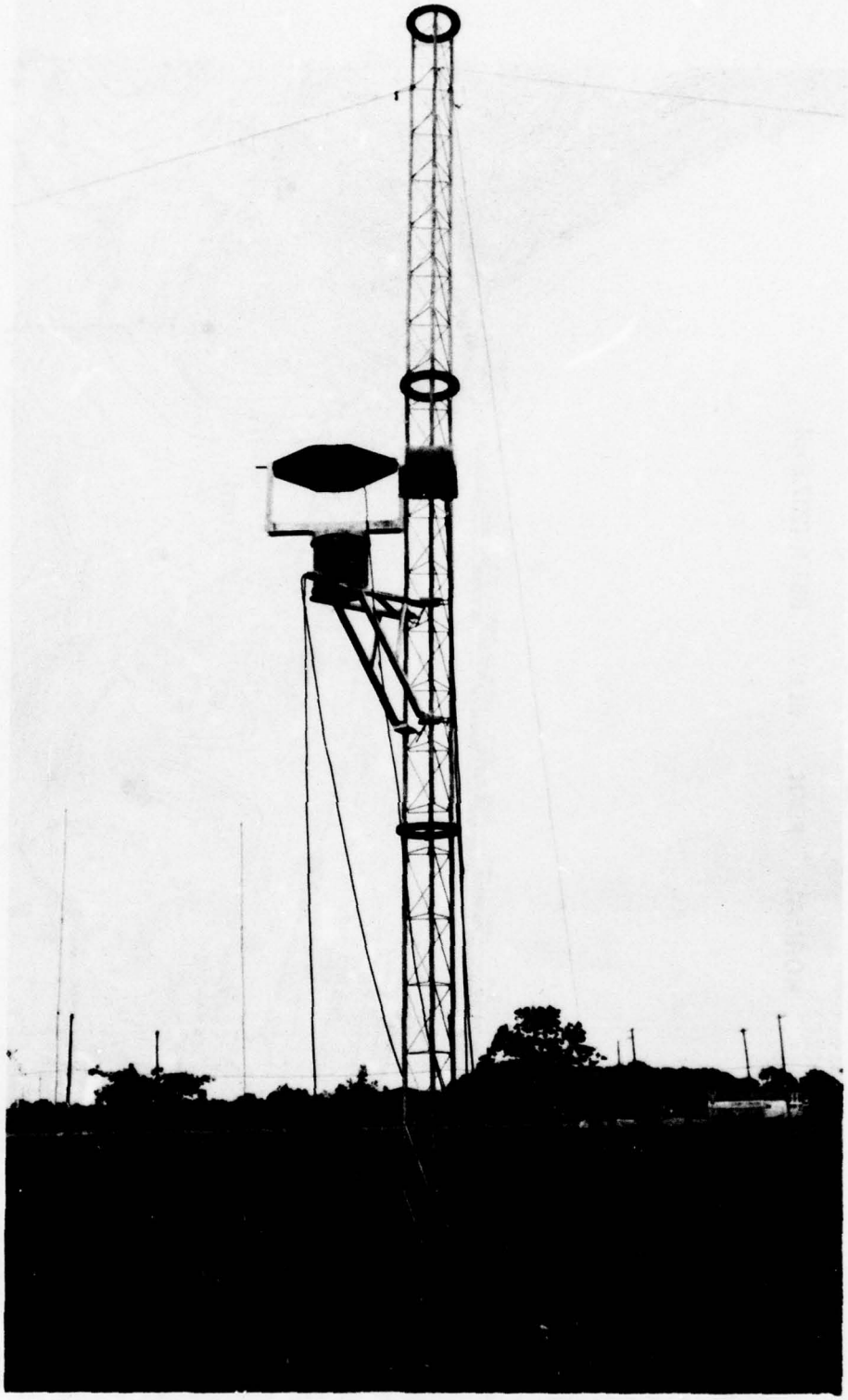

FIGURE 5
TOWER TRANSDUCER CONTROL MECHANISM

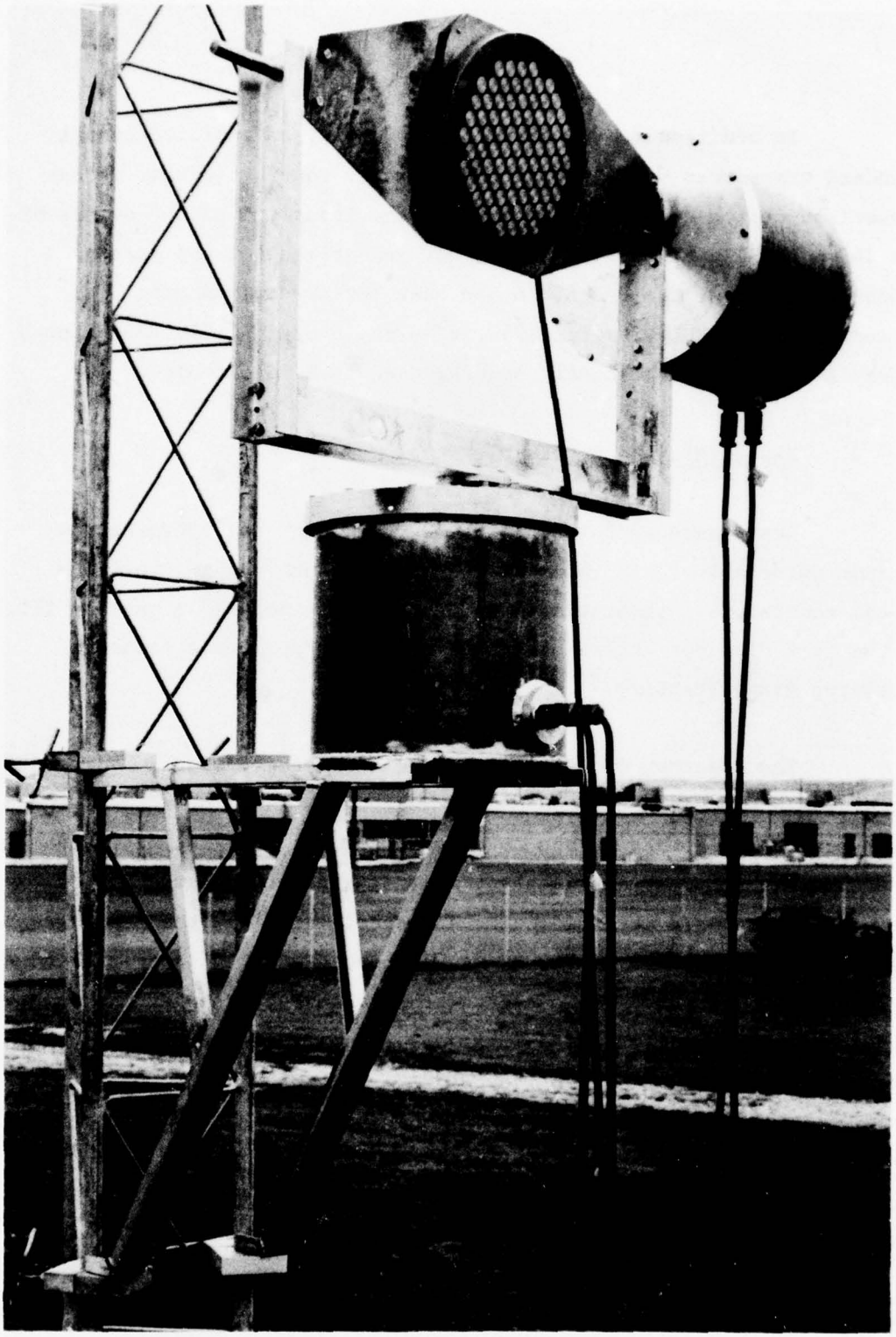

FIGURE 6
CLOSEUP VIEW OF TOWER TRANSDUCER CONTROL MECHANISM

In addition to the PARRAY transducers, an omnidirectional standard transducer was installed on the west tower to permit direct comparison of the ambient noise both at the input and at the output of the 340 m PARRAY. This allows a direct measurement of the spatial processing gain of the PARRAY in the Lake Travis environment. The ambient monitor, NRL/USRD Type F50, required a preamplifier and line driver so that the transducer could be used on a long cable.

2. System Minimum Detectable Level

Tests were performed on the 340 m PARRAY to determine the minimum detectable level (MDL) of the system under varying environmental conditions. These tests are described in detail in section III.A. of the Test Plan for Interim Lake Tests of the Parametric Acoustic Receiving Array (PARRAY).[23]

The spectrum of the signal from an omnidirectional hydrophone located near the PARRAY hydrophone is labeled LN(F50) in Fig. 7. The large peak below 150 Hz is due to machinery noise from the nearby dam even though the hydroelectric plant was not generating power at the time these data were obtained. The spectrum level from the F50 over the frequency range 150 to 800 Hz is shown to gradually taper from 63 to 55 dB re 1 $\mu Pa/\sqrt{Hz}$. The output of the 340 m PARRAY under the same conditions is also illustrated in Fig. 7. The PARRAY output includes the spatial processing gain of the PARRAY which, for an isotropic noise field, is equivalent to the directivity index. The ambient noise levels shown in Fig. 7 represent some of the lowest ambient noise levels measured at Lake Travis. It is therefore enlightening to compare the PARRAY output with ocean ambient noise levels. The curves labeled "B Shipping - DI" and "SS2 - DI" represent the "B Shipping" and "sea state 2" ambient noise levels from curves given in Fig. 8 reduced by the directivity index of the 340 m PARRAY. Thus the 340 m PARRAY is not self-noise limited for ambient noise levels as low as B Shipping and sea state 2.

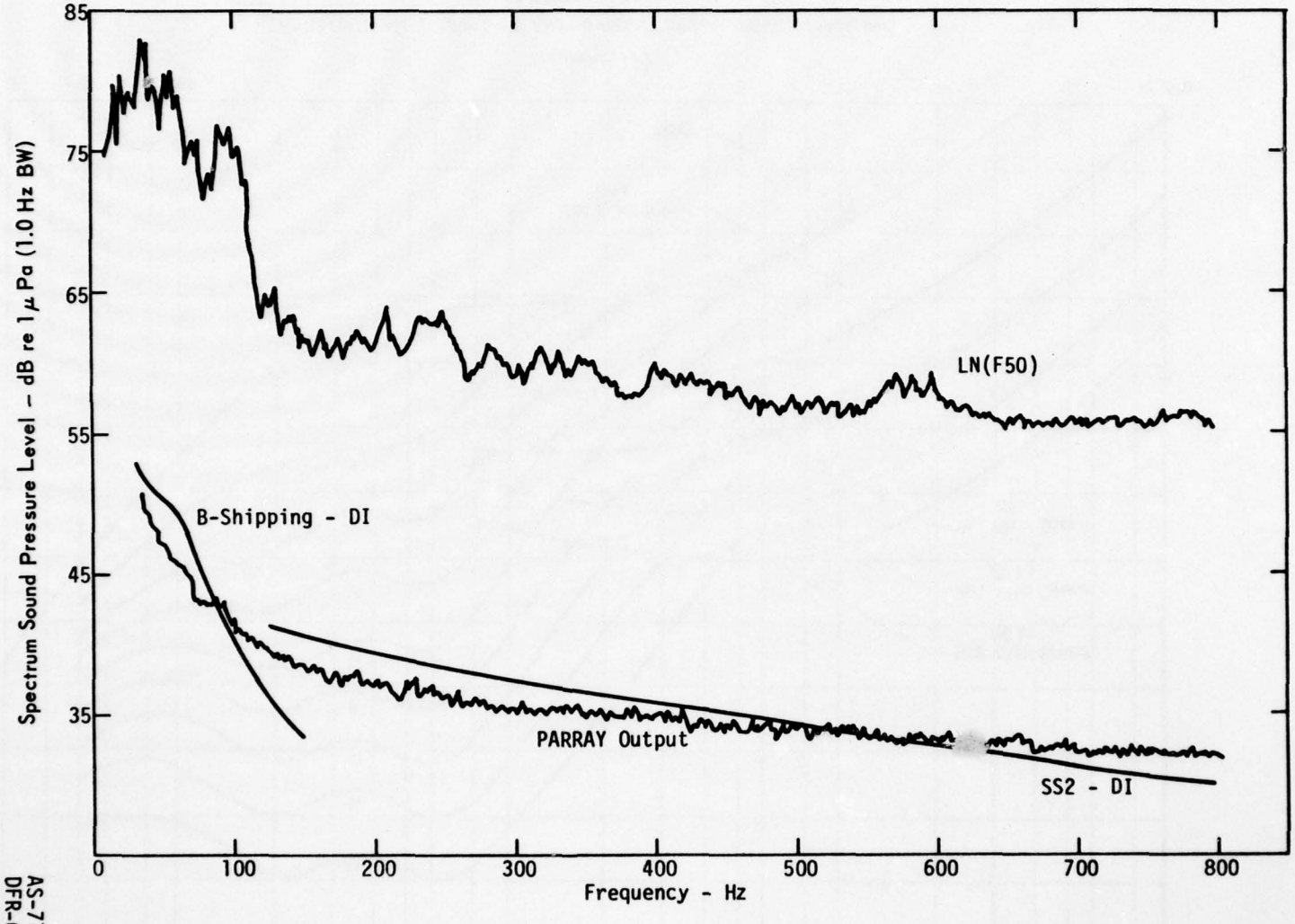

AS-77-2171
DFR-0231-0

FIGURE 7
COMPARISON OF AMBIENT NOISE AT INPUT AND OUTPUT OF 340 m PARRAY - 2-9-77 DATA

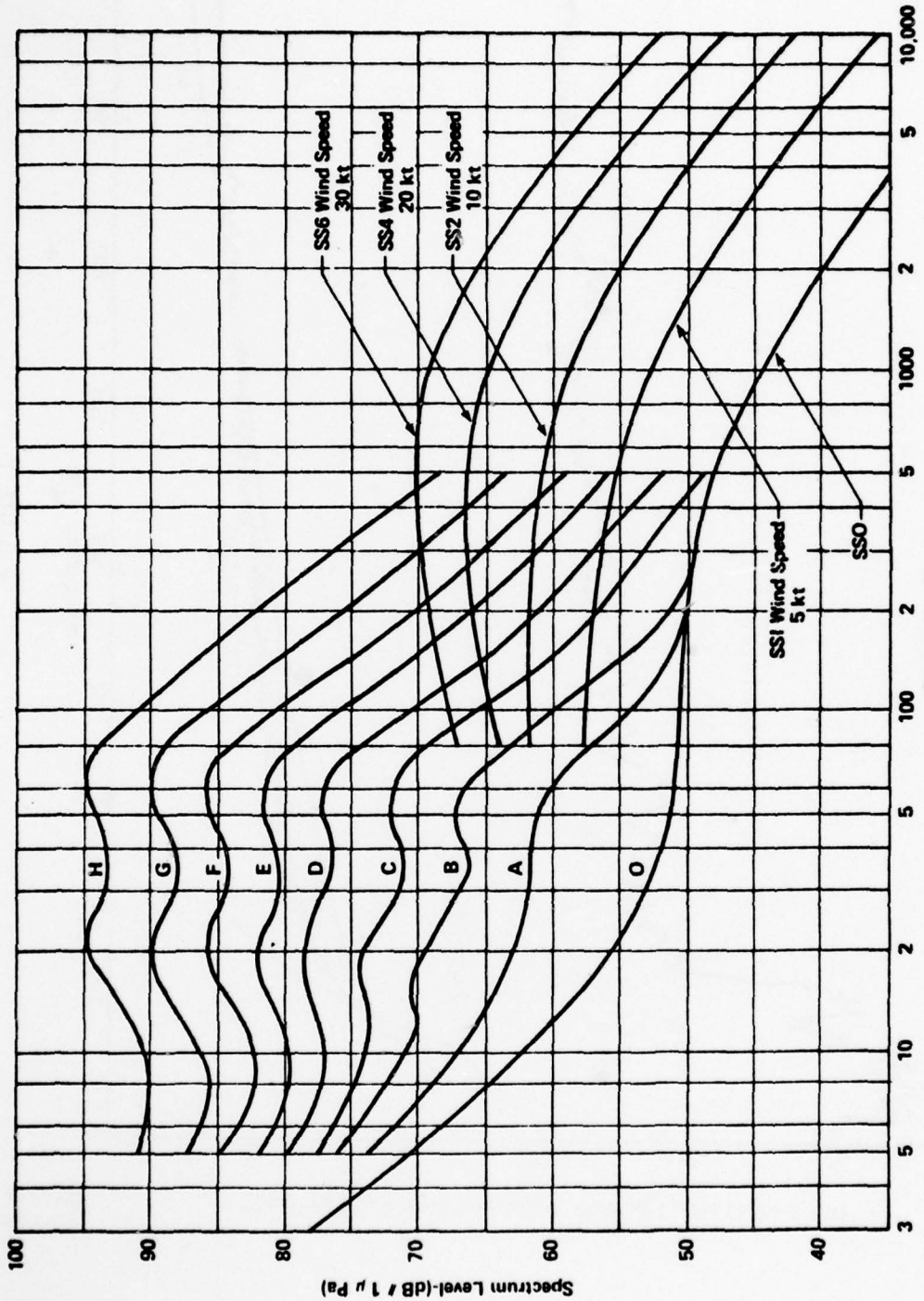

FROM FUTURE SUBMARINE EMPLOYMENT STUDY, TETRA TECH, INC.
29 DECEMBER 1972

FIGURE 8
AMBIENT NOISE CAUSED BY SHIPPING AND SEA STATE

AS-78-336

In summary, these tests have demonstrated that the 340 m PARRAY is ambient noise limited under the quietest conditions encountered in Lake Travis. Furthermore, these tests verify that the predicted spatial processing gain for the 340 m PARRAY is achieved over the frequency range from 35 to 800 Hz.

3. Low Frequency Sensitivity and Array Processing Gain

An experiment was conducted to examine the performance of the PARRAY at very low frequencies. During this experiment a 71 Hz acoustic reference signal was transmitted from the J9 transducer on axis approximately 1500 m from the midpoint of the PARRAY. The data obtained were analyzed using an 800 line spectrum analyzer over the baseband frequency range to 160 Hz; the results are shown in Fig. 9. The noise analysis bandwidth for these data is 0.2 Hz, which results in an SPL 7 dB below spectrum level noise. Although the hydroelectric plant was not generating power at the time these data were obtained, the frequency region below 125 Hz contains a large amount of acoustic energy due to the machinery in the dam. The improvement in signal-to-noise ratio from the PARRAY over that of the F50 omnidirectional sensor is due to the spatial processing gain of the PARRAY which includes the DI and backside rejection.

Another set of data, illustrated in Fig. 10, was obtained under the same experimental conditions, except that the signal frequency was changed to 55 Hz. Again the PARRAY output background noise closely follows the levels due to C Shipping minus the directivity index of the PARRAY over the frequency range from 50 to 100 Hz. From 100 to 160 Hz the PARRAY output approaches that of sea state 2 minus the directivity index of the PARRAY. Even with contaminating machinery noise, the experimental 340 m PARRAY demonstrates a capability of detecting signals from 35 to 45 dB re 1 μPa for a processing bandwidth of 0.2 Hz over the frequency range from 50 to 160 Hz.

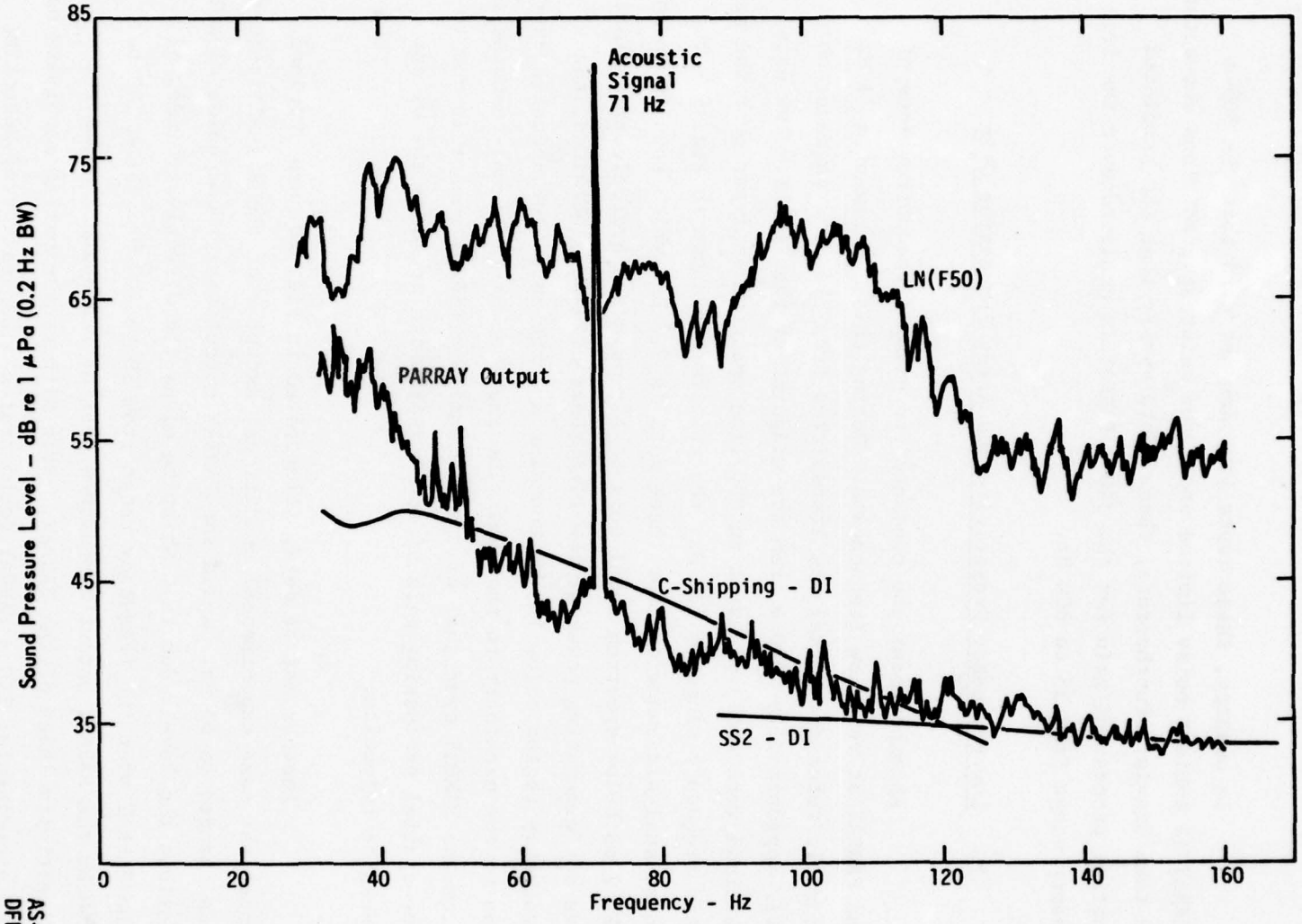

FIGURE 9
COMPARISON OF AMBIENT NOISE AT INPUT AND OUTPUT OF 340 m PARRAY - 2-28-77 DATA

AS-77-2173
DFR-0231-0

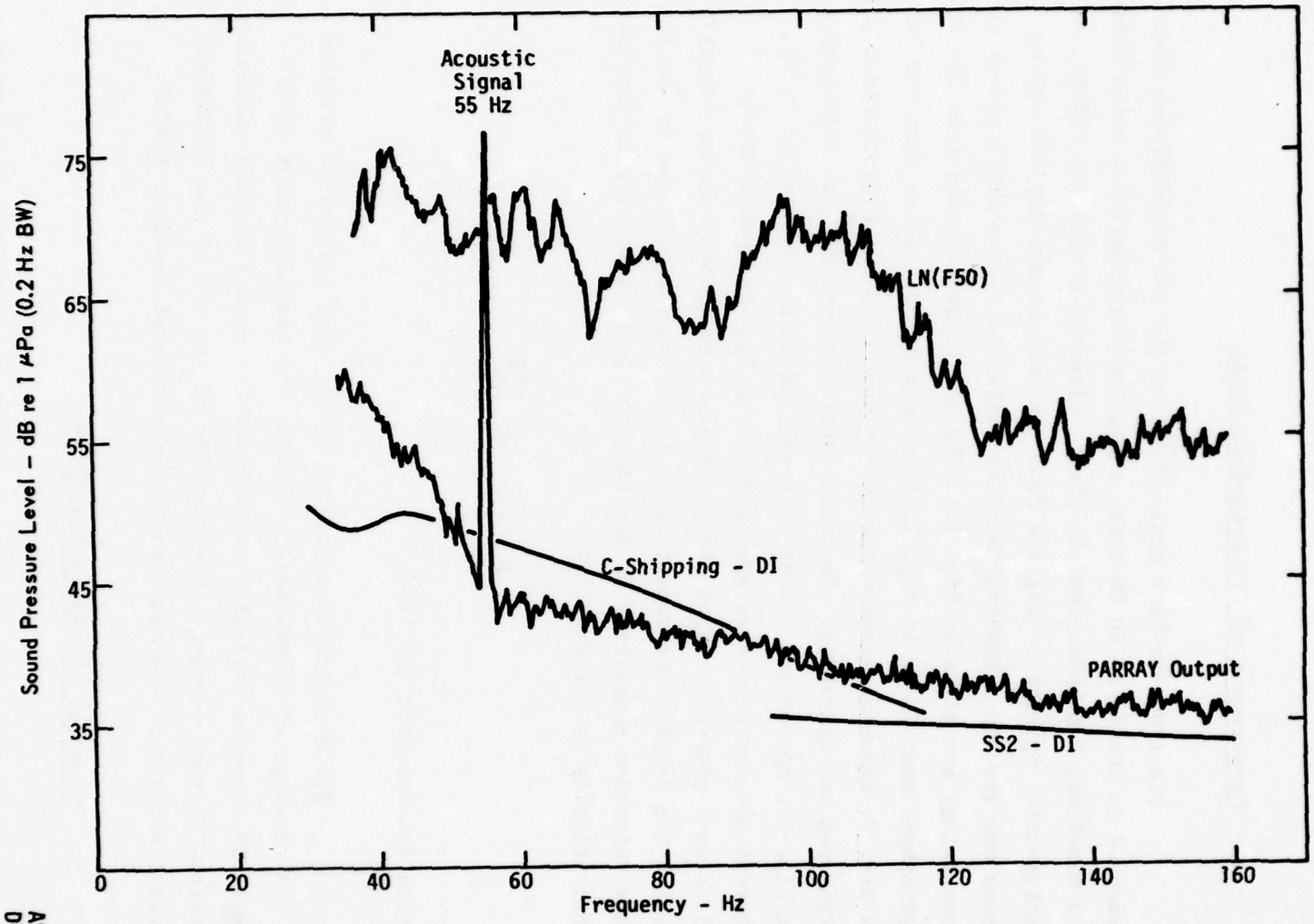

FIGURE 10
COMPARISON OF AMBIENT NOISE AT INPUT AND OUTPUT OF 340 m PARRAY - 3-1-77 DATA

AS-77-2174
DFR-0231-0

4. Measurement of Front-to-Back Ratio

The front-to-back ratio (F/B) of the 340 m PARRAY has been measured in the 70 to 80 Hz range using the high amplitude noise from the Mansfield Dam hydroelectric plant, directly behind the PARRAY, as background. Spectra of signals from the ambient monitor F50 hydrophone and the 340 m PARRAY, obtained while the hydroelectric plant was generating, are given in Fig. 11. The low frequency peak from the F50 hydrophone near 75 Hz in Fig. 11 is nearly 36 dB greater than the level in Fig. 7, whose measurements were obtained when the hydroelectric power plant was not operating. The peak level from the F50, as illustrated in Fig. 11, approaches 119 dB re 1 $\mu Pa/\sqrt{Hz}$ at a frequency of 75 Hz, whereas the corresponding peak from the PARRAY is approximately 75 dB re 1 $\mu Pa/\sqrt{Hz}$. Since the power plant is located almost directly behind the PARRAY, the reduction in level is primarily due to the back-side rejection capability of the PARRAY. This capability is expressed theoretically by the equation

$$\frac{F}{B} = \left[\frac{7}{3}\,\frac{kL}{\sin(kL)}\right]^2 \tag{7}$$

which follows from Eq. (1).

For a signal frequency of 75 Hz, this expression predicts a F/B envelope of approximately 48 dB. The measured value of F/B of 44 dB compares favorably with theory for such a complex radiating source. A more complete investigation of the F/B of the PARRAY was conducted as part of the measurements on the short baseline PARRAY.

5. Temporal and Phase Stability

Another experiment was performed to determine the temporal stability of signals received by the 340 m PARRAY. A stable signal at 71.18 Hz was transmitted from the J9 transducer at a distance of 1500 m on the PARRAY axis. The signal was analyzed with 0.01 Hz resolution and the resulting spectrum is displayed in Fig. 12. For the 0.01 Hz

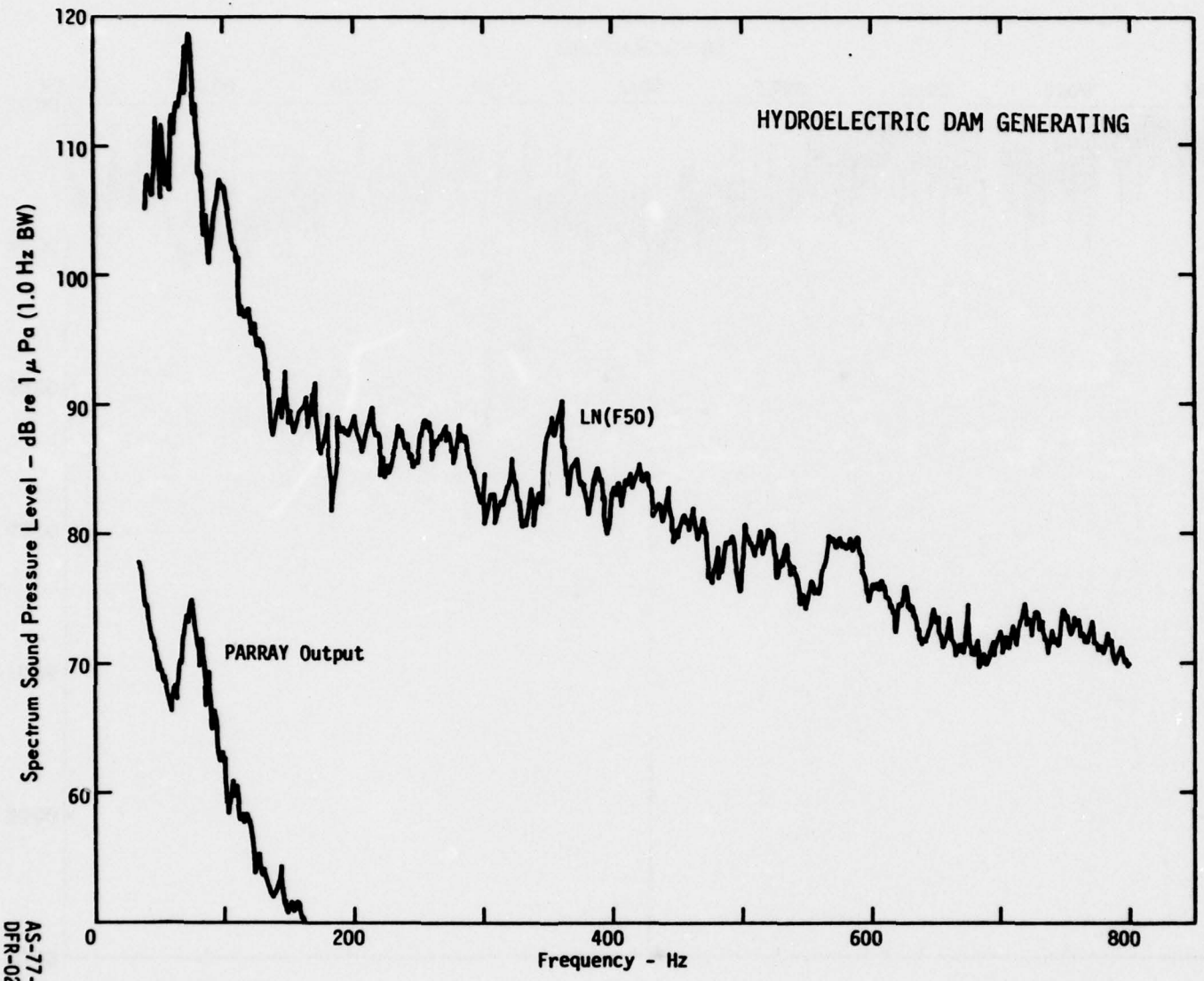

AS-77-2172
DFR-0231-0

FIGURE 11
COMPARISON OF AMBIENT NOISE AT INPUT AND OUTPUT OF 340 m PARRAY - 2-24-77 DATA

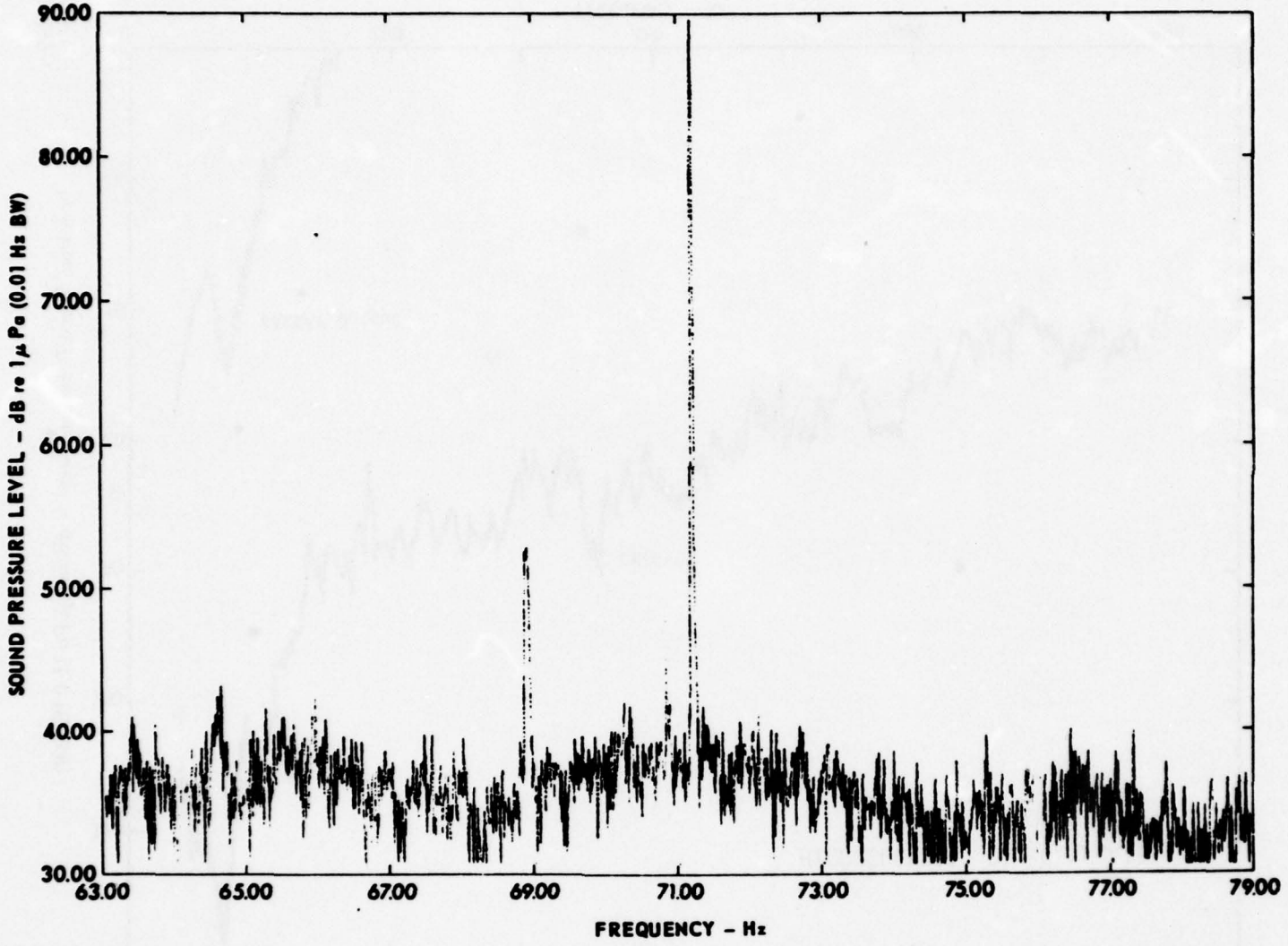

ARL-UT
AS-78-23
DFR-GA
1-13-78

FIGURE 12
340 m PARRAY OUTPUT FOR NARROWBAND PROCESSING 0.01 Hz BANDWIDTH

resolution processing there was no loss in signal level but the background noise level did correctly show a reduction of about 13 dB over that for 0.2 Hz processing bandwidth. However, as shown in Fig. 13, further processing of the data to a resolution of 0.004 Hz did not show a corresponding reduction in background noise. The same 71.18 Hz signal from the reference hydrophone (F50) was similarly processed with 0.01 Hz and 0.004 Hz resolution and the results are shown in Figs. 14 and 15, respectively. The background noise level does show a proper reduction in level commensurate with a reduction in bandwidth. Careful comparison of Figs. 13 and 15 reveals that there is some additional spectral spreading of the 71.18 Hz signal from the PARRAY for 0.004 Hz processing resolution as compared to the same processing for the F50 data. This tends to indicate that the very slight spectral spreading from the PARRAY was not due to the medium, stability of the signal source, or the processing procedure of the data acquisition and processing subsystem (DAPS). For this experiment the data indicate the limit to further processing resolution might be due to very small phase instabilities in the receiving and demodulation process. These instabilities could be eliminated by phase locking the demodulation reference oscillator to the received pump signal.

In summary, low frequency signals were received by the PARRAY and processed to a very narrow frequency resolution of 0.01 Hz with proper processing gain and stability. Processing to 0.004 Hz resolution did not provide additional signal-to-noise improvements with the receiving electronics used in the experiment.

6. Effect of Transducer Motion on PARRAY

The effect of transducer motion on the 340 m PARRAY was investigated experimentally by having divers vigorously shake the antenna mast on which the PARRAY hydrophone was mounted. At frequencies above approximately 80 Hz, the noise floor of the PARRAY was 1 to 2 dB higher than the noise floor measured approximately 45 min earlier, before the

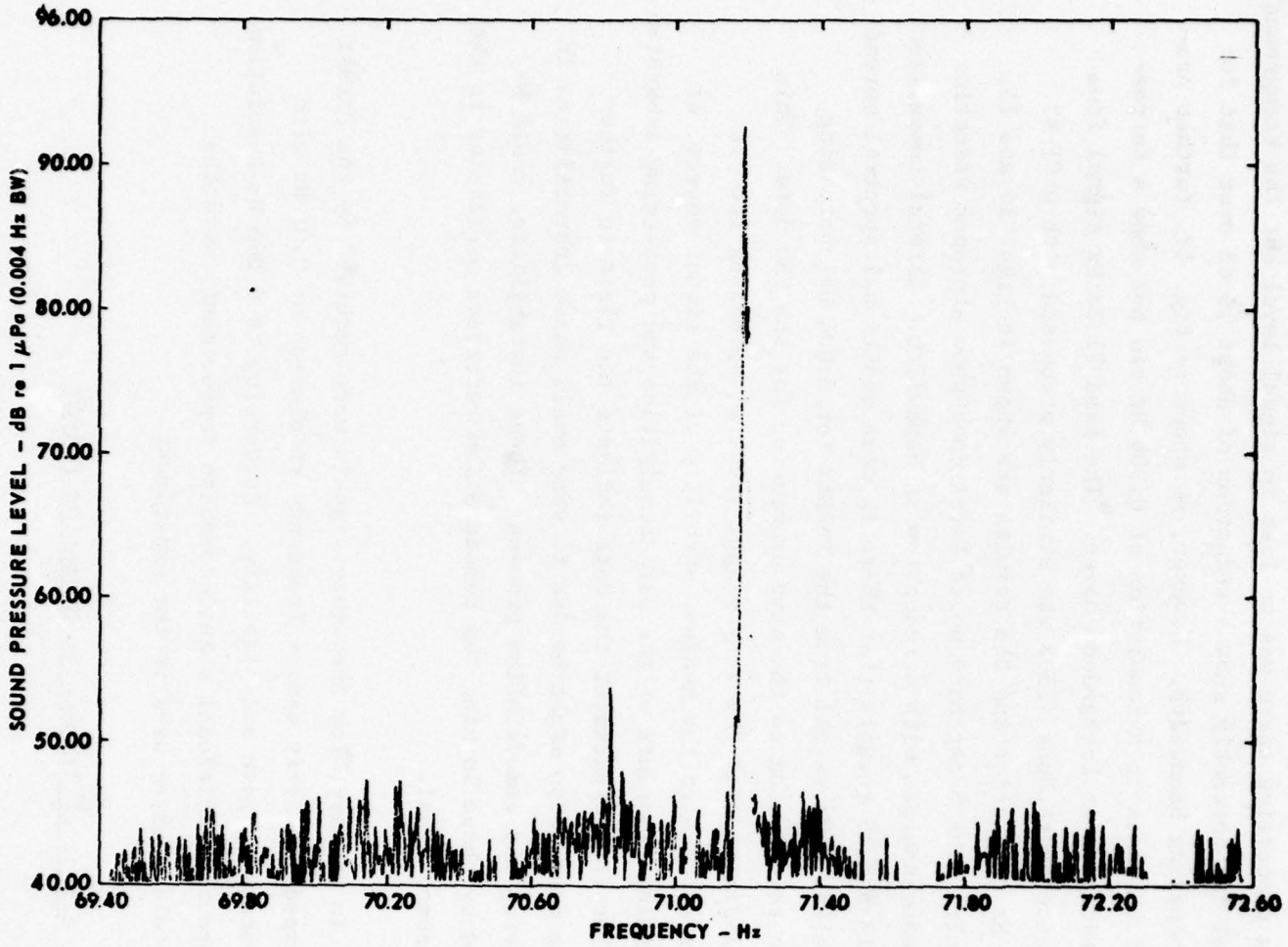

ARL:UT
AS-78-24
DFR-GA
1-13-78

FIGURE 13
340 m PARRAY OUTPUT FOR NARROWBAND PROCESSING 0.004 Hz BANDWIDTH

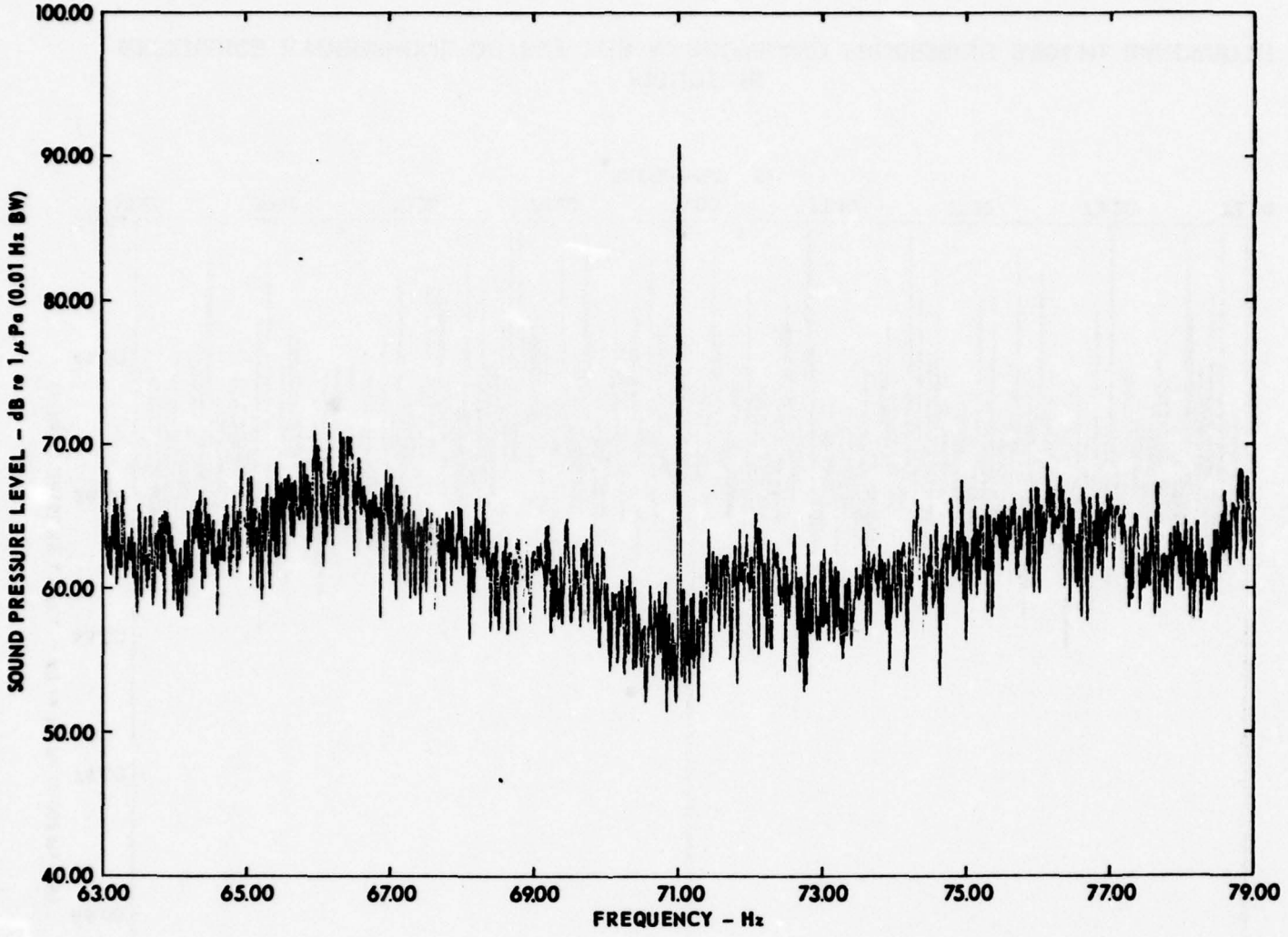

ARL:UT
AS-78-25
DFR-GA
1-13-78

FIGURE 14
REFERENCE HYDROPHONE OUTPUT FOR NARROWBAND PROCESSING 0.01 Hz BANDWIDTH

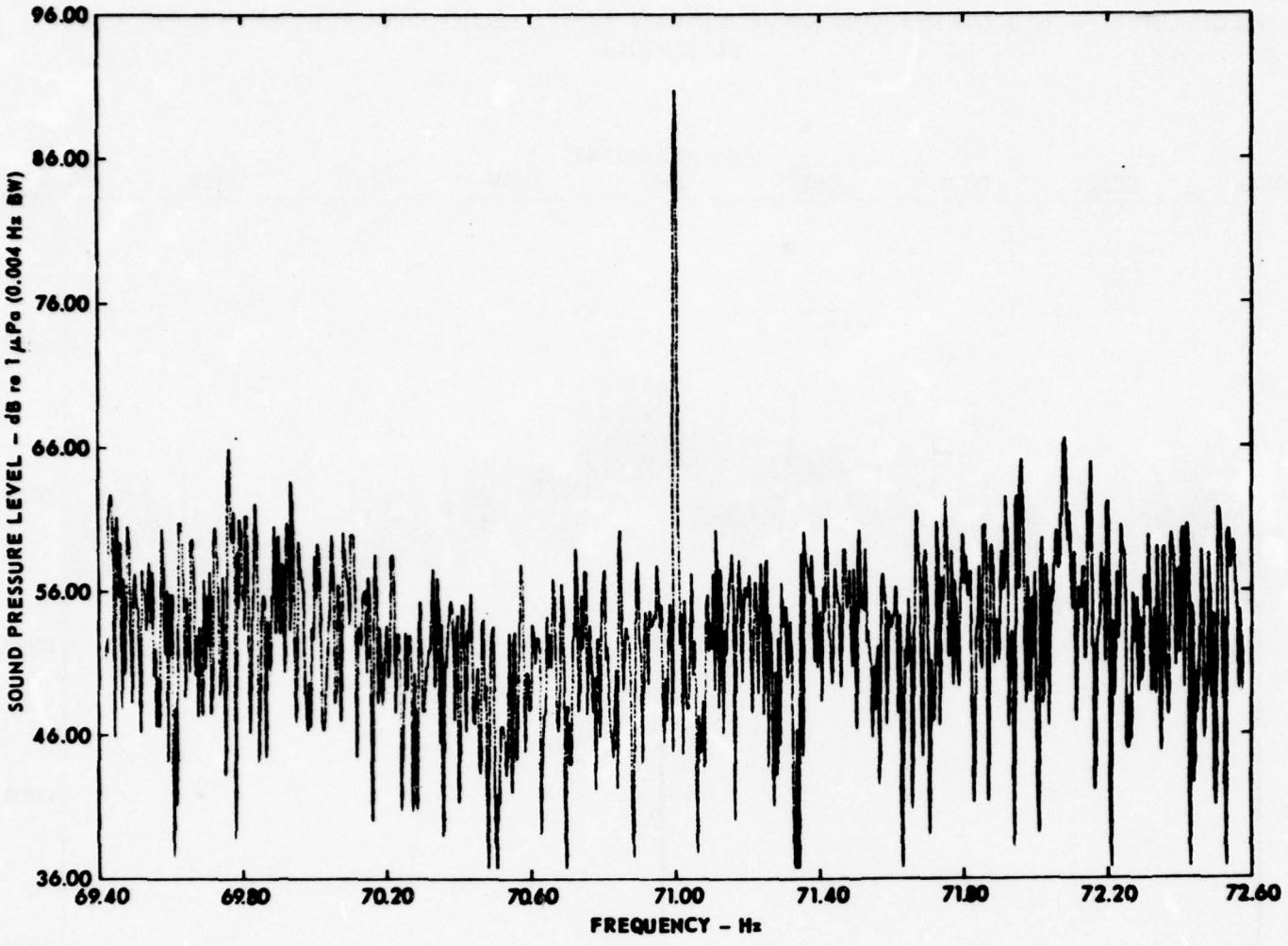

ARL:UT
AS-78-26
DFR-GA
1-13-78

FIGURE 15
REFERENCE HYDROPHONE OUTPUT FOR NARROWBAND PROCESSING 0.004 Hz BANDWIDTH

divers entered the water. This change is less than the variability of the background (ambient) noise over that time period. At frequencies below approximately 70 Hz, there was an increase of as much as 9 dB in the noise floor of the 340 m PARRAY when the divers hovered about 8 m above the PARRAY hydrophone. This noise floor remained at the same level while the divers were shaking the tower. During the time these measurements were being obtained, a 150 Hz acoustic signal was being received with the 340 m PARRAY. The 150 Hz signal was phase modulated by the vibration of the PARRAY hydrophone as shown in Fig. 16. A more detailed inspection of the PARRAY upper sideband revealed several distinct modulation components. The sidebands of the 150 Hz signal were found to be 150 ±0.8 Hz, 150 ±1.6 Hz, and 150 ±2.4 Hz. The levels of these 150 Hz sideband signals were +6 dB, +2 dB, and -5.6 dB referred to the 150 Hz signal level, respectively; the implication is that the signal at 150 Hz was phase modulated with a modulation index of about 1.9 at a frequency of 0.8 Hz. This represents the divers shaking the tower at a frequency of 0.8 Hz with a maximum displacement of 7 mm (14 mm peak-to-peak). These displacements and frequencies of modulation correspond to a peak acceleration of 0.018 g.

Although this level of acceleration is extremely high, the PARRAY operation was not obliterated. To properly relate vibration levels to the operation of the PARRAY, some analysis was performed and is included in section V of this report. Since there are some mobile platform applications for which the PARRAY concept could be useful, further examination of the effect of vibration on the PARRAY was performed in a more controlled experiment on a short baseline PARRAY, described in section B.

7. Nearfield Noise Rejection

The nearfield noise rejection of the 340 m PARRAY was investigated by transmitting a 10 Hz wide band of noise centered at 288 Hz from a transducer located approximately 10 m above the PARRAY

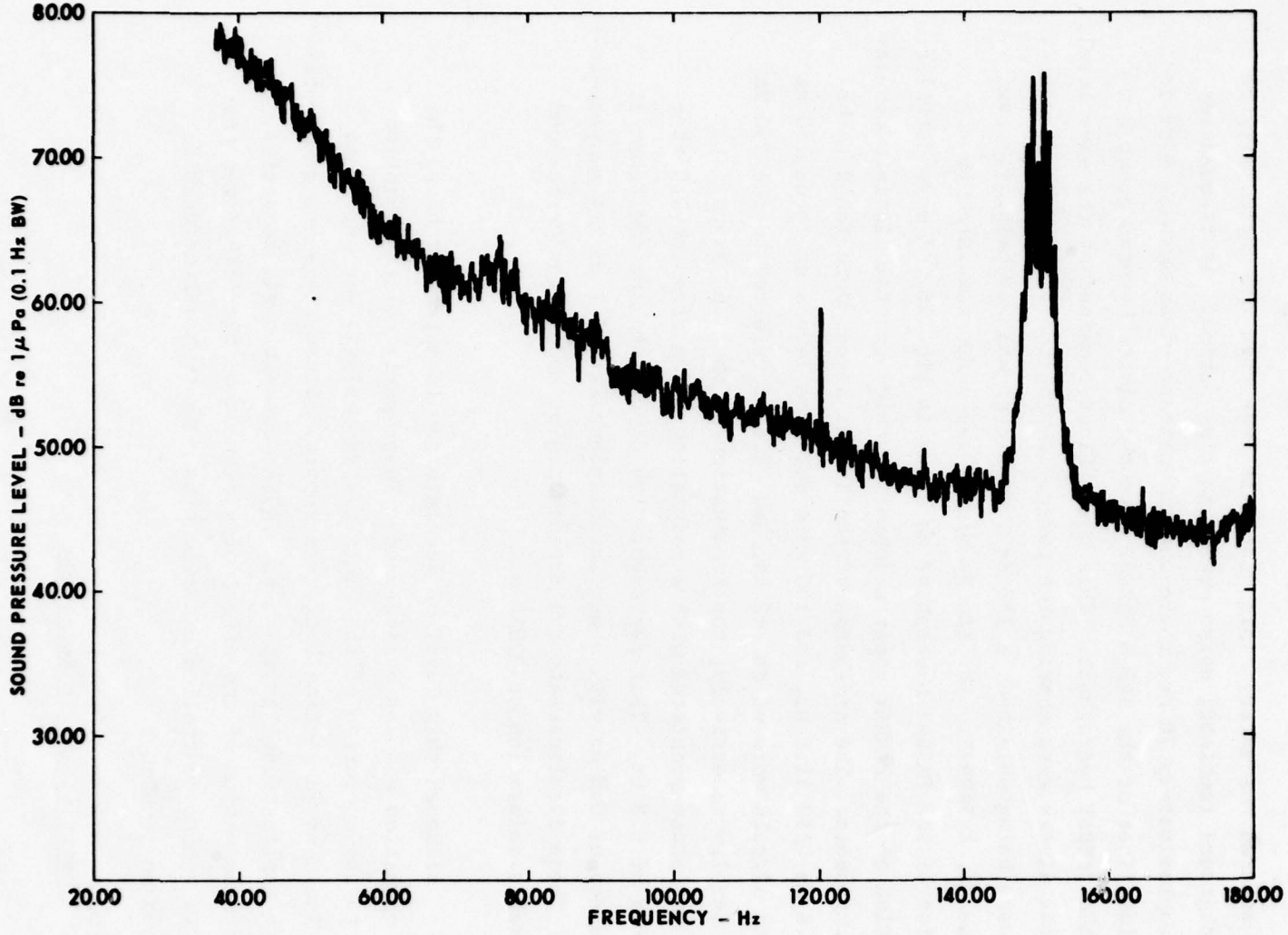

ARL:UT
AS-78-27
DFR-GA
1-13-78

FIGURE 16
340 m PARRAY RESPONSE TO DIVERS SHAKING TOWER

hydrophone. An omnidirectional standard transducer was located beside the PARRAY hydrophone for reference; and an acoustic calibration source at a frequency of 338 Hz was located on axis approximately 1500 m from the center of the PARRAY. The spectrum of the signal from the omnidirectional standard F50 hydrophone is shown in Fig. 17, with the 338 Hz acoustic calibration tone and the 10 Hz BW noise source labeled. Note that the spectrum level of the noise source observed by the F50 is approximately 23 dB greater than the level of the acoustic calibration signal. The response of the 340 m PARRAY to both the calibration source and the nearfield noise is shown in Fig. 18. The spectrum level of the noise source observed by the PARRAY is approximately 19 dB less than the level of the acoustic calibration signal. Since the F50 reference hydrophone provides a measurement of the input signal-to-noise ratio (S/N) of -23 dB to the PARRAY, the simultaneous response of the PARRAY indicates the backside discrimination against the nearfield noise in the form of an output S/N of +19 dB. The discrimination characteristics of the PARRAY are found by subtracting the input S/N in decibels from the output S/N in decibels, which for this example yields a difference of +42 dB. The nearfield noise from the PARRAY was 35 to 45 dB lower than the signal from the omnidirectional standard transducer for various locations and frequencies. These experiments verify an important characteristic of the PARRAY which will be useful in applications with nearby machinery noise or platform noise.

8. Multitone Calibration of PARRAY

Tests were performed on the 340 m PARRAY over a three-day period to determine the sensitivity of the PARRAY as a function of frequency and to observe the statistical variation of the acoustic calibration signals. Most of the data taken previously on the 340 m PARRAY used a 150 Hz acoustic reference signal from an NRL/USRD Type J9 transducer positioned 1500 m from the PARRAY at a depth of approximately 21 m. The new data obtained are in the frequency range from 52 to 793 Hz. The measurements were made using a J13 transducer with four tones summed and transmitted simultaneously. Due to the relatively restricted

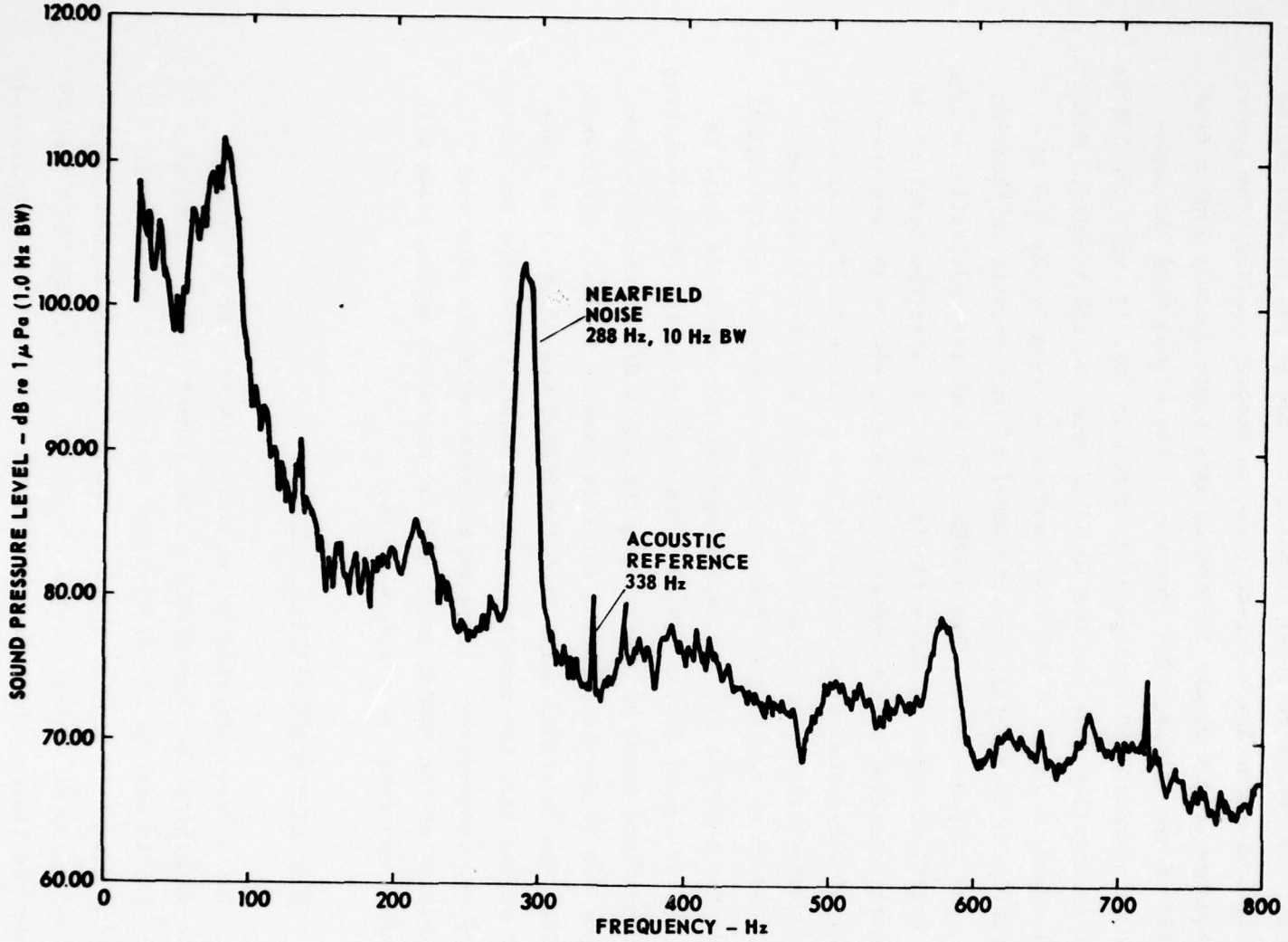

ARL:UT
AS-78-28
DFR-GA
1-13-78

FIGURE 17
REFERENCE HYDROPHONE RESPONSE TO NEARFIELD NOISE

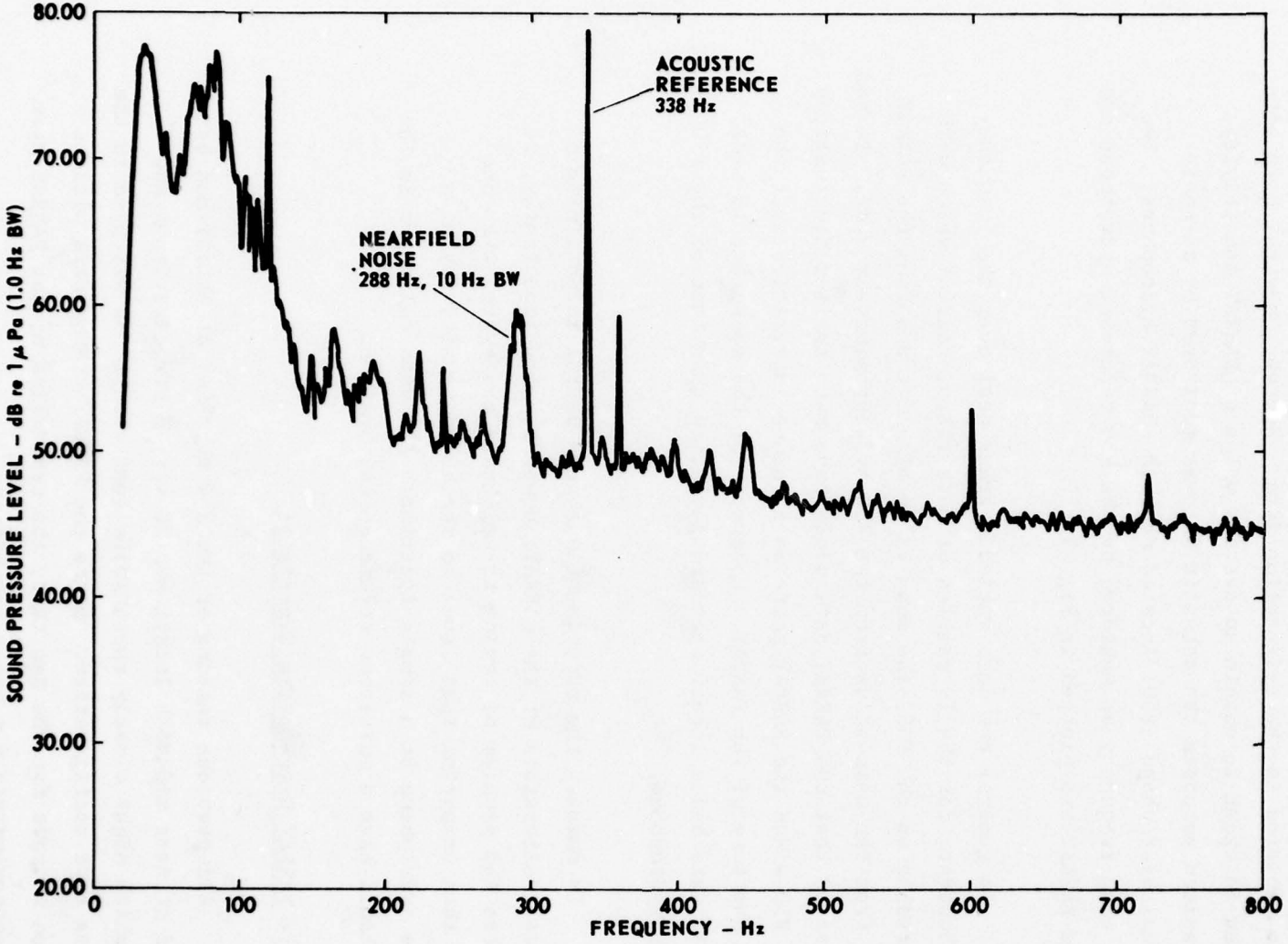

FIGURE 18
PARRAY RESPONSE TO NEARFIELD NOISE

ARL:UT
AS-78-29
DFR-GA
1-13-78

boundary conditions for cw transmissions, some interference between modes was expected in the calibration data. However, several data sets were taken in order to obtain an average value of PARRAY sensitivity. For comparison purposes the acoustic SPL was monitored by an omni-directional hydrophone (F50) located near the PARRAY hydrophone. The SPLs for each frequency as measured by the F50 reference hydrophone and the 340 m PARRAY are plotted in Fig. 19.

In general the data varied a great deal over the frequency range. However, for the 19 samples of data taken, four of which were not observable on the F50, the mean value of all tones from the PARRAY differed from the mean value from the F50 by approximately 2 dB. It had been expected that the PARRAY data would have much smaller fluctuations than the F50 since the PARRAY performs a volume integration over the acoustic aperture of the PARRAY. However, for the measurements made, the PARRAY data had a larger standard deviation than that of the F50 reference hydrophone.

In summary the experiment was very useful in obtaining a statistical calibration of the PARRAY; however, more importantly, it illustrates the problem of trying to calibrate the system with one tone and then comparing that level to the known sensitivity of a reference hydrophone at a single location. All data collected in the future should have a multitone reference calibration.

9. PARRAY Near-Bottom Experiment

All previous testing of the 340 m PARRAY at ARL:UT had been performed at near middepth locations (20 m). A new experiment was desired which might closely approximate test conditions expected in the future sea test configuration. Since the PARRAY transducers will be mounted on tripods for the sea test, the centerline of the PARRAY beam will be approximately 6 m above the bottom.

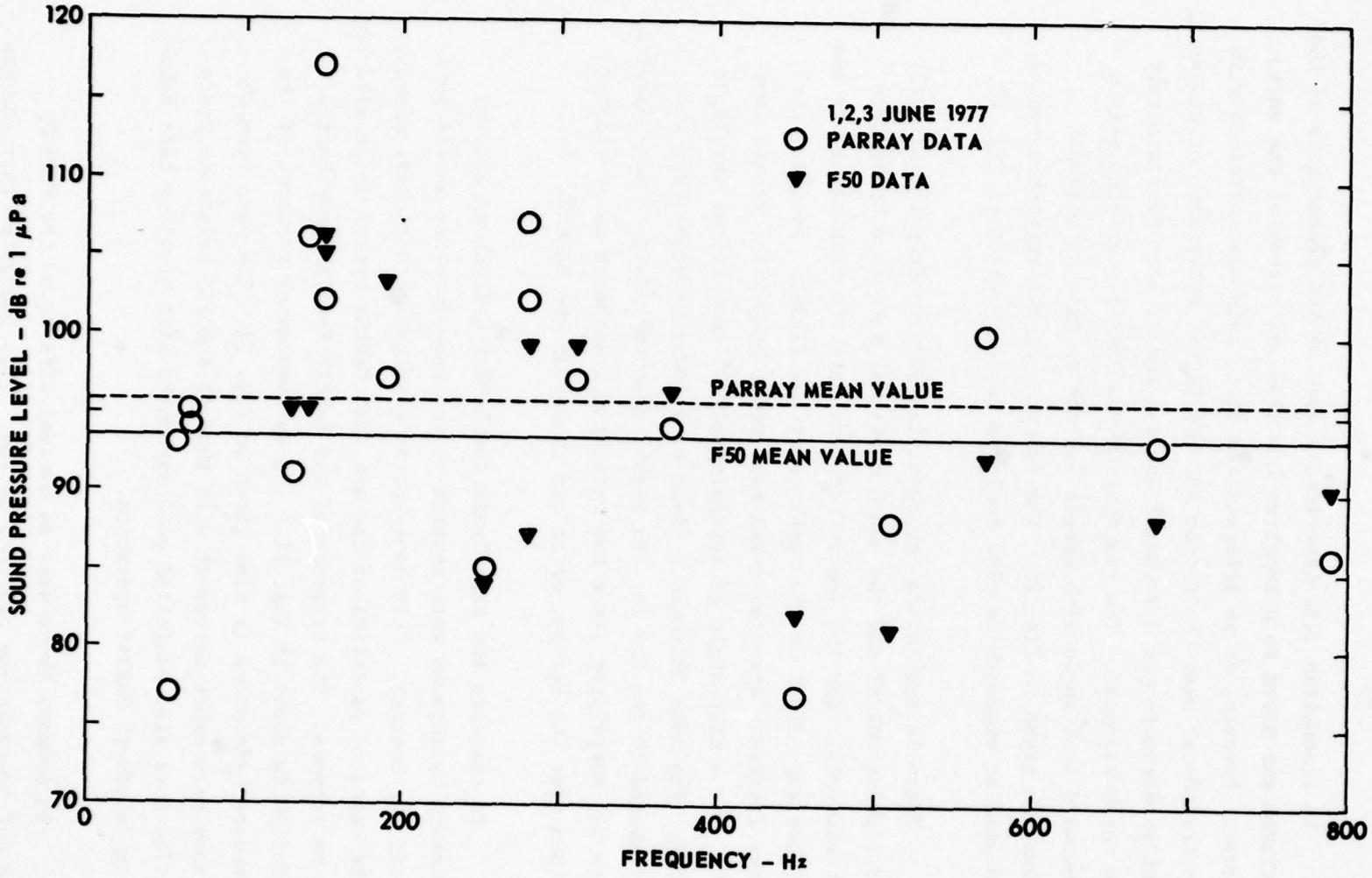

FIGURE 19
COMPARISON OF SPL OF SIGNALS MEASURED WITH 340 m PARRAY LOCATED AT MIDDEPTH AND F50 AT MIDDEPTH

AS-77-2238
DFR 0231-0

To accomplish this experiment, each of the transducers of the PARRAY system was moved to a location 8 m from the bottom of the underwater tower. However, as an intermediate test, data were obtained with the pump transducer near the bottom and the PARRAY hydrophone at middepth. This configuration formed a downward looking PARRAY beam approximately 3° below the horizontal. The response of the PARRAY operating with a small downward look angle with single sources on axis at middepth 1500 m away is given in Fig. 20. The response of the reference hydrophone located at middepth is also included for comparison in Fig. 20.

There is reasonable agreement in the data from the slightly downward looking PARRAY and the omnidirectional reference hydrophone (F50) at middepth. For the lower frequency data the beam should be too broad to see any effect on the response of the PARRAY. However, for the higher frequency data the total half-power beamwidth becomes less than 10°. For a tilt angle of approximately 3° some effect should be observable. The data indicate a trend of a lower response from the PARRAY compared to the F50 for the higher frequency data. These observations are not surprising since the reference hydrophone is at middepth rather than near the bottom, or at the center of the PARRAY.

To complete the experiment the PARRAY hydrophone and the F50 reference hydrophone were lowered to the same location as the pump (8 m above the bottom). This near-bottom configuration closely approximates the expected operation of the sea test PARRAY system which will be mounted on tripods. The response of the PARRAY for the near-bottom configuration is shown in Fig. 21. The corresponding response of the F50 reference hydrophone is also given in Fig. 21. The data from the PARRAY show reasonable agreement with that of the F50 reference hydrophone. The data also exhibited good agreement with previous data taken during the middepth PARRAY operation.

In summary there were no unusual effects on the PARRAY response due to operation near the bottom. This indicates that the sea

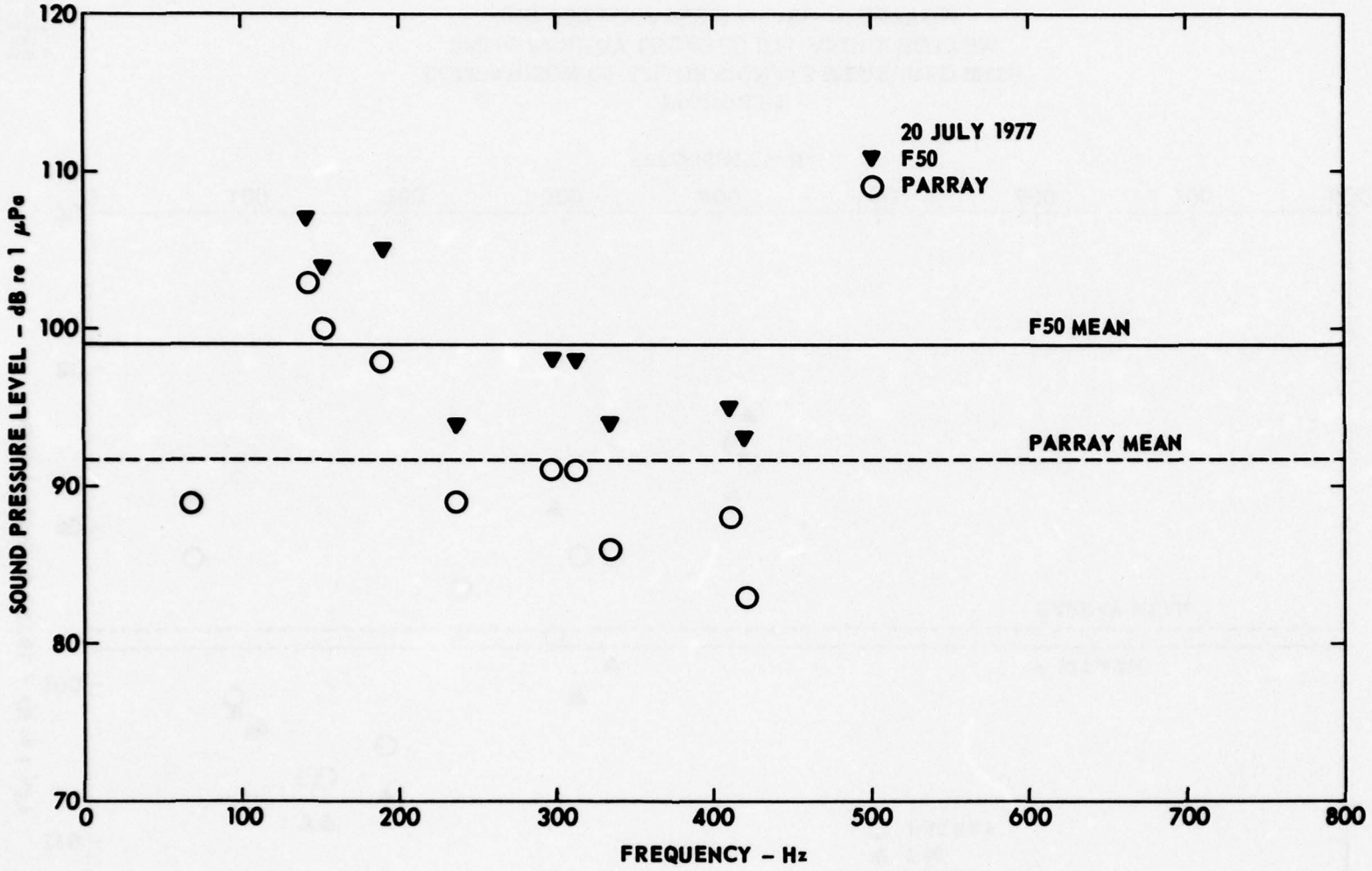

FIGURE 20
COMPARISON OF SPL OF SIGNALS MEASURED WITH
DOWNWARD TILTED 340 m PARRAY AND F50 AT MIDDEPTH

ARL:UT
AS-78-556
DFR-GA
4-10-78

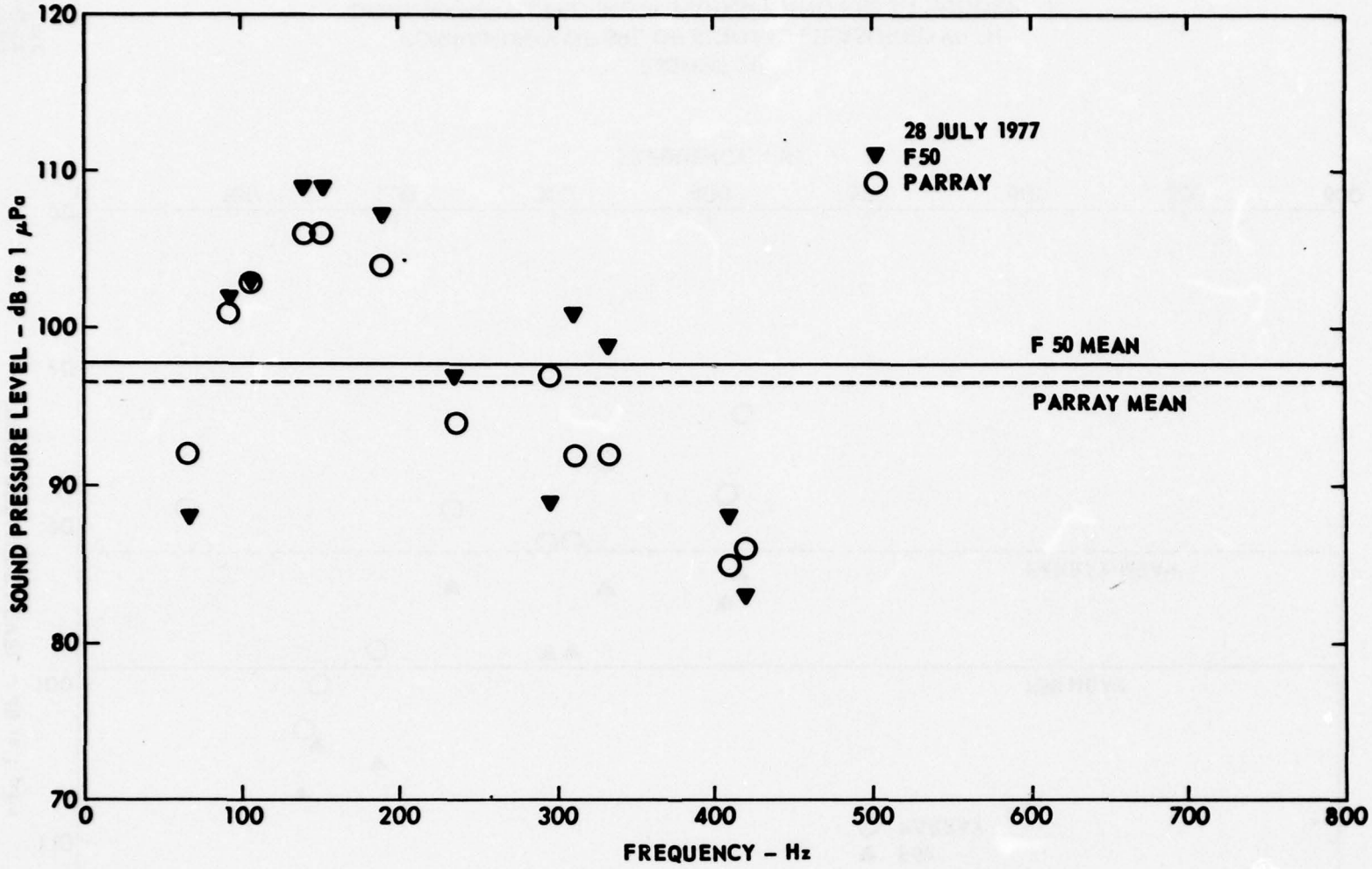

FIGURE 21
COMPARISON OF SPL OF SIGNALS MEASURED WITH 340 m PARRAY LOCATED 8 m ABOVE BOTTOM AND F50 LOCATED 8 m ABOVE BOTTOM

ARL:UT
AS-78-557
DFR-GA
4-10-78

test configuration planned for the PARRAY, consisting of a tripod bottom mounted unit, should not experience adverse operation.

B. 5 m PARRAY On a Column

In planning the test of the experimental PARRAY at LTTS, it was recognized that the relatively small Lake Travis basin would preclude direct measurement of beam patterns with the 340 m PARRAY. To circumvent this problem we were able to exploit the fact that the beam pattern of the PARRAY is determined by the acoustic aperture, kL, rather than being a function of the pump-hydrophone separation only. Thus we implemented a short PARRAY on a column located on the main barge to obtain beam patterns by scaling the frequency of the signal to correspond to the smaller pump-hydrophone separation. This is discussed in more detail in the test plan for the interim lake tests.[23] However, since the interim lake tests on the 340 m PARRAY were so successful, the instrumentation of the short PARRAY on the column was expanded to investigate the effects of transducer vibration on the PARRAY. For this purpose a vibrator was constructed to vibrate the PARRAY transducers in a controlled manner, and accelerometers were developed for the specialized conditions of the PARRAY. This vibrator and the accelerometers were installed on the PARRAY transducers.

1. Test Fixtures

The special short baseline PARRAY consisted of a pump and hydrophone mounted on a horizontal boom attached to a rotating vertical column. One of the purposes of this fixture was to obtain beam pattern measurements by rotating the PARRAY instead of moving the sound source. Since the pump-hydrophone separation is small, the PARRAY has good directional characteristics (narrow beamwidth and high F/B) only at high signal frequencies; however, the beam patterns obtained at high frequencies on this short array are theoretically the same as would be obtained with a longer array at lower frequencies. Because of this

tradeoff between signal frequency and array length, both the frequency and array length are scaled to make the experimental results applicable to the long baseline PARRAY.

Since the frequencies to be used for the short baseline experiments would be high compared to those used for the long baseline LTTS experiments, small transducers were needed to reduce the shadowing and reflection problems from the transducer housings. A pair of 4-element arrays was fabricated for use in the scaled PARRAY experiments. These 4-element arrays were constructed using the same techniques developed for the larger PARRAY transducers, which are discussed in section IV.D. A significant problem was encountered in integrating the 4-element transducers into a PARRAY. The problem was matching the high transducer impedance to a power amplifier at high power levels. Series tuning the transducer with two inductors reduced this impedance and lowered the inductor dissipation somewhat.

Tests of the 5 m PARRAY using these transducers showed the array noise floor to be dependent on the pump power level. This was assumed to be due to transducer cavitation. Maximum projected sideband noise-to-carrier ratio occurred at approximately 1.5 W pump power for the shallow depth of 4.5 m. At this pump power level the PARRAY noise floor was dominated by the 65 kHz ambient noise in the lake because of the small DI of the 4-element arrays. This meant that either higher pump levels or a more directional PARRAY hydrophone (or both) was needed to maximize low frequency sensitivity of the 5 m PARRAY. However, because of cavitation at the shallow operating depth, an increase in pump source level required a larger pump transducer. Therefore, to obtain higher pump source level and more directionality in the PARRAY hydrophone, existing single ended, 19-element transducers were modified for use with the 5 m PARRAY. A new housing design was developed to allow a transformer to be mounted behind the transducer face. This allowed the transducers to be driven from a balanced line transducer cable, thus reducing line frequency pickup.

The 19-element transducers were installed, aligned, and tuned on the 5 m PARRAY, and provided an improved acoustic sensitivity and a lower sensor noise floor.

2. Beam Patterns with Scaled PARRAY

Several preliminary beam patterns were obtained using the scaled PARRAY at Lake Travis Test Station. These beam patterns were made at relatively high frequencies; however, the short length of the scaled PARRAY provides the proper scaling such that the results are representative of patterns that would be obtained for normal frequencies of interest and a much longer baseline PARRAY. For example, the beam pattern of a 5 m PARRAY at a signal frequency of 2500 Hz would correspond to the beam pattern of a 500 m PARRAY at a signal frequency of 25 Hz; this represents a scale factor of 100.

Data were obtained using a pump frequency of 65 kHz with the 19-element planar array. The output of the PARRAY hydrophone was coupled into a band elimination receiver (BER-2) which suppressed the carrier and amplified the near sideband information. This single sideband (SSB) information was then translated to baseband and processed by an 800-line spectrum analyzer in a 64-exponential average mode with 0.5 Hz resolution. The output of the 2500 Hz frequency cell was then monitored by a PDP 11/04 processing system and plotted on a Zeta digital incremental plotter. The signal source consisted of an NRL/USRD Type J13 transducer driven with a cw signal of 2500 Hz. This source was at a depth of 4.57 m and a range of approximately 18 m.

A representative beam pattern obtained under these conditions is illustrated in Fig. 22. The major lobe structure is well defined and is close to the expected pattern. The back lobe structure has some asymmetry and deviates from that expected.

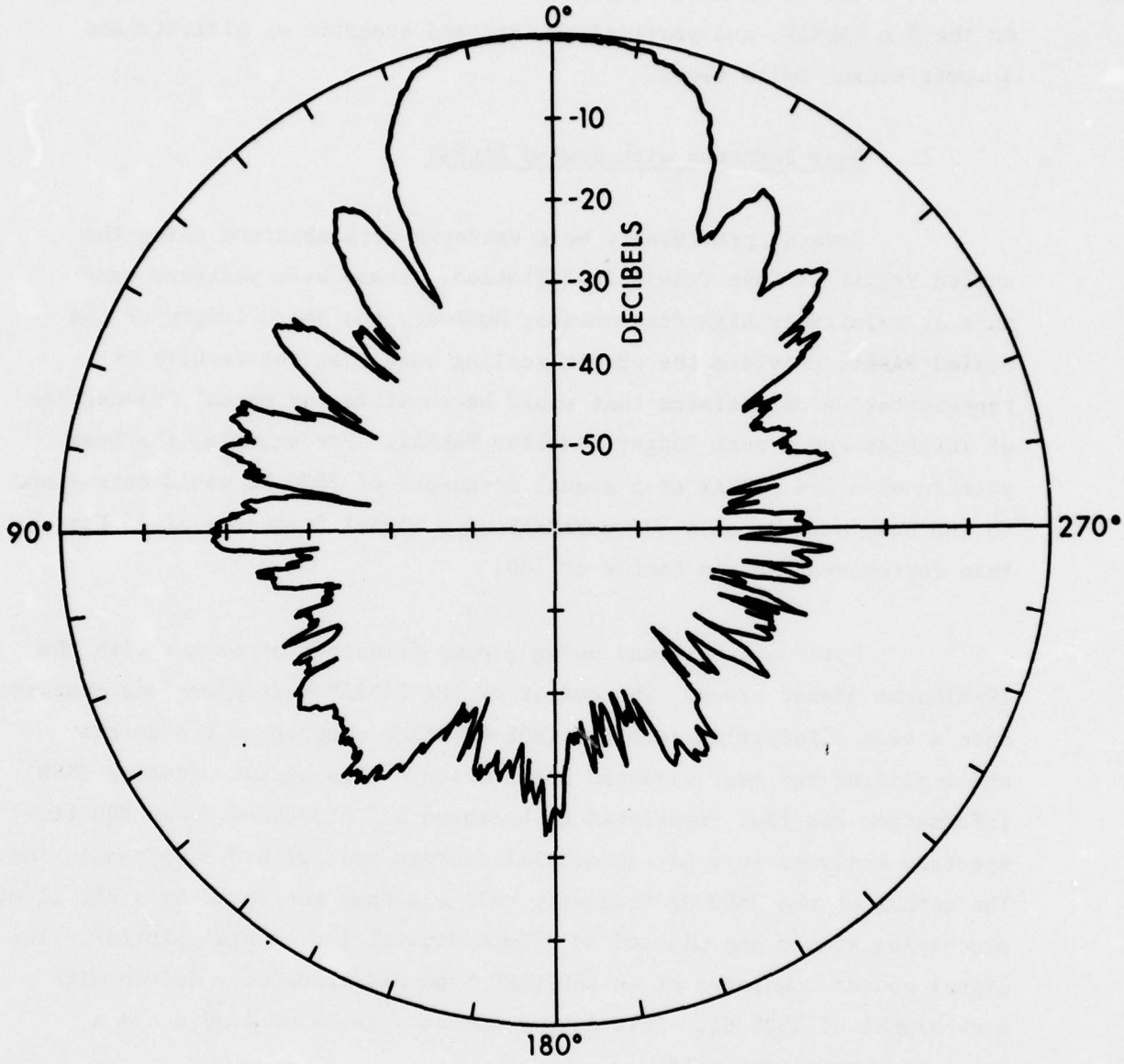

FIGURE 22
EXPERIMENTAL BEAM PATTERN FOR 5 m PARRAY AT 2500 Hz

ARL - UT
AS - 77 - 1249
DFR - GA
10 - 19 - 77

An expression for the directional response of the PARRAY was given in Eq. (1). A theoretical beam pattern for a PARRAY at a signal frequency of 2500 Hz with a length of 5 m is shown in Fig. 23.

A comparison of beam patterns is shown in Fig. 24 for a signal frequency of 2500 Hz. The major lobe and first minor lobes are in good agreement; however, the back lobe structure on the experimental pattern is larger and not well behaved. Further investigations using pulsed data indicated that there were very strong reflections from the flotation material supporting the barges at LTTS. A more isolated platform would be desirable for more detailed observations of scaled PARRAY operations.

3. Measurement of Vibration

Instrumenting the PARRAY transducers to measure transducer vibration while the PARRAY was operating presented some unique problems. First, commercially available accelerometers immersed in water are quite sensitive to acoustic energy in the water. This makes it difficult to distinguish the accelerometer output due to acoustic waves in the water from the accelerometer output due to mechanical vibration of the surface on which the accelerometer is mounted. Second, the vibration levels which we desired to measure were much smaller than the vibration levels in the transducer housing generated by the high level 65 kHz pump signal to which the accelerometers were quite sensitive.

The design approach to solving this problem was to isolate the accelerometer from the 65 kHz vibration by means of a mechanical low pass filter and to isolate the accelerometer from the waterborne acoustic signals by enclosing the accelerometer and mechanical filter in an air filled canister. A further constraint was that the accelerometer, mechanical filter, and canister had to be small enough to mount on the back of the PARRAY transducers without adversely affecting the operation

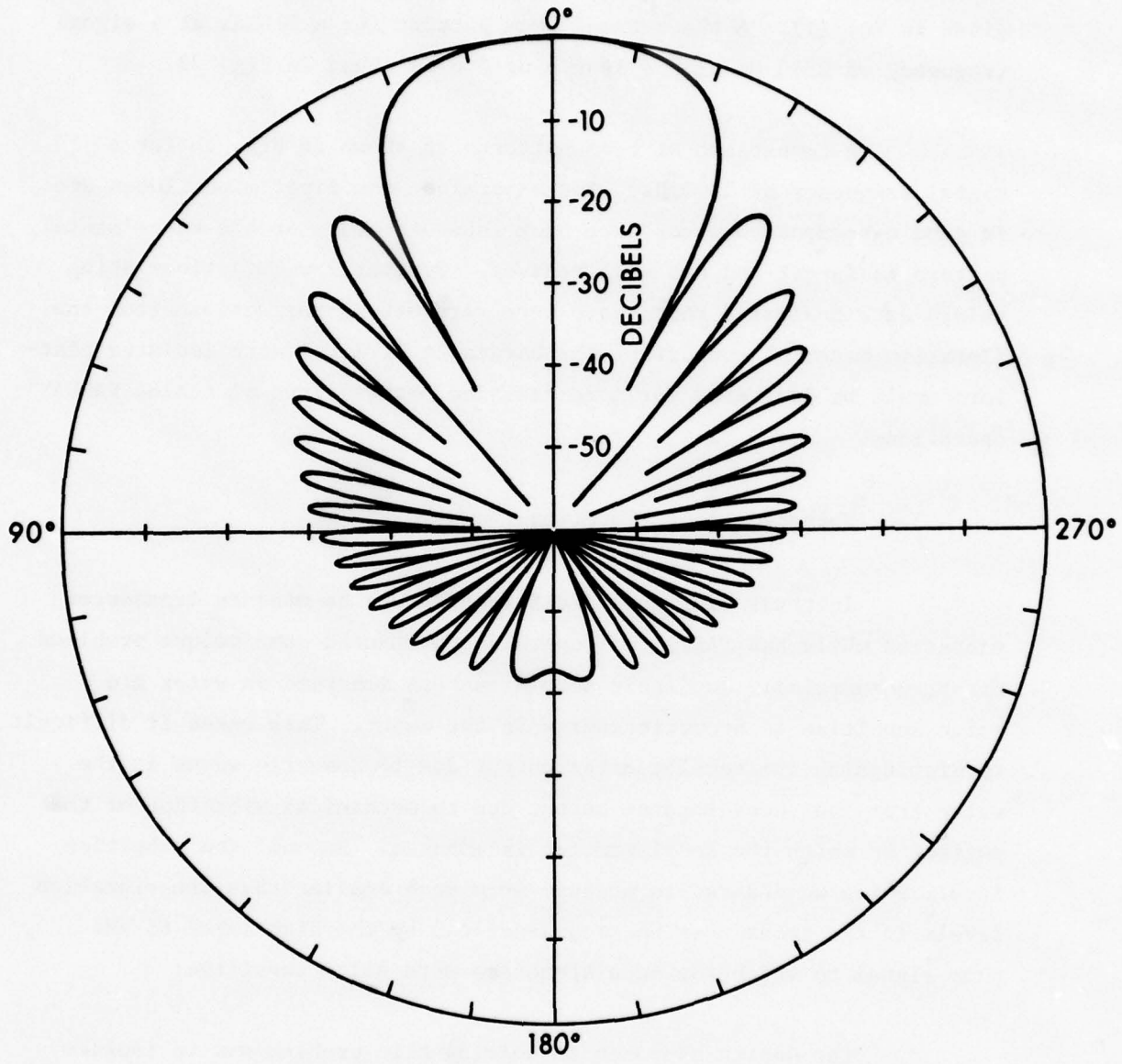

FIGURE 23
THEORETICAL BEAM PATTERN FOR 5 m PARRAY AT 2500 Hz

ARL - UT
AS - 77 - 1250
DFR - GA
10 - 19 - 77

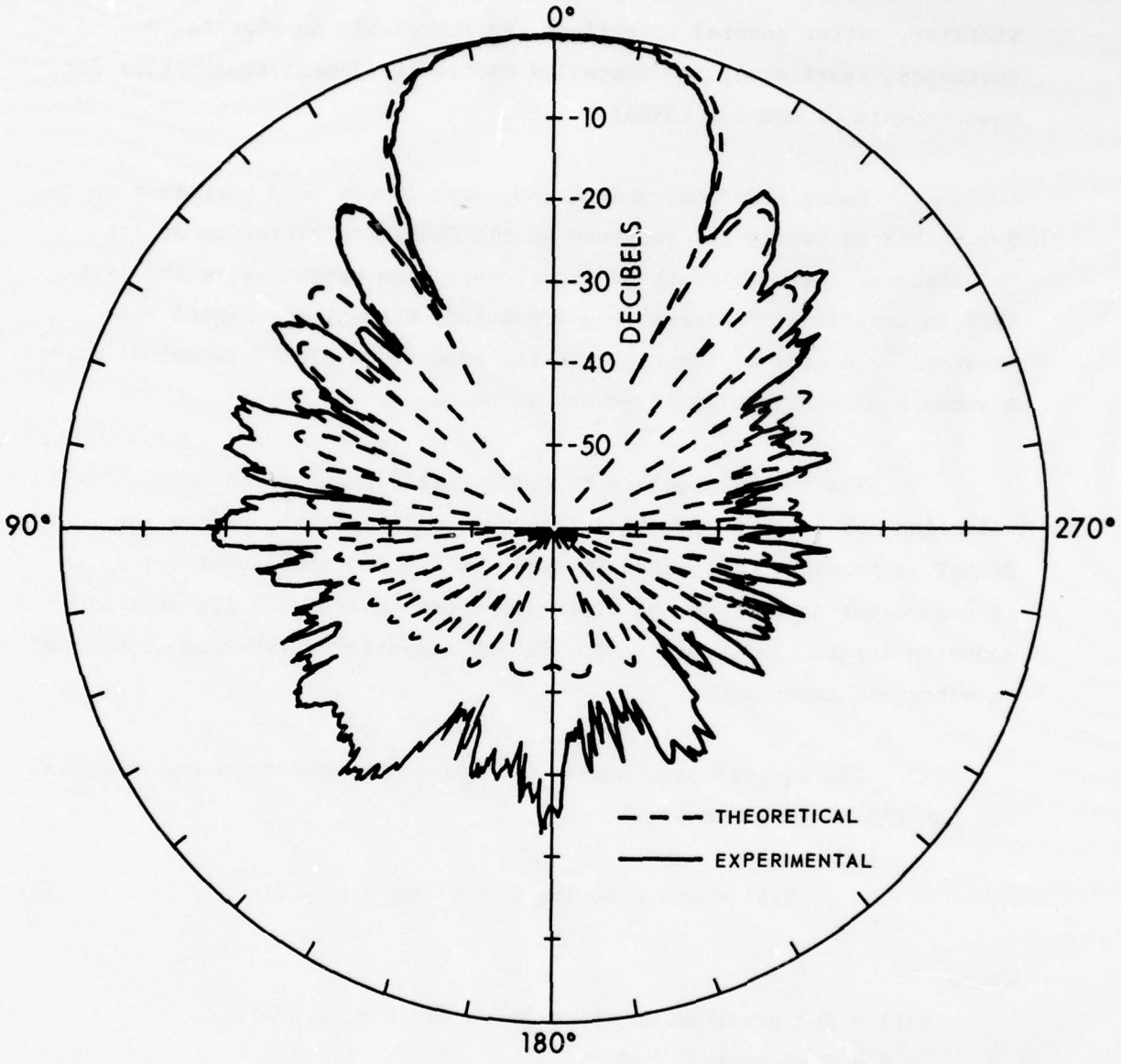

FIGURE 24
COMPARISON OF THEORETICAL AND EXPERIMENTAL BEAM PATTERNS FOR 5 m PARRAY AT 2500 Hz

ARL - UT
AS - 77 - 1251
DFR - GA
10 - 19 - 77

of the transducers or changing the response of the total assembly to the vibrator. After several iterations, an acceptable combination was developed, fabricated, and installed on the 19-element transducers for measurements on the 5 m PARRAY.

Using this instrumentation, experiments were performed on the 5 m PARRAY to verify the response of the PARRAY to vibration of its transducers. Results of these experiments were presented at the 1978 IEEE International Conference on Acoustics, Speech, and Signal Processing.[31] A copy of the paper is included in an ARL:UT technical report.[16] A summary of the results is presented below.

The theory predicts that the PARRAY responds to both vibration and acoustic inputs in a very similar manner. Since the PARRAY is normally calibrated in terms of its acoustic sensitivity, it is convenient to express the vibration input in terms of its equivalent acoustic input. This permits the PARRAY acoustic calibration to be used in vibration experiments.

The equivalence between vibration and on-axis acoustic signal for the PARRAY is given by

$$P(f) = 164 - 40 \log f - 20 \log L + G(f) \quad , \tag{8}$$

where

$P(f)$ = the pressure spectrum level in dB re 1 $\mu Pa/\sqrt{Hz}$,

f = frequency in hertz

L = PARRAY length in meters, and

$G(f)$ = the vibration spectrum level in dB re 1 $\mu g/\sqrt{Hz}$.

For the 5 m PARRAY this is

$$P(f) = 150 - 40 \log f + G(f) \quad . \tag{9}$$

The experimental technique used to verify this relationship was to measure the acceleration spectrum, convert the acceleration spectrum to its equivalent spectrum SPL using Eq. (9), and compare the resulting SPL spectrum with the SPL spectrum measured by the PARRAY using its normal acoustic calibration. For this experiment the PARRAY was set up for normal operation except that the hydrophone was instrumented with both a shaker and accelerometer so that vibration of the hydrophone could be induced and accurately measured.

Figure 25 shows an acceleration spectrum measured with an accelerometer mounted on the PARRAY hydrophone while the hydrophone was being shaken at frequencies of 146 Hz and 292 Hz. Note the narrowband acceleration spectral components at those frequencies. Figure 26 shows the output of the PARRAY and the output of a reference hydrophone, both measurements being made while the PARRAY hydrophone was being shaken. From Fig. 26 it is apparent that the PARRAY tonal outputs at 146 and 292 Hz must be caused by the shaker because the reference hydrophone shows that there are no acoustic signals at those frequencies.

These experimental data are compared with the theoretical predictions, Eq. (9), by transforming the acceleration data of Fig. 25 to its acoustic equivalent, using Eq. (9), and comparing the result with the measured acoustic data. This comparison is shown in Fig. 27. The agreement at 146 Hz and 292 Hz of ±2 dB is well within expected experimental variation.

The same experiment was repeated several times at various frequencies with similar results. Figure 28 shows the agreement between measured and predicted response of the PARRAY to vibration at the various frequencies. These differences are believed to be due primarily to problems in accurately measuring the vibration levels. Nevertheless, the results confirm the theoretical relationships developed for the PARRAY vibration response.

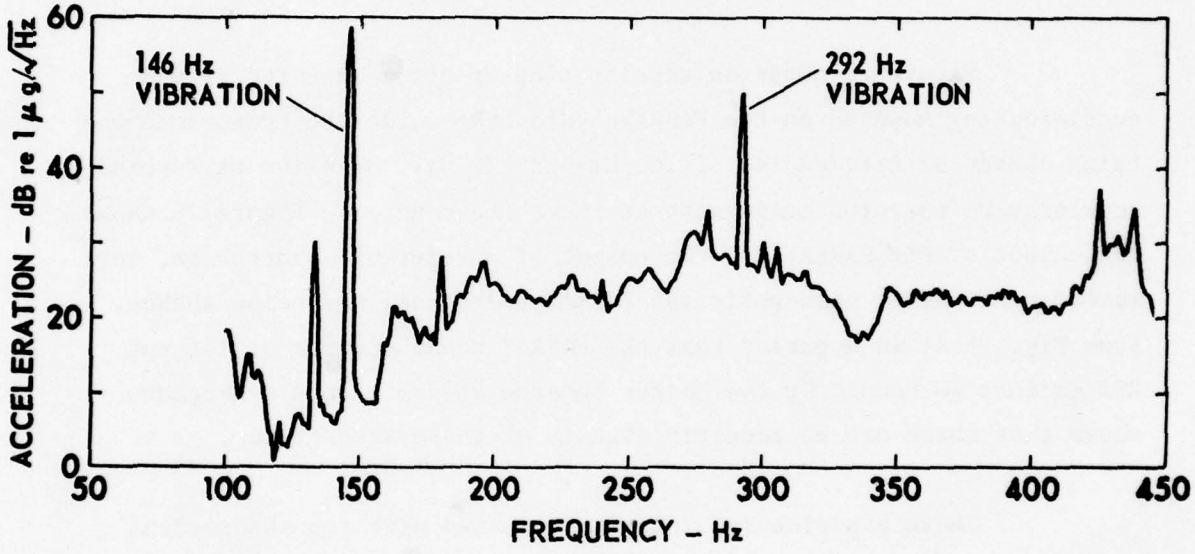

FIGURE 25
ACCELERATION SPECTRUM MEASURED WITH ACCELEROMETER

ARL:UT
AS-77-1417-S
CRR-GA
12-8-77

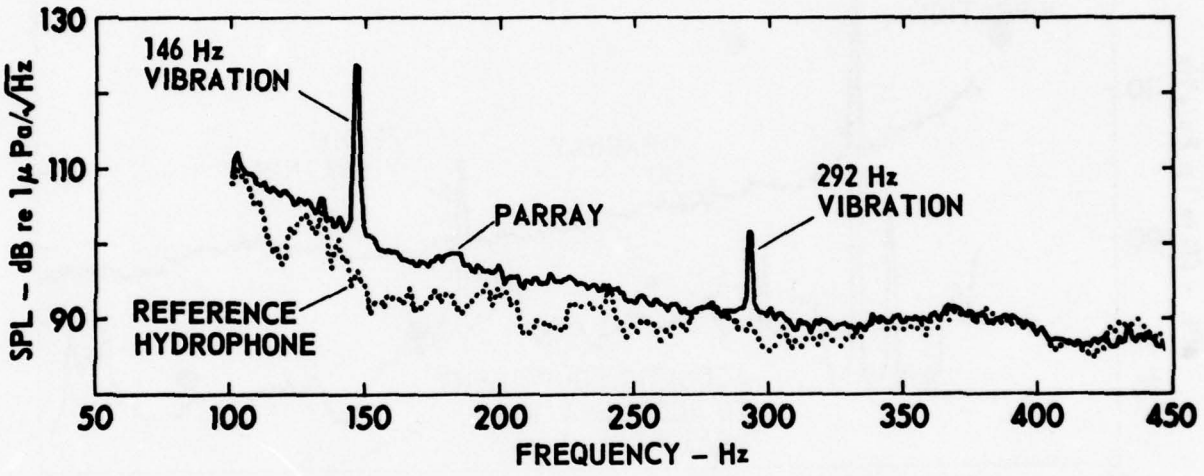

FIGURE 26
SOUND PRESSURE LEVEL SPECTRUM

ARL:UT
AS-77-1416-5
CRR-GA
12-8-77

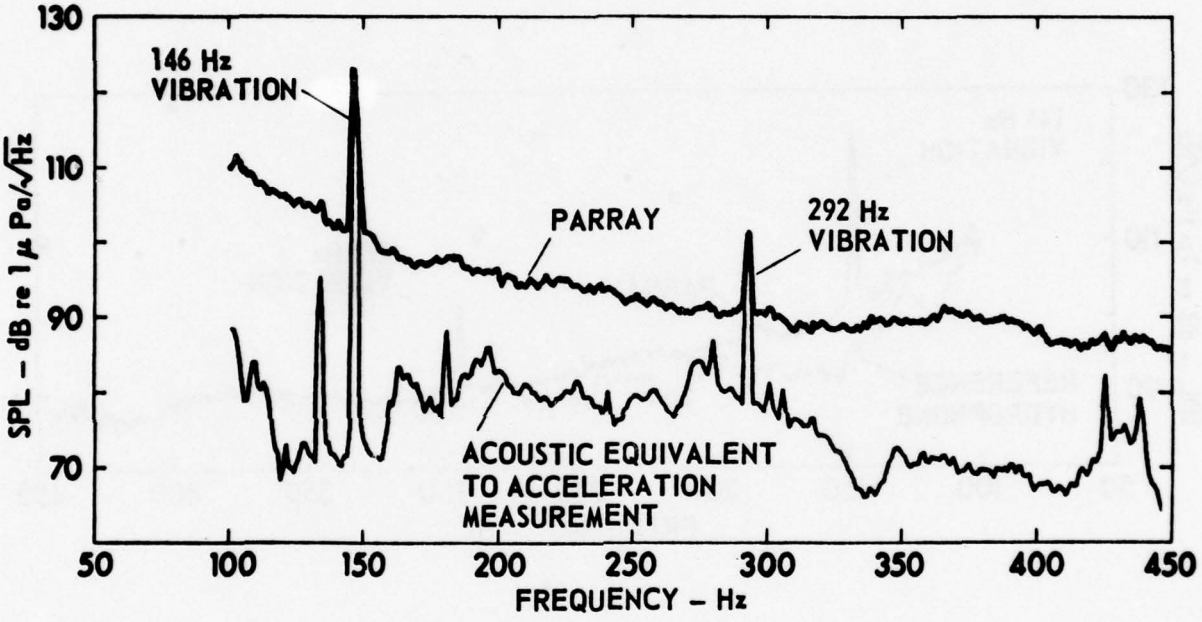

FIGURE 27
COMPARISON OF PARRAY OUTPUT WITH ACOUSTIC EQUIVALENT TO ACCELERATION MEASUREMENT

ARL:UT
AS-78-554-S
CRR-GA
3-23-78

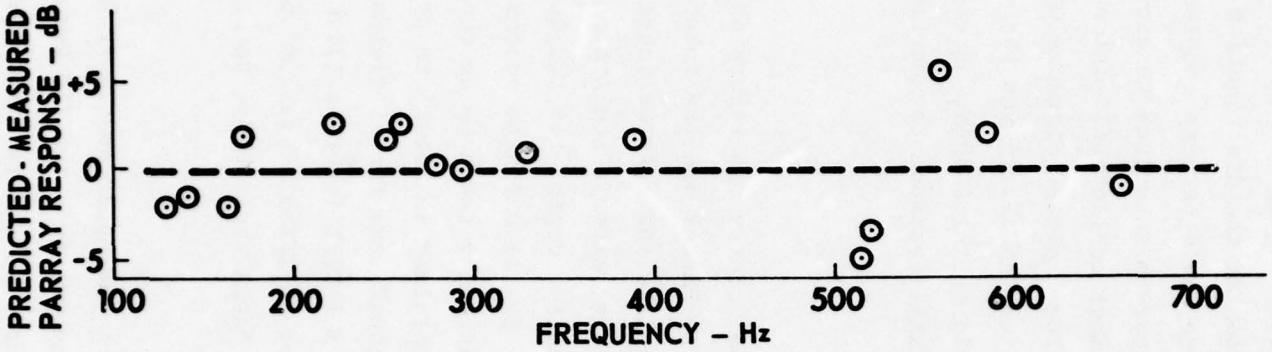

FIGURE 28
COMPARISON OF THEORETICAL AND EXPERIMENTAL RESPONSE OF PARRAY TO VIBRATION

ARL:UT
AS-77-1400-P
CRR-GA
12-8-77

C. Measurements with 11 m PARRAY on Submerged Rotator

The response of the PARRAY to platform noise is critical in mobile sonar applications. A description of the distribution of contaminating noise in both frequency and space would be very complex. Also, the distribution of contaminating sources is unique to each platform. However, a parameter common to most mobile applications is the distance to interfering noise sources. The expected distance would be quite small, especially for a submarine mounted PARRAY. Since the expected noise sources would be in the nearfield of the PARRAY, an experiment was performed to investigate the PARRAY response to nearfield noise sources.

1. System Description

An existing submerged rotator was refurbished and instrumented with an 11 m PARRAY at LTTS. The PARRAY and the rotator are shown in Fig. 29. When installed in the lake the rotator rests on a flotation collar moored above the lake floor; after installation the rotator is winched down and held at the desired depth, for the duration of the experiment, by a 3-point moor. The 11 m PARRAY system, as shown in the block diagram of Fig. 30, is basically the same as that used for the 340 m PARRAY, which has been explained in detail in previous reports.[18-23] The transducers for the 11 m PARRAY were two 19-element transducers, the same as had been used on the 5 m PARRAY (section III.C.) An omni-directional reference hydrophone (NRL/USRD Type F50) was installed on the rotator directly below the PARRAY hydrophone to measure the ambient noise.

During the experiment the upper and lower sidebands of the receiver preprocessor and the output from the F50 were recorded on the DAPS. Simultaneous realtime plots of the received spectrum were made using the Sanders spectrum analyzer.

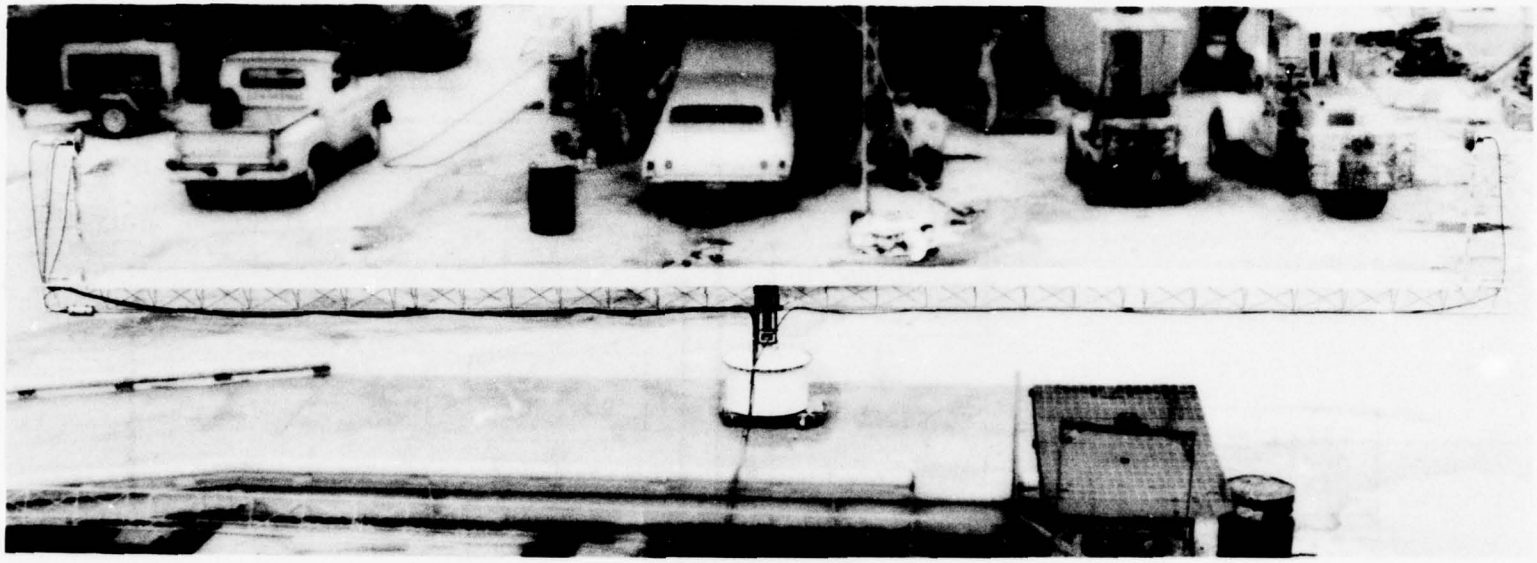

FIGURE 29
PHOTOGRAPH OF ROTATOR AND PARRAY BEFORE SUBMERGENCE

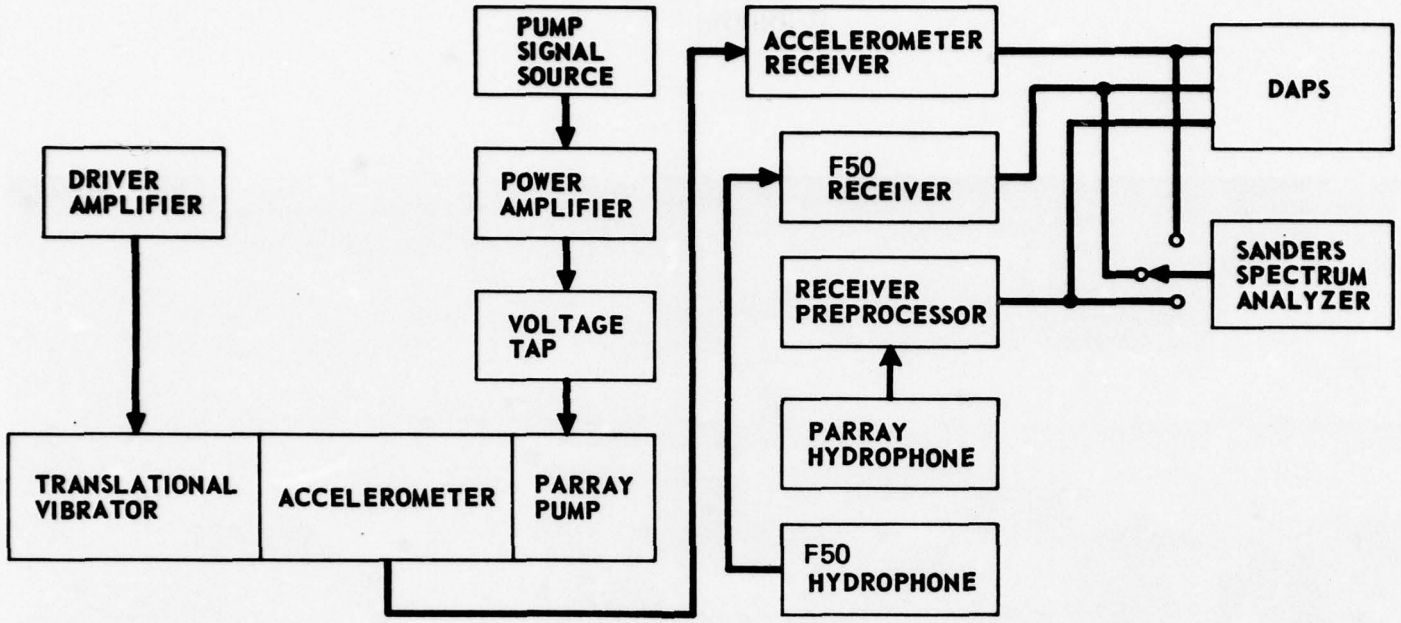

FIGURE 30
BLOCK DIAGRAM OF 11 m PARRAY ON SUBMERGED ROTATOR

ARL:UT
AS-78-610
DFR-GA
4-10-78

2. Response of the PARRAY to Nearfield Noise

The response of the PARRAY to localized bandlimited noise was measured using several sources at different locations. To measure the envelope of the PARRAY response instead of the interference patterns from a single tone, a bandlimited white noise generator was used to drive an NRL/USRD Type J9 transducer as the source of the nearfield noise. The J9 transducer was mounted in four different locations as indicated in Fig. 31: (1) directly beneath the hydrophone (H); (2) midway between the pump and hydrophone and 1 m below the PARRAY axis (M); (3) beneath the pump (P); (4) and midway between the pump and hydrophone but near the axis of the PARRAY (MT). Simultaneous with the nearfield measurements, four acoustic reference tones were transmitted from a source in the farfield and on the axis of the PARRAY. These tones serve as an acoustic calibration between the PARRAY and the reference hydrophone F50.

The response of the PARRAY was measured with a 10 Hz bandlimited source at several frequencies and at the four locations previously described. As shown in Fig. 32, the 10 Hz bandlimited noise, centered at a frequency of 165 Hz and at location H, produced an output from the PARRAY that was much lower (-27 dB) than the value measured from the reference hydrophone. The response of the PARRAY was again measured but with a 10 Hz bandlimited noise centered at a frequency of 650 Hz, as illustrated in Fig. 33. The response from the PARRAY was 34 dB below that of the reference hydrophone. The acoustic reference tones in each case showed reasonable agreement. The nearfield noise rejection for each location as a function of frequency is given in Fig. 34. There are several important observations that can be made from the experimental measurements:

(1) the nearfield noise is rejected from 10 to 40 dB depending on the location and frequency of the source,
(2) the nearfield noise is rejected more at higher frequencies than at lower frequencies,

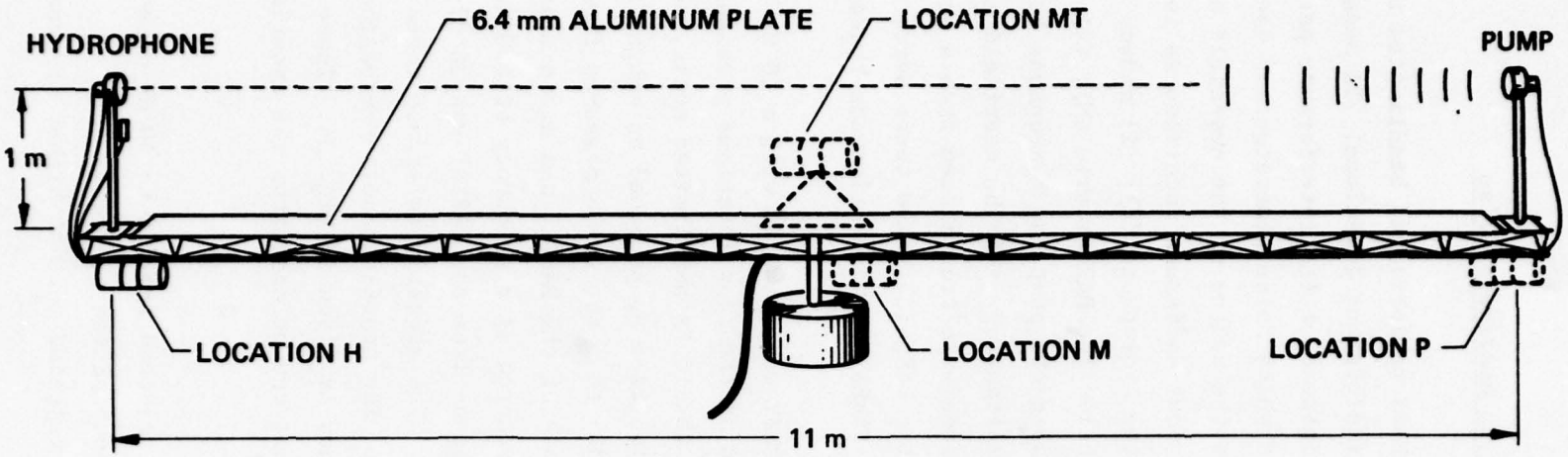

FIGURE 31
LOCATIONS FOR NEARFIELD NOISE REJECTION EXPERIMENT
11 m PARRAY ON SUBMERGED ROTATOR AT LTTS

ARL: UT
AS-78-765
DFR-GA
5-15-78

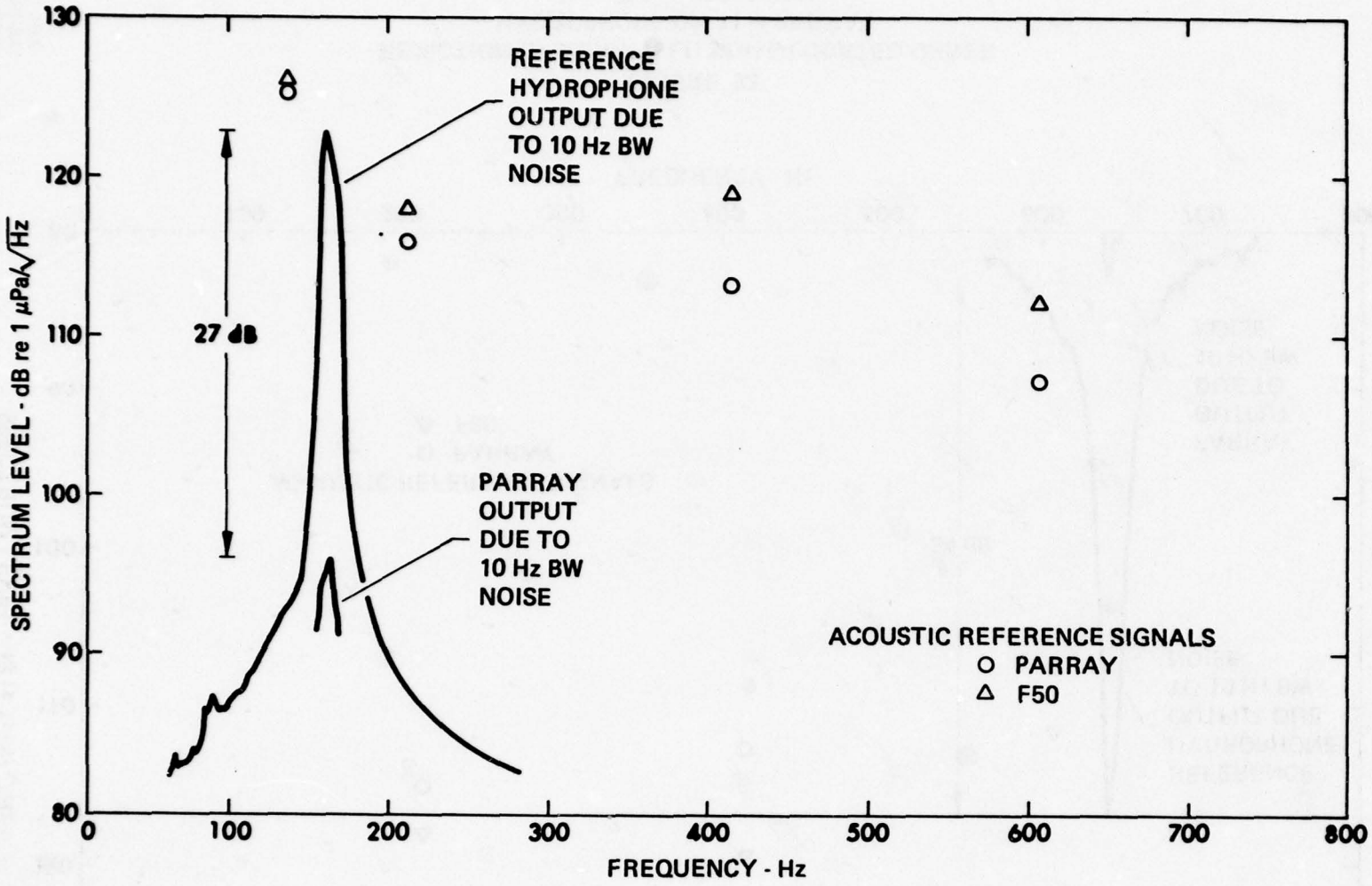

FIGURE 32
REJECTION OF NEARFIELD NOISE LOCATED UNDER HYDROPHONE ON 11 m PARRAY
F_n = 165 Hz (10 Hz BW)

ARL: UT
AS-78-766
DFR-GA
5-15-78

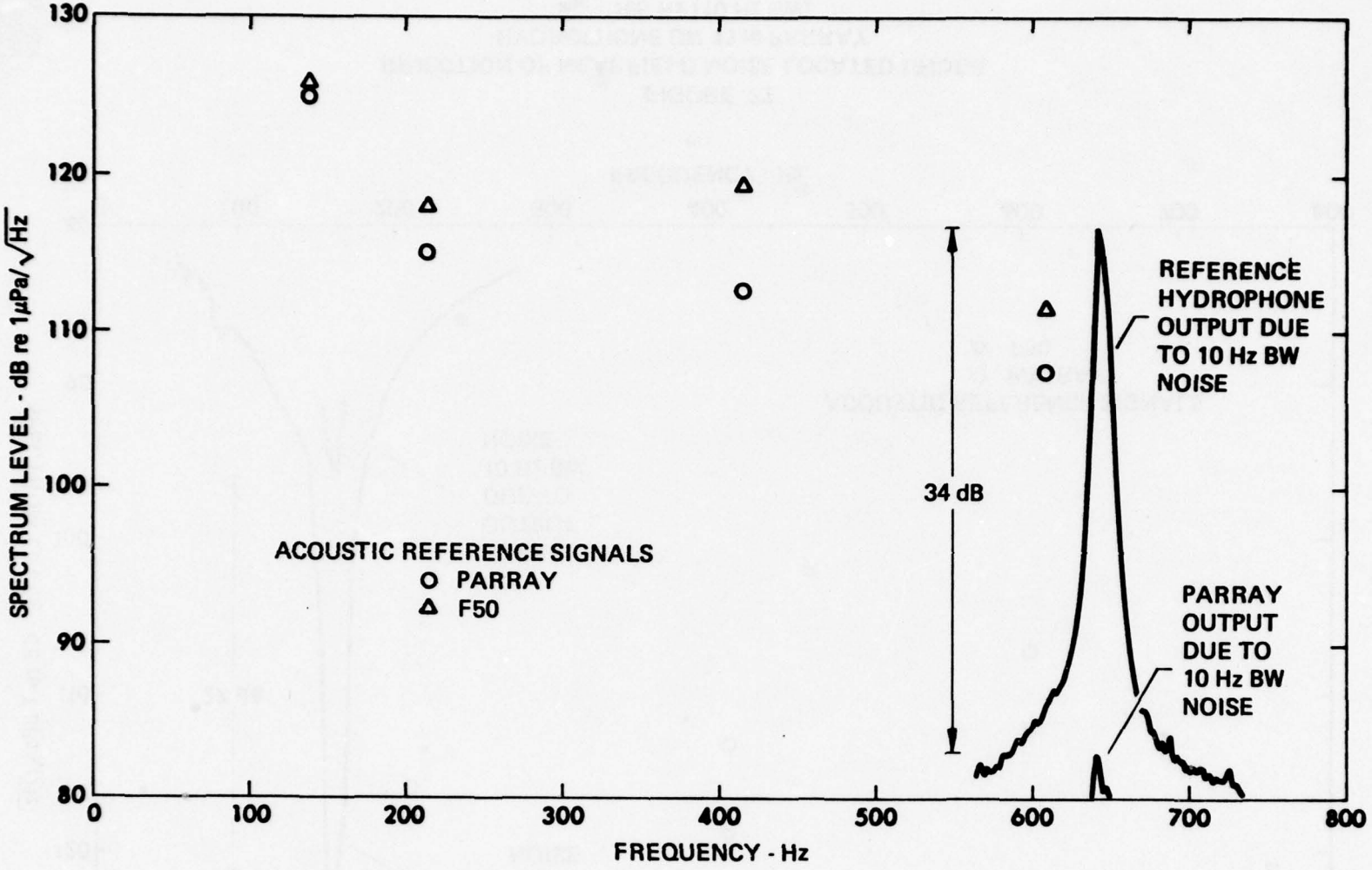

ARL: UT
AS-78-767
DFR-GA
5-15-78

FIGURE 33
REJECTION OF NEARFIELD NOISE LOCATED UNDER HYDROPHONE ON 11 m PARRAY
F_n = 650 Hz (10 Hz BW)

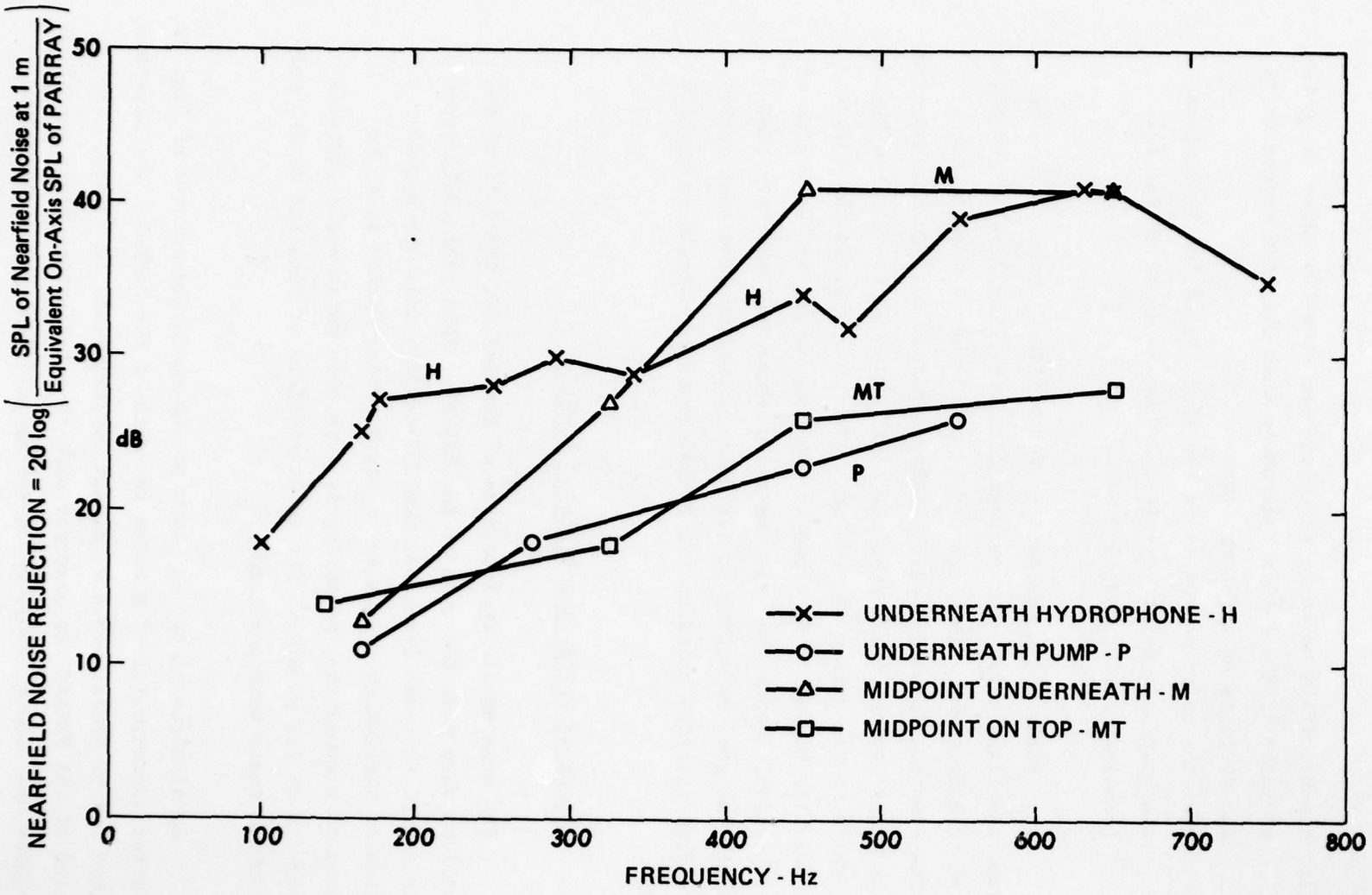

FIGURE 34
NEARFIELD NOISE REJECTION OF 11 m PARRAY ON SUBMERGED ROTATOR

ARL: UT
AS-78-788
DFR-GA
5-15-78

(3) the nearfield noise is rejected more when the noise is in the vicinity of the PARRAY hydrophone than when the source is in the vicinity of the pump, and

(4) when the noise source is in the vicinity of the hydrophone the nearfield noise is rejected from 25 to 40 dB for frequencies greater than 150 Hz.

In conclusion, measurements of the PARRAY response to some localized nearfield noise sources were obtained. The level of rejection was high in many cases. The trend in rejection was favorable for a submarine mounted, forward looking PARRAY application. In this application the higher noise levels from the platform would be near the hydrophone, which is the region of greatest rejection, whereas the quieter levels near the bow would be close to the pump, which is the region of least rejection. Hence the experimental measurements indicate that the PARRAY has good rejection to nearfield noise and thus that interference from platform noise on the PARRAY operation should be greatly reduced.

3. Effect of Reflecting Plate on PARRAY

For some mobile applications of the PARRAY, the hull of the ship will be very near the axis of the PARRAY. This hull could cause reflections of the pump beam that would interfere with the normal operation of the PARRAY. Because an experimental PARRAY is to be evaluated on a submarine, measurements were made which would indicate the severity of the problem. Due to constraints of time and funds, only very limited tests were performed.

An aluminum plate, as shown on the submerged rotator of Fig. 29, was mounted approximately 1 m below the axis of the PARRAY. The aluminum plate was 6.4 mm thick, 0.6 m wide, and approximately 11 m long. The operation of the PARRAY was observed with this reflecting plate installed. A reference hydrophone (F50), which was mounted just below the PARRAY

hydrophone, was monitored simultaneously with the PARRAY output. The responses of the PARRAY and the reference hydrophone are given in Fig. 35. The output of the PARRAY reasonably matched the response of the reference hydrophone. The average value of the sensitivity of the PARRAY was very near the theoretically predicted value. Hence a reflecting plate located near the axis of the PARRAY seemed to have no gross effects on the PARRAY sensitivity.

The effect of the plate on the beam pattern of the PARRAY was also measured. An experimental beam pattern for the 11 m PARRAY for a signal frequency of 1645 Hz is shown in Fig. 36. The pattern exhibits the expected sidelobe structure and has the expected main lobe 3 dB beamwidth. The lobes are greater than 30 dB down on the backside of the pattern. The limitations on obtaining further reduction in the measured sidelobes are due to the S/N available in the analysis bandwidth.

A theoretical beam pattern for a pump-hydrophone separation of 11 m and a signal frequency of 1645 Hz was computed using Eq. (1) and is shown in Fig. 37.

A comparison of the measured and theoretical beam patterns is shown in Fig. 38. The overall agreement is very good. The sidelobe levels of the measured pattern show good agreement with the theoretical sidelobe levels in the region 30° to 90° on either side of the (maximum response) axis, where there is a high S/N. The main lobe of the measured pattern is in good agreement with the theoretical pattern except for a slight skew to the left. This is probably due to a slight misalignment of the PARRAY pump and hydrophone transducers. This skewing effect was observed in some earlier experiments at ARL:UT.[12]

In summary, the PARRAY beam pattern did not show unusual effects due to the presence of a reflecting plate. The response of the experimental PARRAY at 1645 Hz was typical of that obtained at other frequencies. The slight deviations from theoretical predictions have

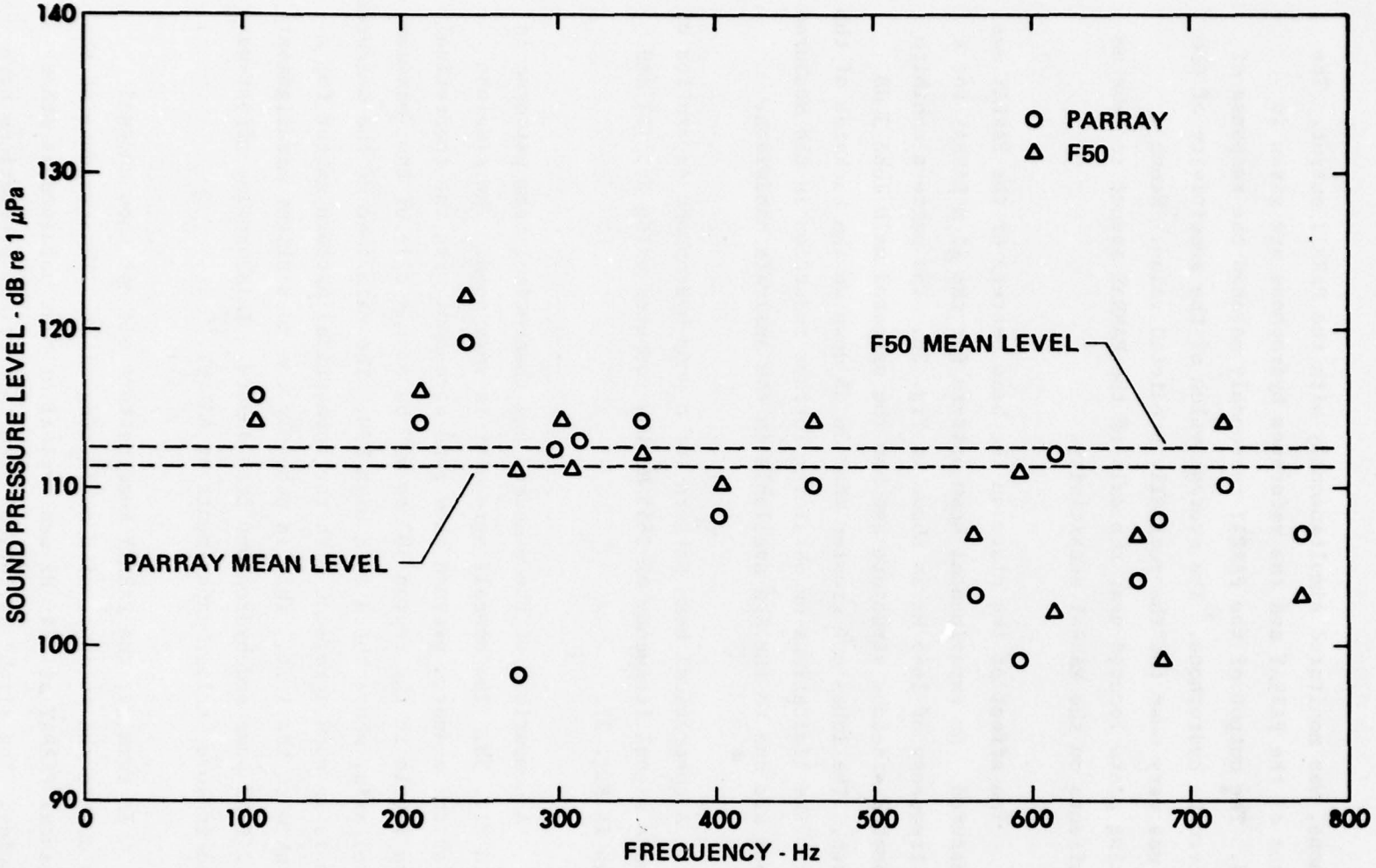

ARL: UT
AS-78-769
DFR-GA
5-15-78

FIGURE 35
COMPARISON OF 11 m PARRAY OUTPUT ON SUBMERGED ROTATOR TO REFERENCE HYDROPHONE OUTPUT

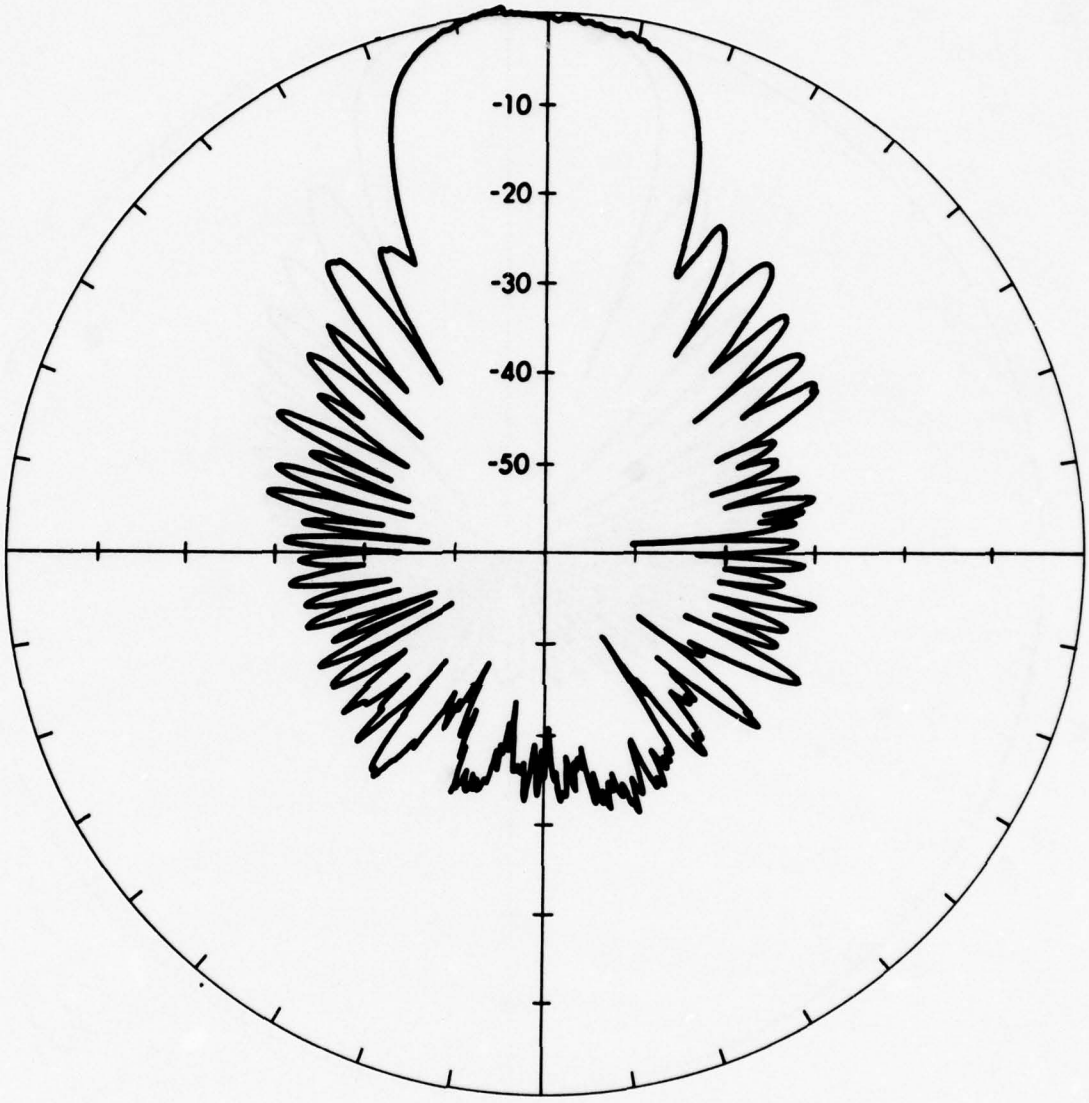

FIGURE 36
EXPERIMENTAL BEAM PATTERN FOR 11 m PARRAY
F_s = 1645 Hz

ARL: UT
AS-78-770
DFR-GA
5-15-78

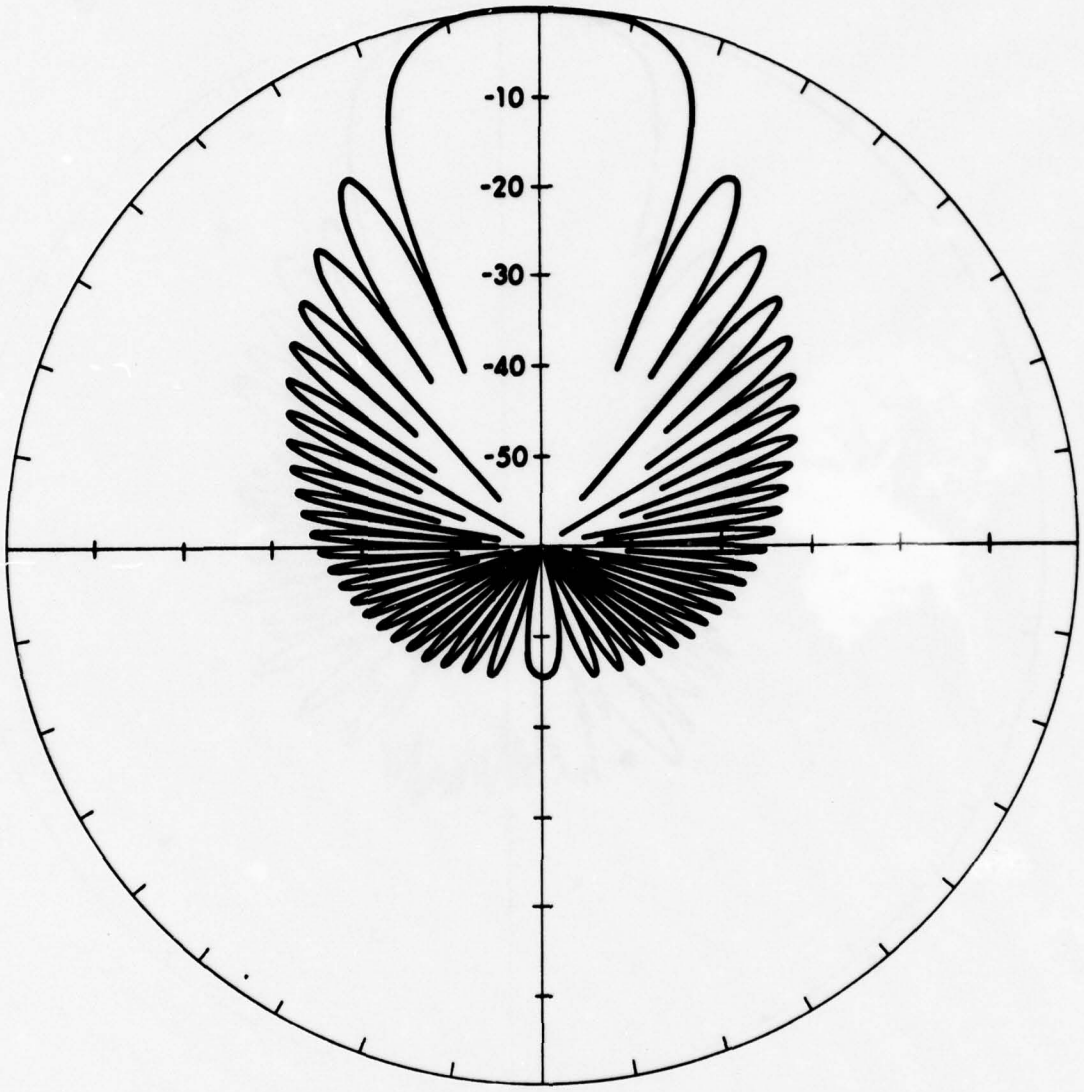

FIGURE 37
THEORETICAL BEAM PATTERN FOR 11 m PARRAY
F_s = 1645 Hz

ARL: UT
AS-78-771
DFR-GA
5-15-78

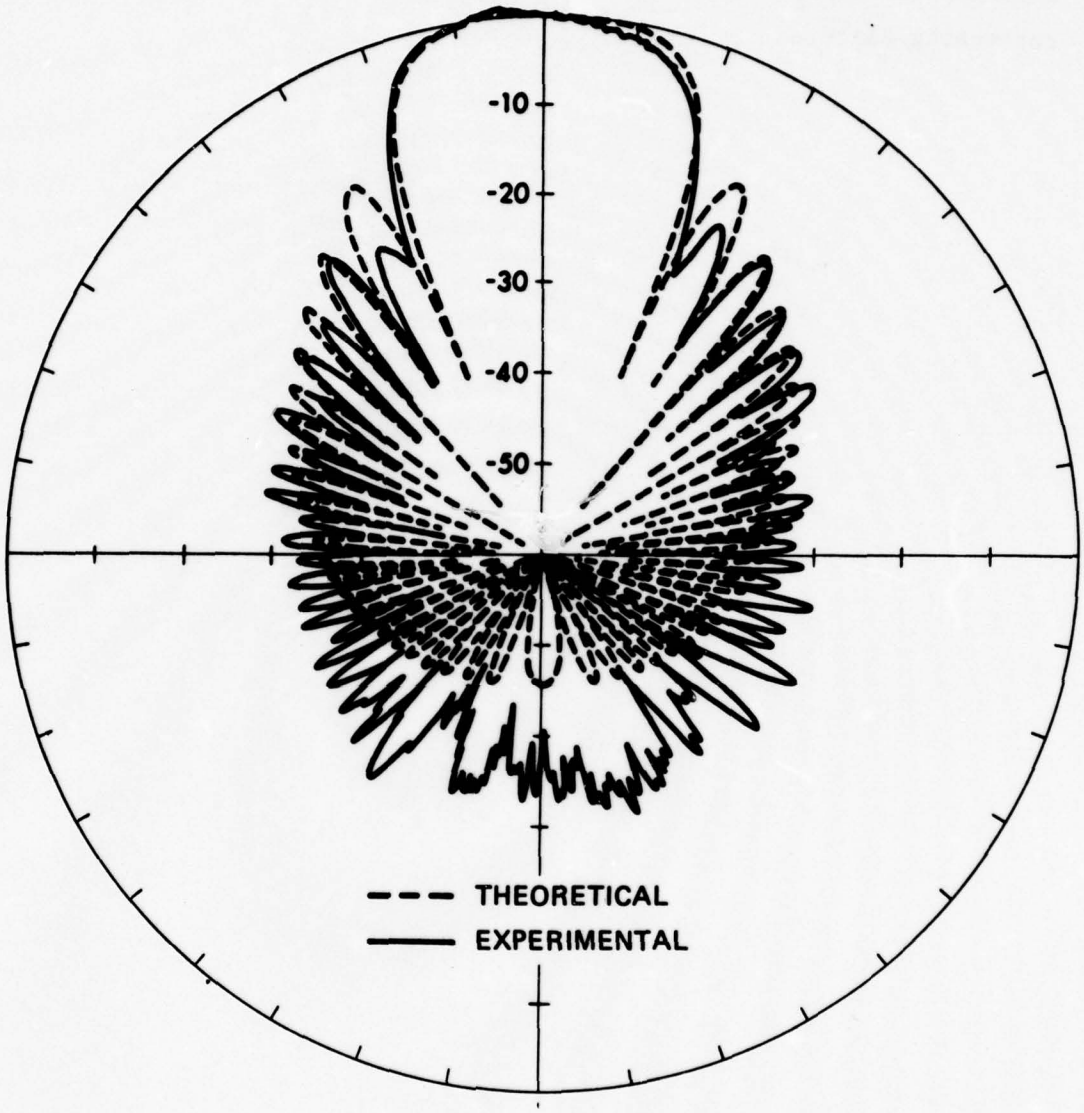

FIGURE 38
COMPARISON OF THEORETICAL AND EXPERIMENTAL BEAM PATTERNS FOR 11 m PARRAY AT 1645 Hz

ARL: UT
AS-78-772
DFR-GA
5-15-78

either been observed in previous experiments or they are entirely within experimental error and cannot be attributed to the presence of a reflecting plate.

IV. HARDWARE DEVELOPMENT AND EVALUATION

A. Receiver Preprocessor

A receiver preprocessor was constructed for use in the experimental PARRAY tested by ARL:UT at LTTS. The function of the receiver preprocessor is to suppress the high level carrier while simultaneously amplifying the low level, near-sideband signals.

A block diagram of the band elimination preprocessor is shown in Fig. 39. The signal from the hydrophone is connected directly to the input of a band elimination crystal filter, which is followed by a 20 dB gain low noise preamplifier. Two subsequent stages of band elimination crystal filtering and variable gain amplification provide greater than 120 dB of carrier suppression. The characteristics of the band elimination crystal filters are illustrated by the test data of a typical filter shown in Fig. 40. The double sideband suppressed carrier signal from the last filter and amplifier stage is then coupled into a pair of balanced modulators operating in phase quadrature. One of several reference signals may be used in the phase locked loop oscillator which provides the phase quadrature reference signals to the balanced modulators. Reference signals which may be used are (1) an internal local oscillator, (2) the pump frequency carrier signal from the hydrophone, (3) the pump crystal oscillator source, and (4) an external frequency synthesizer. The signal from each balanced modulator is then low pass filtered and phase shifted by quadrature phase shifters. The signals from the phase shift circuits are summed with appropriate polarities to simultaneously yield the upper and lower sideband signals.

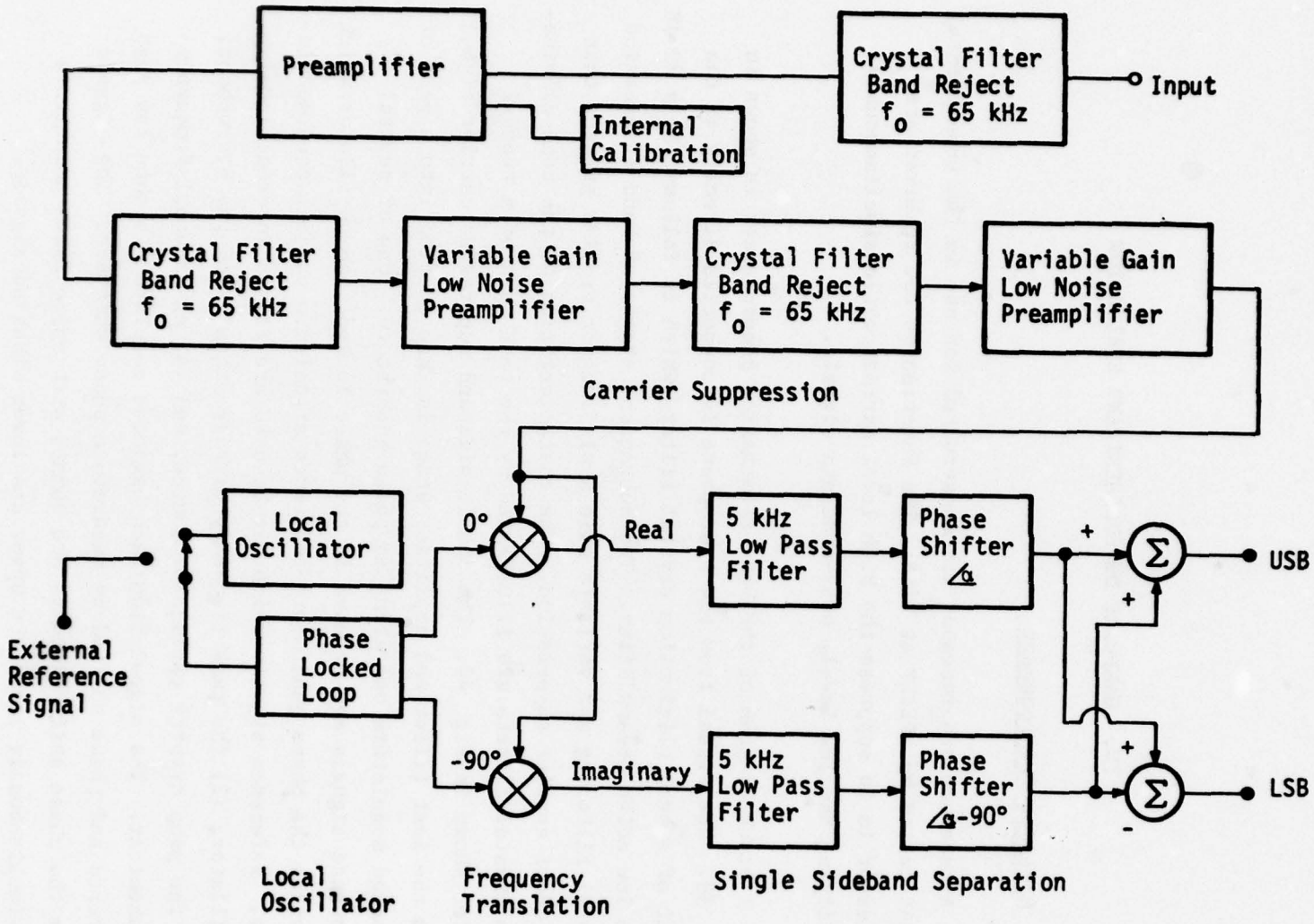

FIGURE 39
BLOCK DIAGRAM OF BAND ELIMINATION RECEIVER PREPROCESSOR

AS-76-2313
DFR-0231-0

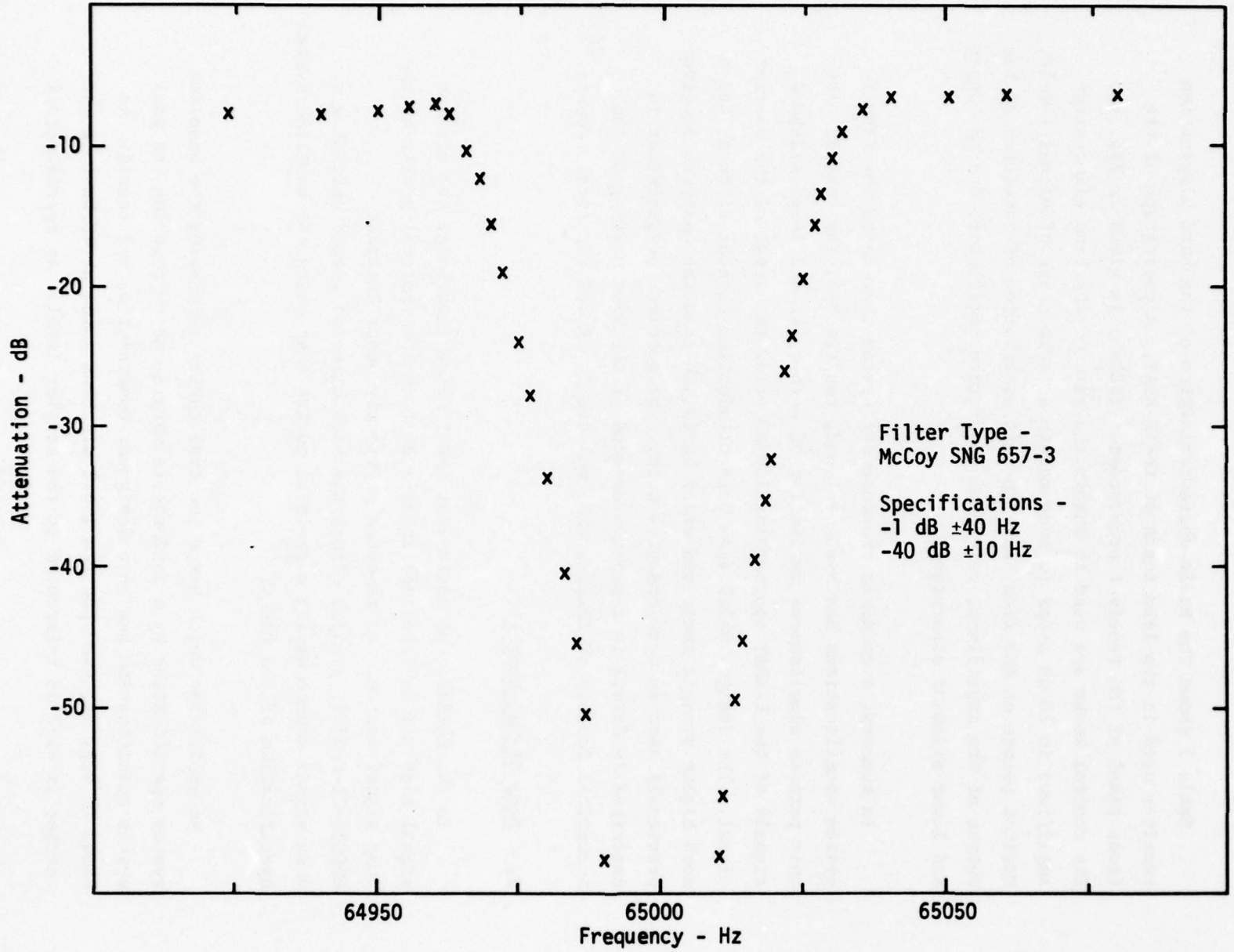

FIGURE 40
MEASURED RESPONSE OF BAND ELIMINATION FILTER

AS-76-2314
DFR-0231-0

Table I shows the basic characterisitics of the band elimination receiver used in the lake tests of the PARRAY. A photograph of the front panel of the receiver preprocessor (BER-2) is given in Fig. 41. The control knobs are used to change the gain of the band elimination amplifiers in 10 dB steps to accommodate a large range of signal levels. Monitor points on the front panel permit observation of waveforms at the output of the amplifiers, reference quadrature oscillator, and the upper and lower sideband separators.

In summary, a receiver preprocessor system that meets the PARRAY system specifications has been designed, constructed, and tested. The unit permits simultaneous monitoring of both upper and lower sideband signals of the PARRAY approaching 180 dB below the level of the carrier signal. The design, which uses band elimination crystal filters, has a much higher dynamic range and wider bandwidth than the bandpass receiver previously used in developmental work. The receiver preprocessor is described in detail in a paper presented at the 92nd Meeting of the Acoustical Society of America and included in ARL:UT technical reports.[28,16]

B. Pump Signal Source

In the PARRAY, the equivalent input noise (and hence the minimum signal that can be detected) is dependent on the spectral purity of the pump signal source. As reported previously under Contract N00039-75-C-0207, a major effort has been directed toward obtaining a pump signal source having a spectral purity that meets the baseline system specification of the PARRAY.[17]

An oscillator which has a spectral purity surpassing the baseline system specification by a comfortable margin and approaching the goal system specification has been designed, constructed, and tested. As shown in Fig. 42, the spectrum level sideband noise at 40 Hz from the carrier is -157 dB referenced to the carrier level. At approximately

TABLE I

CHARACTERISTICS OF THE BAND ELIMINATION RECEIVER (BER 2)

Number of band elimination crystal filters	3
Single sideband signal gain	100 dB
Receiving band (for each sideband)	40 Hz to 4 kHz
Noise figure (referenced to 15 kΩ source)	6 dB
Maximum carrier to sideband-noise floor	~180 dB

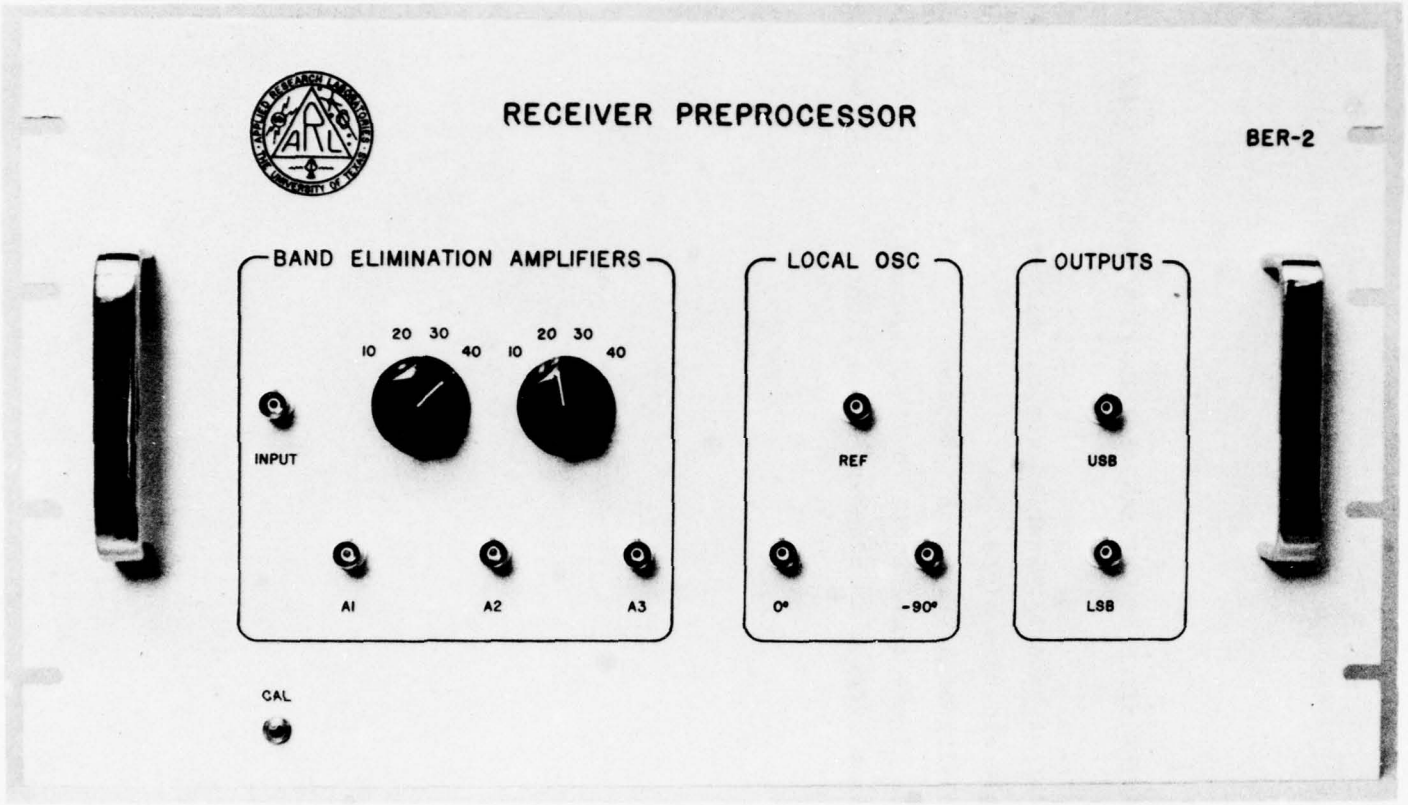

FIGURE 41
PHOTOGRAPH OF THE BAND ELIMINATION RECEIVER PREPROCESSOR (BER-2)

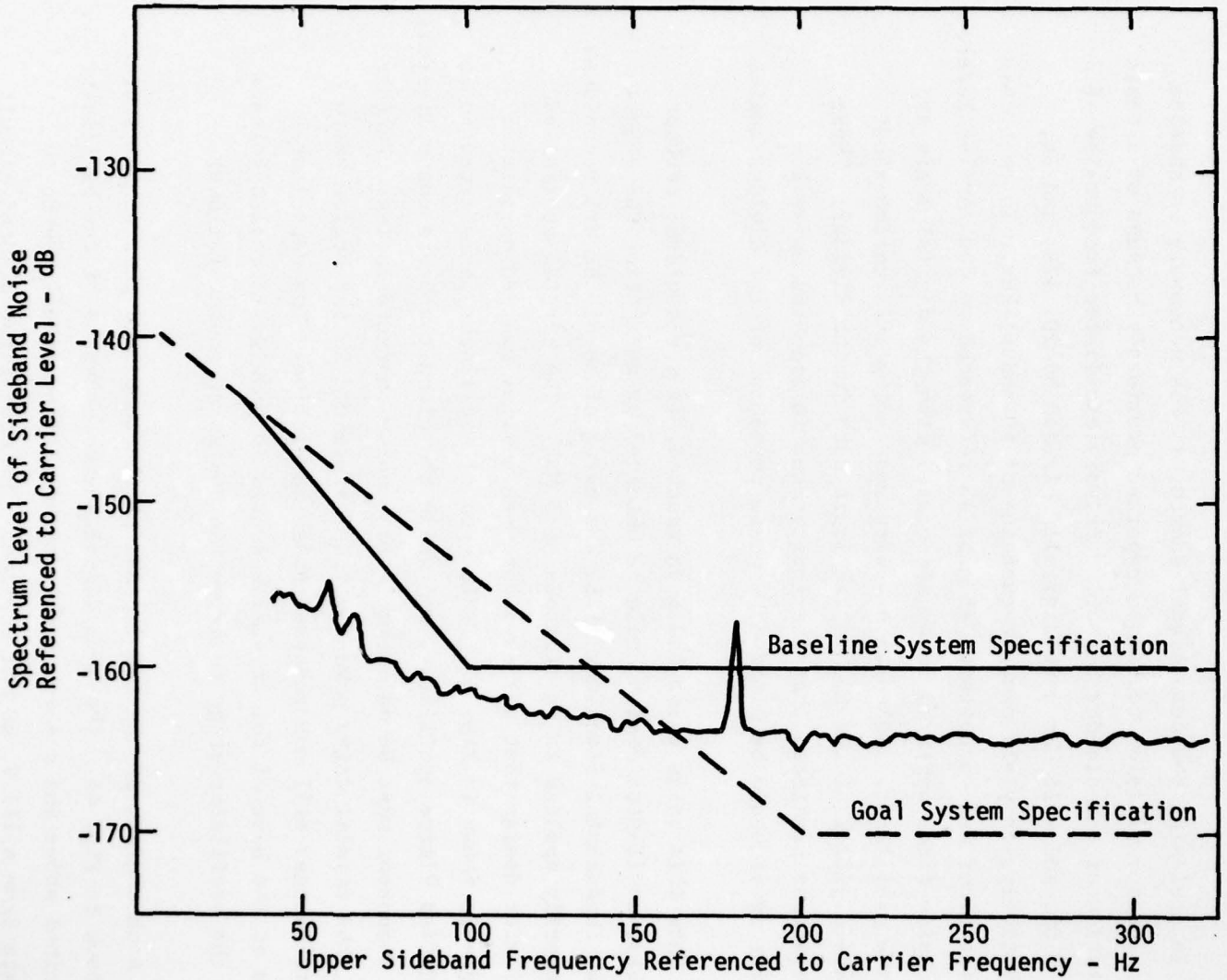

FIGURE 42
SIDEBAND NOISE OUT OF 65 kHz CRYSTAL OSCILLATOR

150 Hz from the carrier, the noise decreases to the noise floor at -164 dB referenced to the carrier level.

In designing the pump signal source, it was necessary to abandon the frequency division technique reported previously because of a basic limitation of the divider logic.[17] Primary oscillator frequencies of 1.2, 7.68, and 4.16 MHz were digitally divided by 20, 128, and 64, respectively, to yield pump frequencies of 60 and 65 kHz. In each case a noise floor was encountered at -152 dB referenced to the carrier level. This noise floor appeared to be associated with the digital logic and not the oscillator. Calculations were made using information about the phase jitter of the high speed logic used in the divider. These calculations predicted that the improvement in sideband noise-to-carrier level could be limited by phase noise out of the divider logic.

Once this noise floor had been reached, it was decided, perhaps the best oscillator design could be obtained by generating the signal at the fundamental frequency of 65 kHz using state-of-the art techniques customarily applied to oscillators at 5 MHz. The crystal controlled oscillator design that was developed--an emitter coupled oscillator design--is shown in Fig. 43. This type of oscillator is referred to as a modified Pierce oscillator, and while the circuit appears uncomplicated, each component must be selected for low noise characteristics. Furthermore, the crystal drive power must be maintained in the region where minute changes will not generate phase modulation. The capacitor shown at the base of the crystal was used to provide increased voltage from the oscillator stage to drive the bootstrap source follower.

A photograph of the front panel of the completed pump signal source is shown in Fig. 44. The pump signal source consists of the oscillator described above and a power supply to permit the signal source to operate from a 117 V, 60 Hz, ac line. The oscillator printed circuit board is mounted inside a metal can, which is then mounted inside the pump signal source chassis. The oscillator can be operated from an

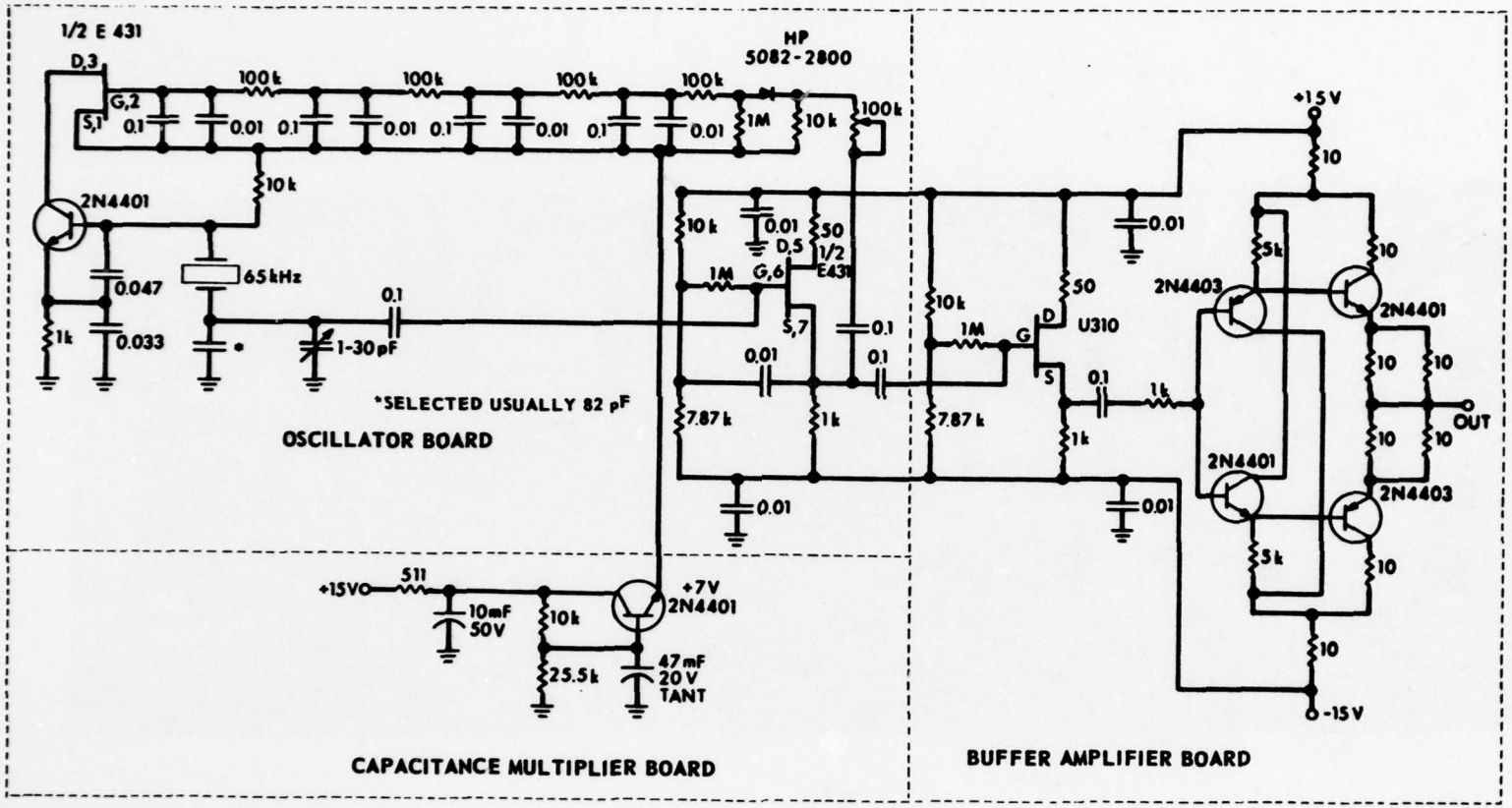

FIGURE 43
SCHEMATIC OF PUMP SIGNAL SOURCE

ARL - UT
AS-77-1071
WSO - RFG
9 - 20 - 77

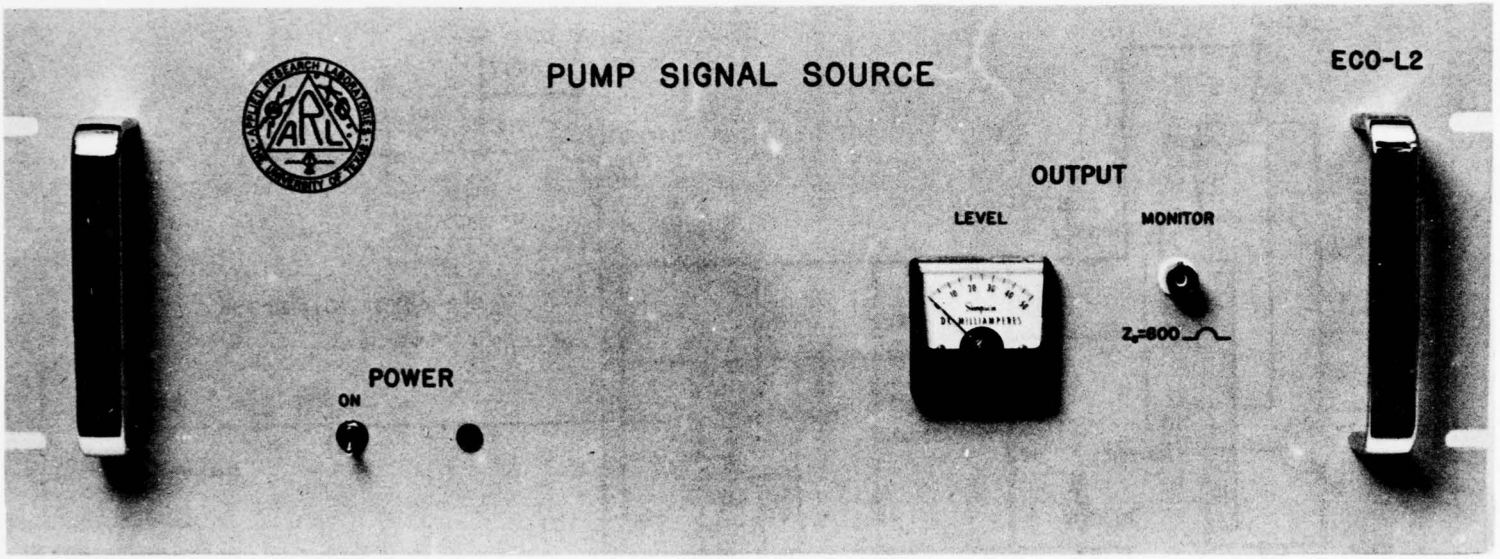

FIGURE 44
FRONT VIEW OF PUMP SIGNAL SOURCE

external dc supply, e.g., batteries, through a connector provided for that purpose on the rear of the chassis.

The pump signal source is described in more detail in a paper presented at the 92nd Meeting of the Acoustical Society of America and included in ARL:UT technical reports.[26,16]

C. Power Amplifier

A 1 kW power amplifier for the PARRAY pump was developed under Contract N00039-75-C-0207. This amplifier, shown in Fig. 45, consists of four 250 W amplifier modules operating in parallel. The amplifier may also be operated in a 500 W capacity by switching out two of the modules. The front panel meter on the amplifier is used to monitor various internal currents and voltages as well as total output power. Monitor lights are provided to indicate fault conditions in each of the individual modules.

For the tests at LTTS, this amplifier was interfaced to an 84-element transducer used as the PARRAY pump. The spectral purity of the amplifier output signal when driving the pump transducer was measured using the band elimination receiver. Sideband noise-to-carrier ratios better than -160 dB were obtained, as shown in Fig. 46. This level of spectral purity is sufficient to make the pump sideband noise contribution to the PARRAY output negligible under most conditions for LTTS tests.

D. Transducers

Six transducers, each consisting of arrays of small individual elements, have been designed and constructed for the lake tests of the PARRAY: two with 19 elements, two with 84 elements, and two with

FIGURE 45
PARRAY 1 kW POWER AMPLIFIER

0207-2

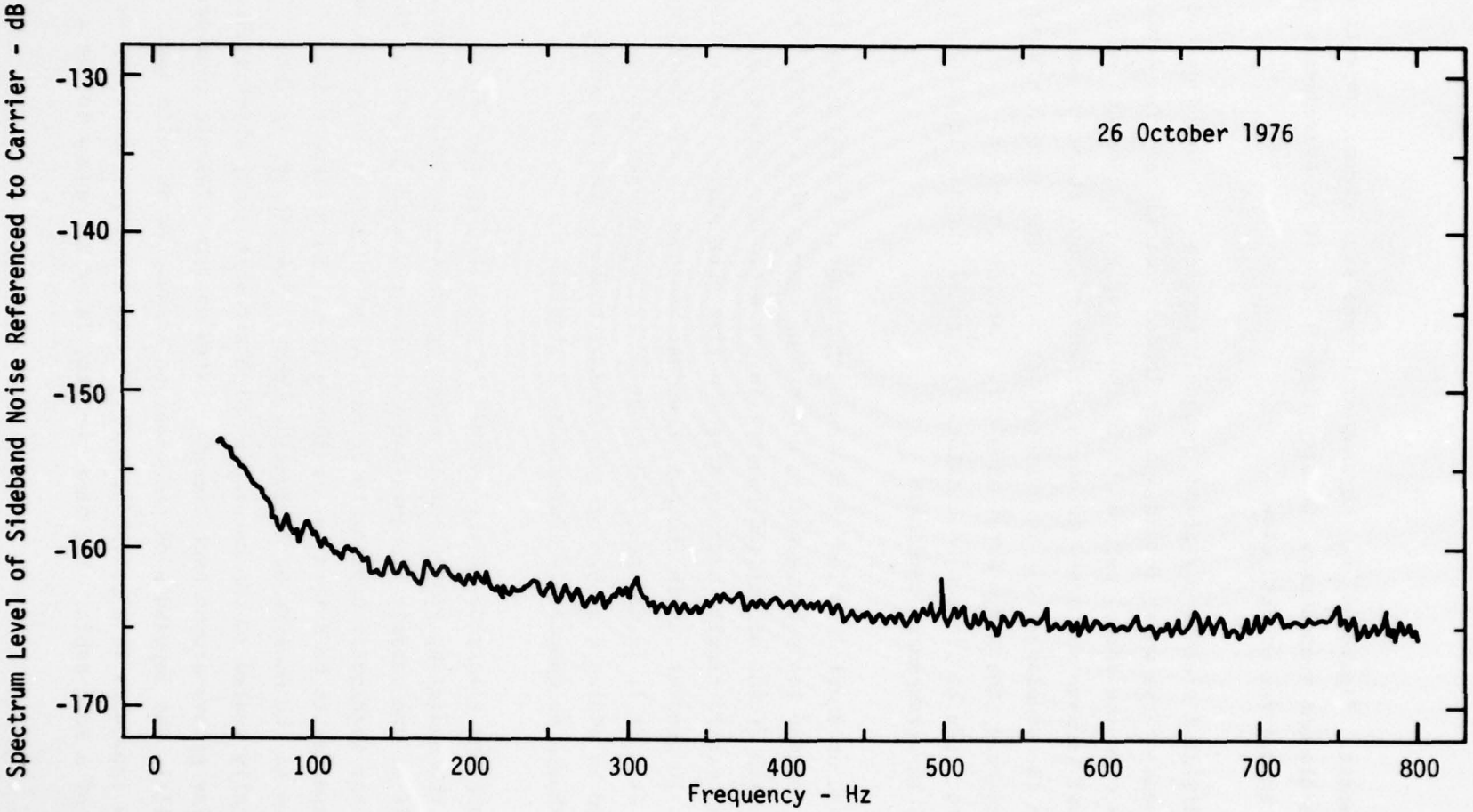

FIGURE 46
PUMP SIDEBAND NOISE INTO TRANSDUCER CABLE

432 elements. Figures 47 and 48 show front and back views, respectively, of an 84-element transducer. Construction of the other transducers is similar except for overall size.

Individual element efficiency probably exceeds 95%, based on the measurement of the water loaded and air loaded admittance. The actual efficiency in the array, referenced to the major lobe, does not reach this level because the array is not a perfect piston; there is more power in the sidelobes than is expected for a uniform piston. However, measurements on the large array show that a source level of 230 dB re 1 μPa at 1 m can be obtained with an electrical input of only 400 W at the transducer terminals.

Based on static loading of the support flange, the design was tested without failure for submergence to a depth of nearly 915 m (3000 ft). The strength of the air filled housing is not a problem, since each mounting hole is totally supported by the flat back plate. The wiring is inset in grooves cut in the main housing, as shown in the photograph in Fig. 48. If it is desired, the front of the transducer can be protected by adding a screen or thin window; however, the radiating piston should be completely immersed in a liquid.

Since one electrode of the ceramic is connected to the water through the radiating piston, it is advantageous to construct the array with half of the ceramic elements mounted with reversed polarity. This permits the transducer housing to be maintained at ground potential and the transducer to be driven as a balanced load. Each element is connected to the housing by conductive epoxy. The element is then hermetically sealed to the housing by high strength epoxy which fills an annular groove around each element. With so many elements connected in parallel, the impedance of the complete transducer is quite low. This low impedance is a potential problem when the array is driven at the end of a long cable. For best results, it is necessary to use a

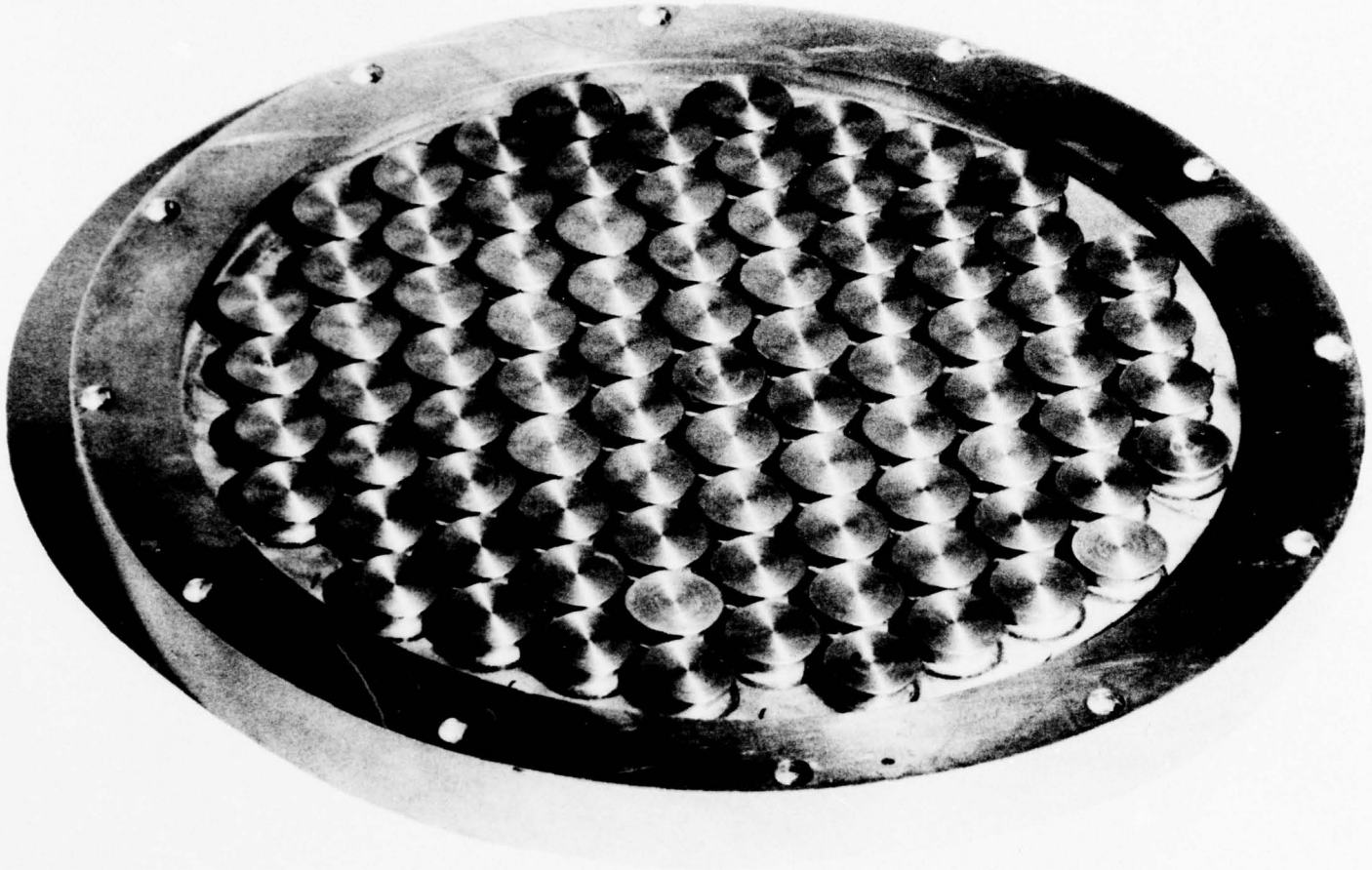

FIGURE 47
FRONT VIEW OF 84-ELEMENT TRANSDUCER

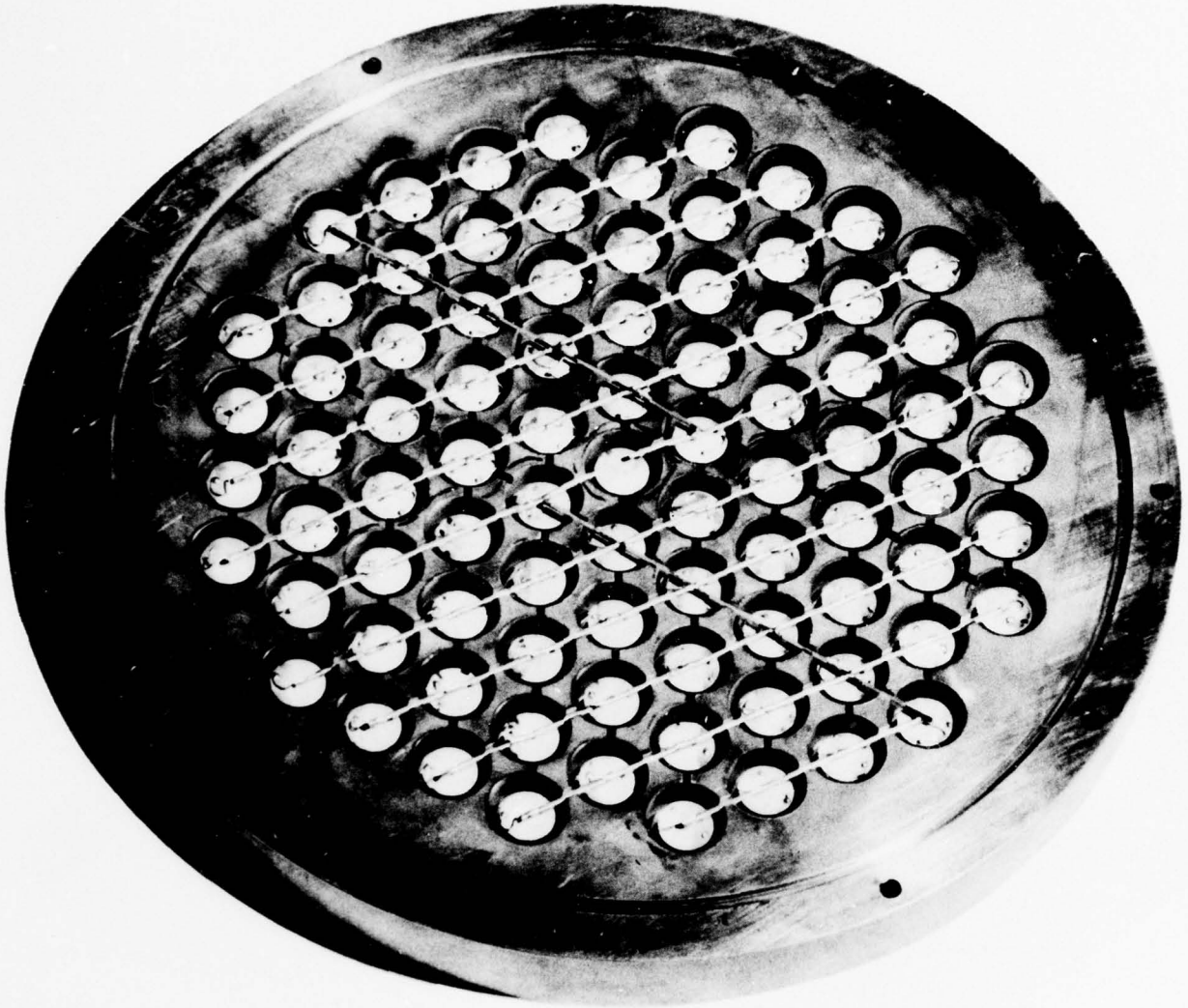

FIGURE 48

BACK VIEW OF 84-ELEMENT TRANSDUCER WITH BACK PLATE REMOVED

transformer and inductive tuning to allow the cable to operate at its characteristic impedance. Even so, there is a significant power loss in the cable.

Characteristics of some of the transducers are summarized in Table II. These characteristics were measured with the transducers on 12.2 m long cables. These same transducers with different cables were used in the experimental PARRAY; their performance was somewhat different from that reflected in Table II because of the different cable lengths used in the various experimental arrangements.

Beam patterns for the 84-element and 432-element arrays are shown in Figs. 49 and 50, respectively. The major lobe directivity and the first few sidelobes appear as expected. The F/B is very good; however, there are some anomalous sidelobes that result from the discrete circular elements being used to approximate a circular piston. The approximation is not as effective for the 432-element array, with its high directivity, as it is for the 84-element array. The calibration shows that the expected improvement in source level was not quite reached; this may be due to the fact that the energy in the anomalous sidelobes is significant.

These transducer elements and arrays are described in greater detail in papers presented at the 92nd Meeting of the Acoustical Society of America and at a specialists meeting of the Underwater Acoustics Group of the Institute of Acoustics.[27,30] Copies of these papers are included in an ARL:UT technical report.[16]

E. Data Acquisition and Processing Subsystem

The purpose and function of the data acquisition and processing subsystem (DAPS) in the PARRAY is to gather data output by the receiver, make a permanent record of those data, and process the data to yield useful characterizations of receiver system performance. The DAPS functions as a part of the PARRAY system in the following ways:

TABLE II

TRANSDUCER CHARACTERISTICS

ARL Transducer No.	Array Size Number of Elements	Directivity Index (dB)	Half Power Beamwidth (deg)	Transmit			Receive		
				Transmit Response μPa/W at 1 m	Shunt Tuning L	Balanced Impedance (Ω)	Open Circuit Sensitivity dB//1 V/μPa	Shunt Tuning L	Balanced Impedance (Ω)
347-1	19	25	10.5	195.7	--	--	--	--	--
348-1	84	29	5.6	199.9	0.9 mH	1337	-161.8	1 mH	1200
348-2	84	29	5.6	--	--	--	--	--	--
349-1	432	36	2.4	205.6	200 μH	172	-162.3	220 μH	195
349-2	432	36	2.4	206.4	135 μH	120	--	--	--

Note: 1. Characteristics measured at a frequency of 65 kHz

2. Transducer responses obtained with 12.2 m of 92 Ω twisted pair Vector cable type B-10113-R-2

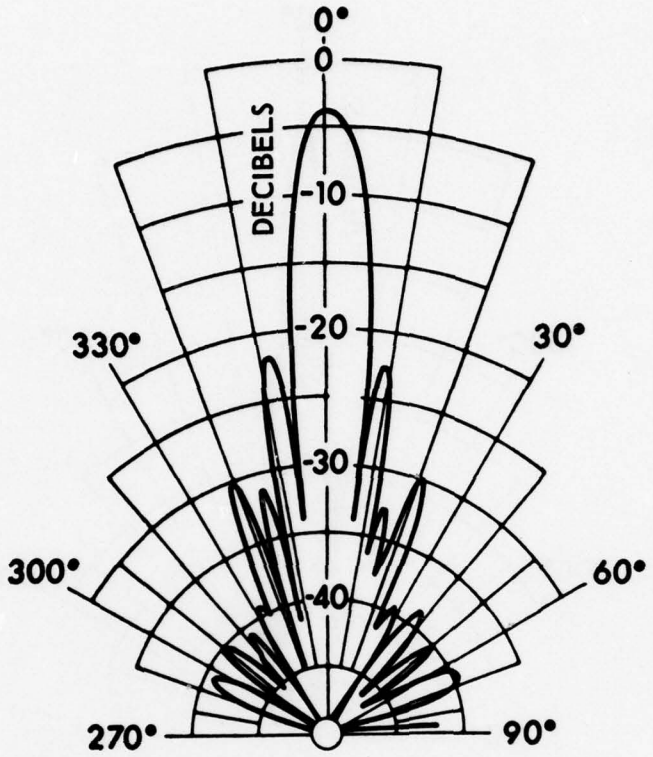

FIGURE 49
POLAR RESPONSE 84-ELEMENT ARRAY

ARL - UT
AS-76-2311-S
MWW - DR
10 - 5 - 76

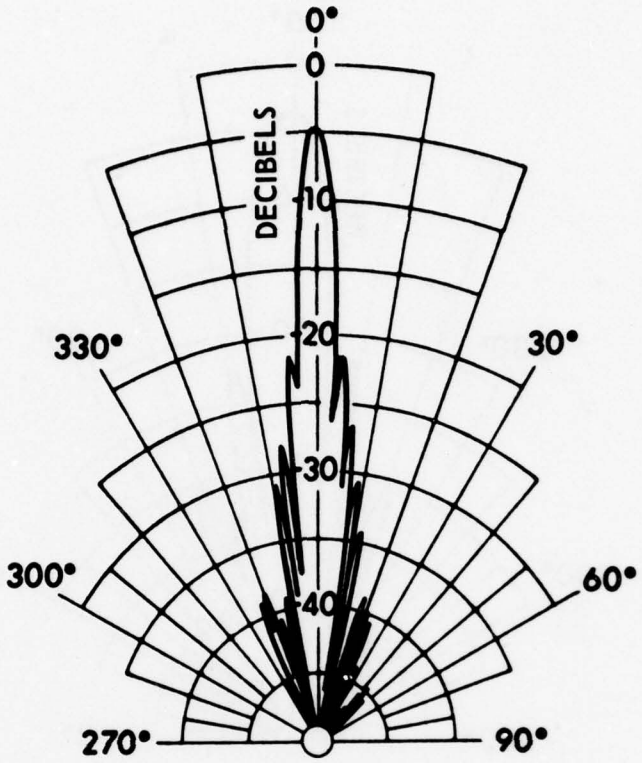

FIGURE 50
POLAR RESPONSE 432-ELEMENT ARRAY

ARL - UT
AS-76-2312-S
MWW - DR
10 - 5 - 76

(1) it serves as a realtime performance monitor to aid in setting up and conducting the various experiments performed during the program,

(2) it provides a permanent record of system performance in a form amenable to further analysis off-line, and

(3) it performs the data processing required to accurately measure the performance parameters of the PARRAY during the various tests.

Because of the wide variety of DAPS functions, the DAPS has been implemented as a minicomputer based, general purpose signal processing system. The advantage of this approach is that the required flexibility is obtained at a reasonable cost. Figure 51 shows the DAPS block diagram and how it is interfaced to the PARRAY receiver preprocessor and other sensors. The primary operating modes of the DAPS are:

(1) realtime monitoring by means of the SA-240 spectrum analyzer and CRT display,

(2) digital recording by the CPU and digital magnetic tape drives, and

(3) playback of the recorded data for detailed analysis both in the CPU and the spectrum analyzer.

The operating system used in the DAPS CPU is RT-11, a realtime, disk based operating system obtained from Digital Equipment Corporation. This system contains a number of support programs which make programming and using the DAPS relatively easy. Most of the applications programs are written in FORTRAN, a widely used high level language.

F. Auxiliary Instrumentation

Some auxiliary instrumentation was designed and constructed to facilitate test and evaluation of the experimental PARRAY.

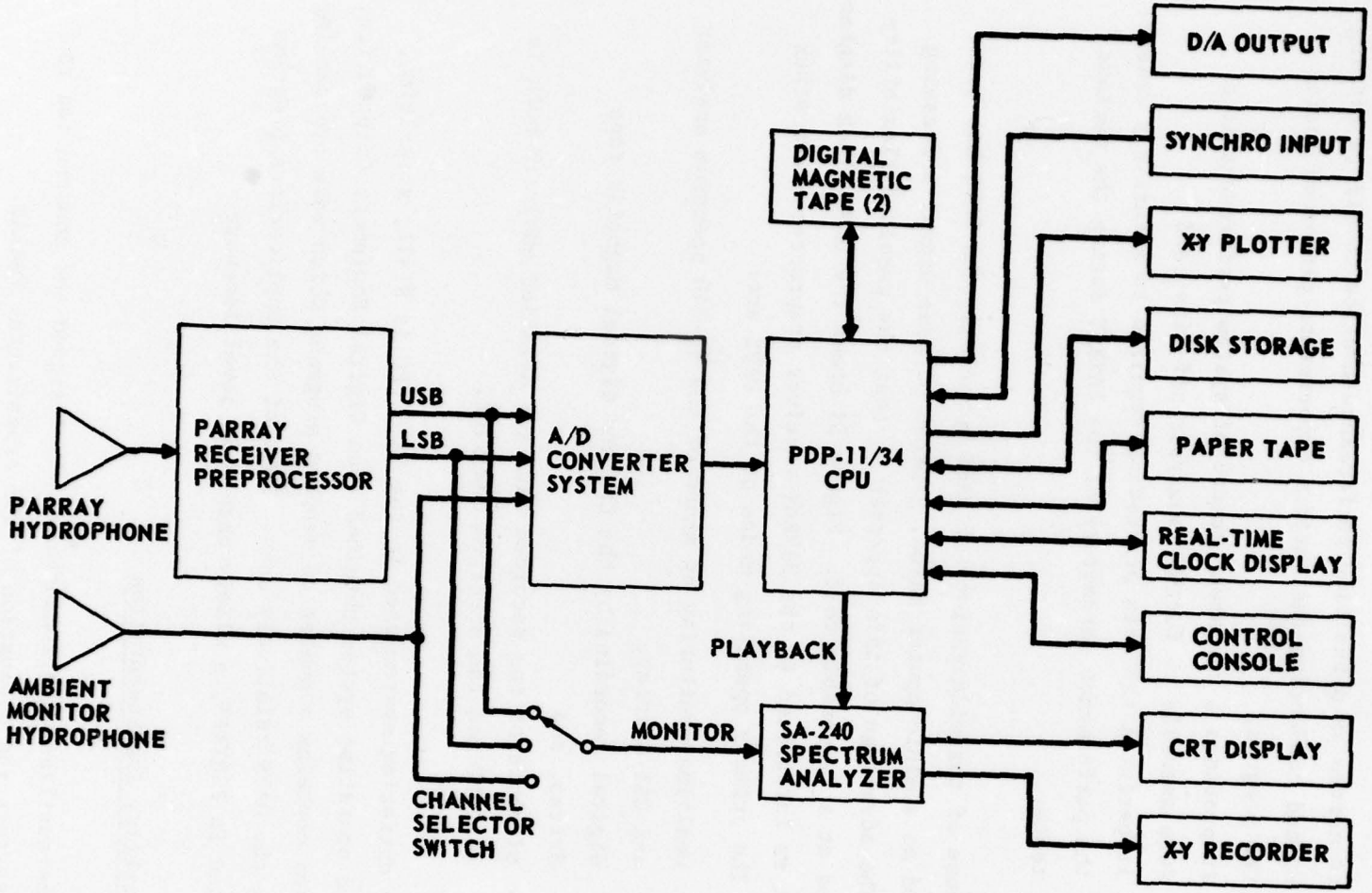

FIGURE 51
DATA ACQUISITION AND PROCESSING SUBSYSTEM - (DAPS)

ARL:UT
AS-78-791
CRR-GA
5-19-78

1. Accelerometers

For certain experiments, accelerometers were mounted on each of the PARRAY transducers to measure their vibration. Any relative motion of the transducers causes a shift in PARRAY pump frequency and therefore generates a PARRAY sideband signal. Measuring the vibration of the transducers helps localize the source of any sideband signals which are not the result of acoustic signals. The accelerometers used in this system measure the force applied to a piezoelectric ceramic element resulting from the acceleration of a mass. The output impedance is capacitive and the low frequency response is determined by the input impedance of the amplifier used to amplify the signal.

An FET input amplifier was used because it has an adequately high input impedance and a low bias current. The Analog Devices 540 was chosen because it had the lowest noise figure at low frequencies for an input impedance of 100 MΩ. Schematic diagrams of the electronics for the accelerometer are shown in Figs. 52 and 53. Signal and power are both on the same twinaxial cable connecting the shore receiver to the pre-amplifier. Since the accelerometer has a high output impedance and is single ended, a very short, low noise cable connects the accelerometer to the preamplifier.

The response of the accelerometer is flat to about 10 kHz, depending upon the particular accelerometer used, and has a resonance peak at some higher frequency, after which the sensitivity decreases. Unfortunately, the accelerometer is still sensitive at 65 kHz, which results in an extremely high level output at that frequency due to the pump signal. This high level signal cannot be effectively filtered electrically due to the capacitive source impedance. Since it is necessary to put the accelerometer in a separate waterproof housing, this housing is also used to mechanically isolate the accelerometer from high frequency signals.

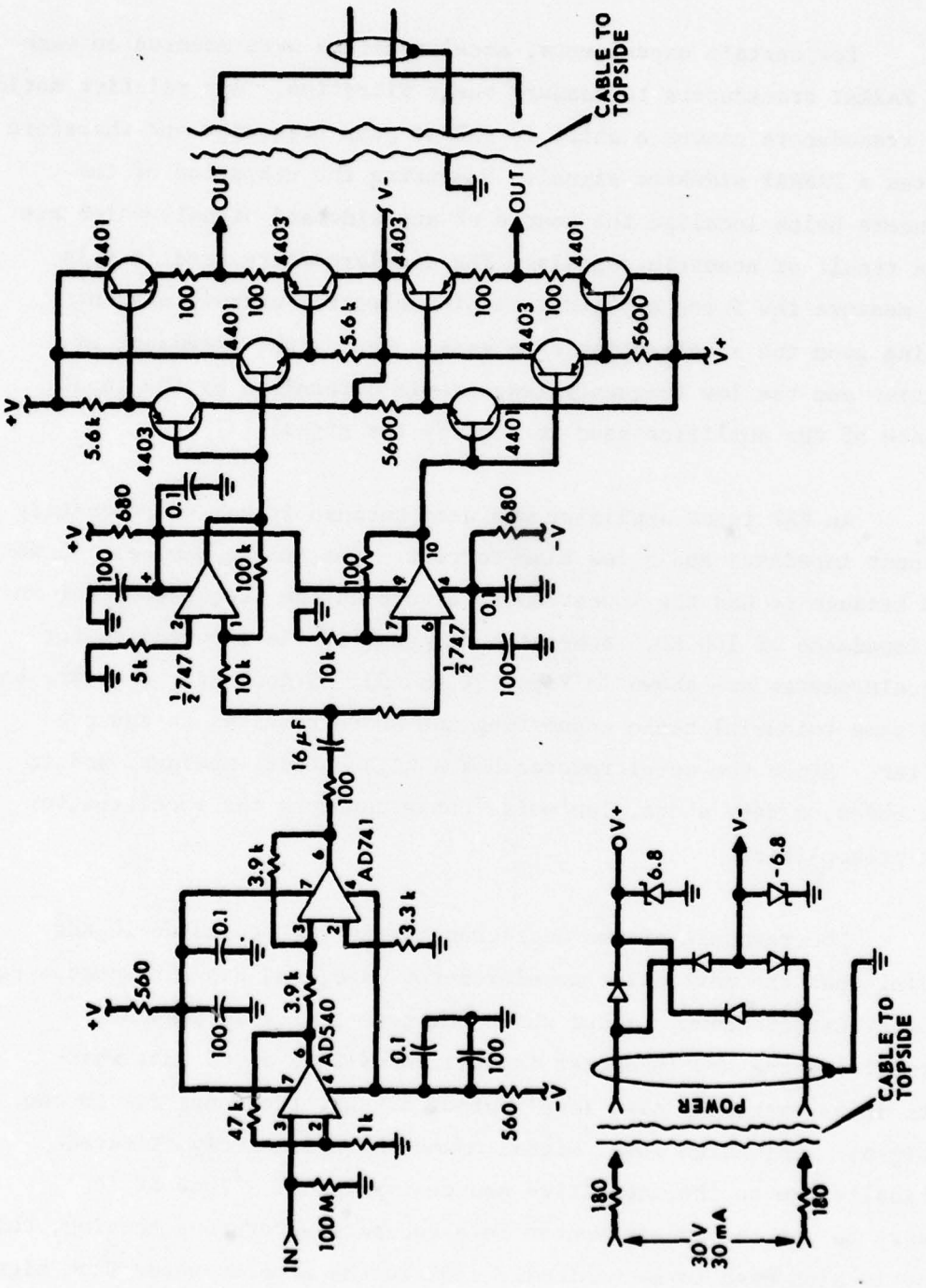

FIGURE 52
ACCELEROMETER PREAMPLIFIER

ARL - UT
AS-77-1230
VEM - GA
10 - 14 - 77

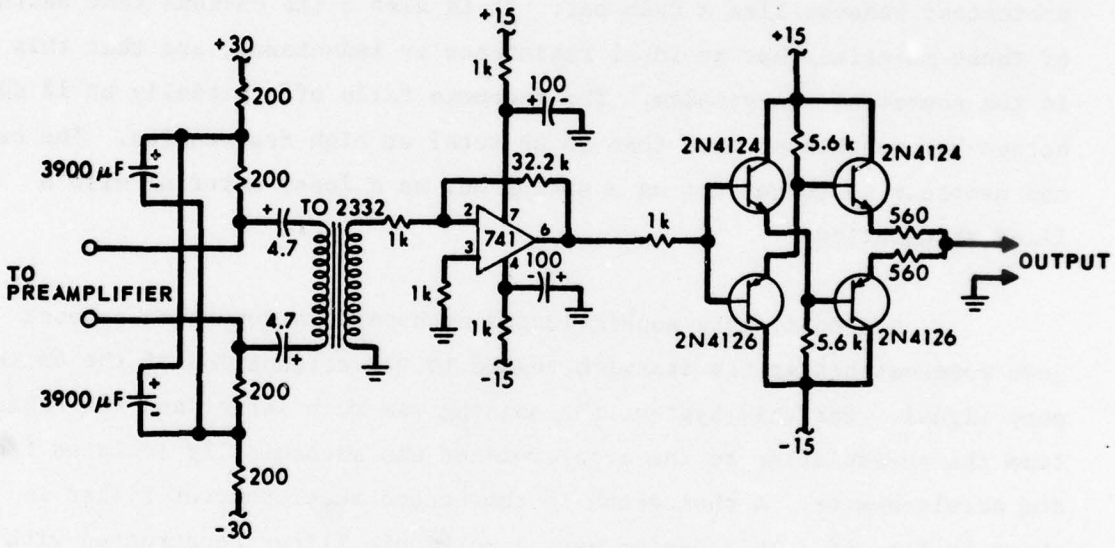

FIGURE 53
ACCELEROMETER RECEIVER

ARL - UT
AS-77-1231
VEM - GA
10 - 14 - 77

Two mechanical isolation devices were developed during this effort. The first, diagrammed in Fig. 54, is essentially a 2-pole mechanical filter. This mechanical isolation circuit behaves like a spring, mass, and dash pot; i.e., it is the mechanical analog of an electrical RLC, which gives 12 dB/octave roll off at frequencies greater than the resonance frequency. The frequency response of the system is shown in Fig. 55. As can be seen, the response can be adjusted by using various materials. The cork and neoprene serve as the spring and the Scotchcast behaves like a dash pot. It is also quite obvious that neither of these materials has an ideal resistance or inductance, and that this is the source of the problem. The response falls off initially at 12 dB/ octave but reaches no more than 30 dB total at high frequencies. The cork and neoprene no longer act as a spring but as a lossy material with a fixed attenuation.

A second, more sophisticated mechanical attenuation network gave somewhat better results with regard to the attenuation of the 65 kHz pump signal. For this system, the housing was much larger and the cable from the preamplifier to the accelerometer was mechanically isolated from the accelerometer. A photograph of the second accelerometer-filter is shown in Fig. 56. This design uses a multipole filter constructed with much lower loss material. This mechanical filter arrangement had extremely good attenuation at high frequency, as evidenced by Fig. 57. Side-by-side comparison of hard mounted and soft mounted accelerometers in the same mechanical configuration demonstrated an attenuation of 78 dB at 65 kHz for the soft mounted accelerometer.

Comparison of the output of a nonmounted accelerometer with the output of an accelerometer mounted in a large case, attached to a 19-element transducer, showed that the large housing greatly affected the vibrational characteristics of the transducer and did not give accurate data. The solution was to return to the cork and neoprene gasket material and Scotchcast attenuator, which gave 30 dB of attenuation, and use this with a lower sensitivity accelerometer. Although some S/N was sacrificed,

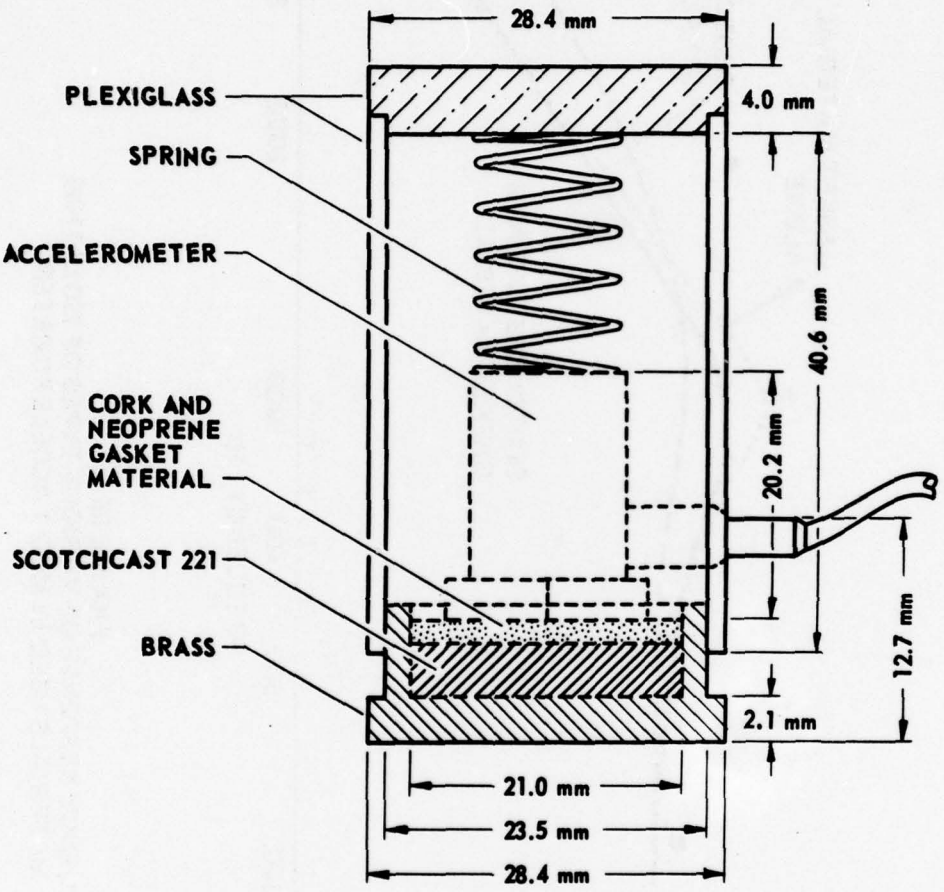

FIGURE 54
ACCELEROMETER HOUSING No. 1

ARL - UT
AS-77-1241
VEM - GA
10 - 19 - 77

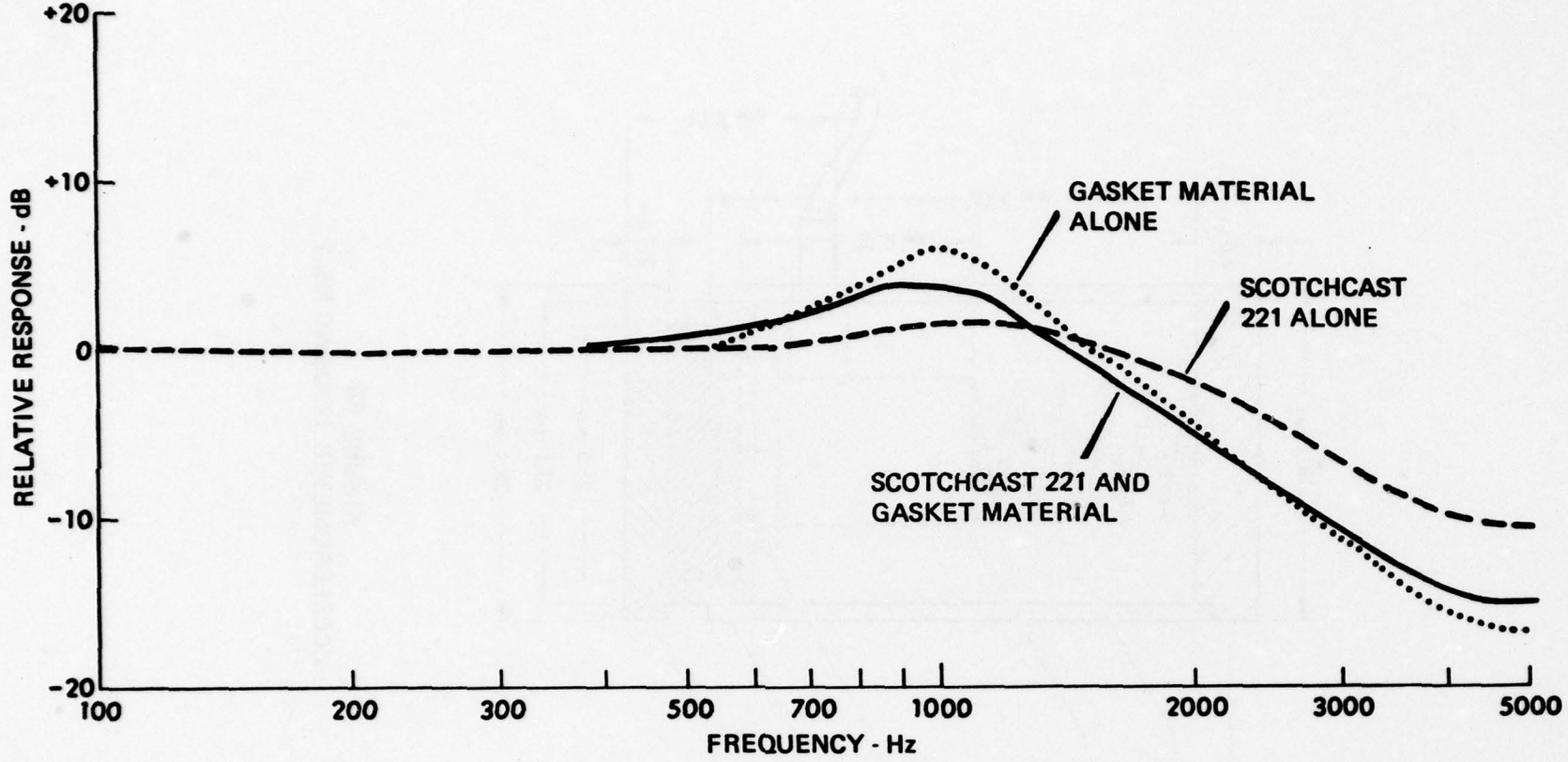

FIGURE 55
FREQUENCY RESPONSE OF VARIOUS TYPES OF ISOLATION MATERIALS USED IN MOD 1 ACCELEROMETER

ARL - UT
AS-77-1232
VEM - GA
10 - 14 - 77

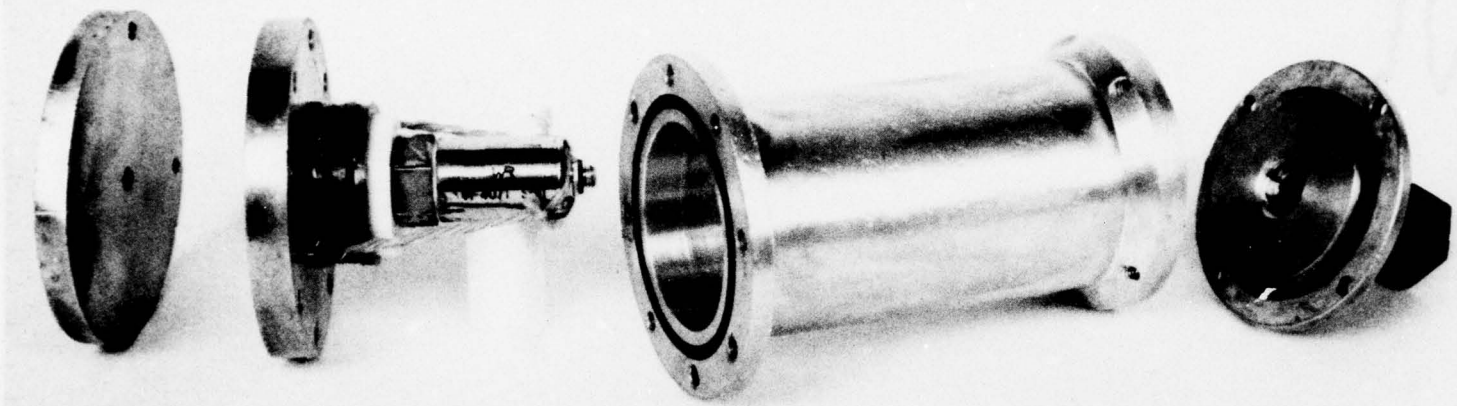

FIGURE 56
PHOTOGRAPH OF ACCELEROMETER HOUSING No. 2

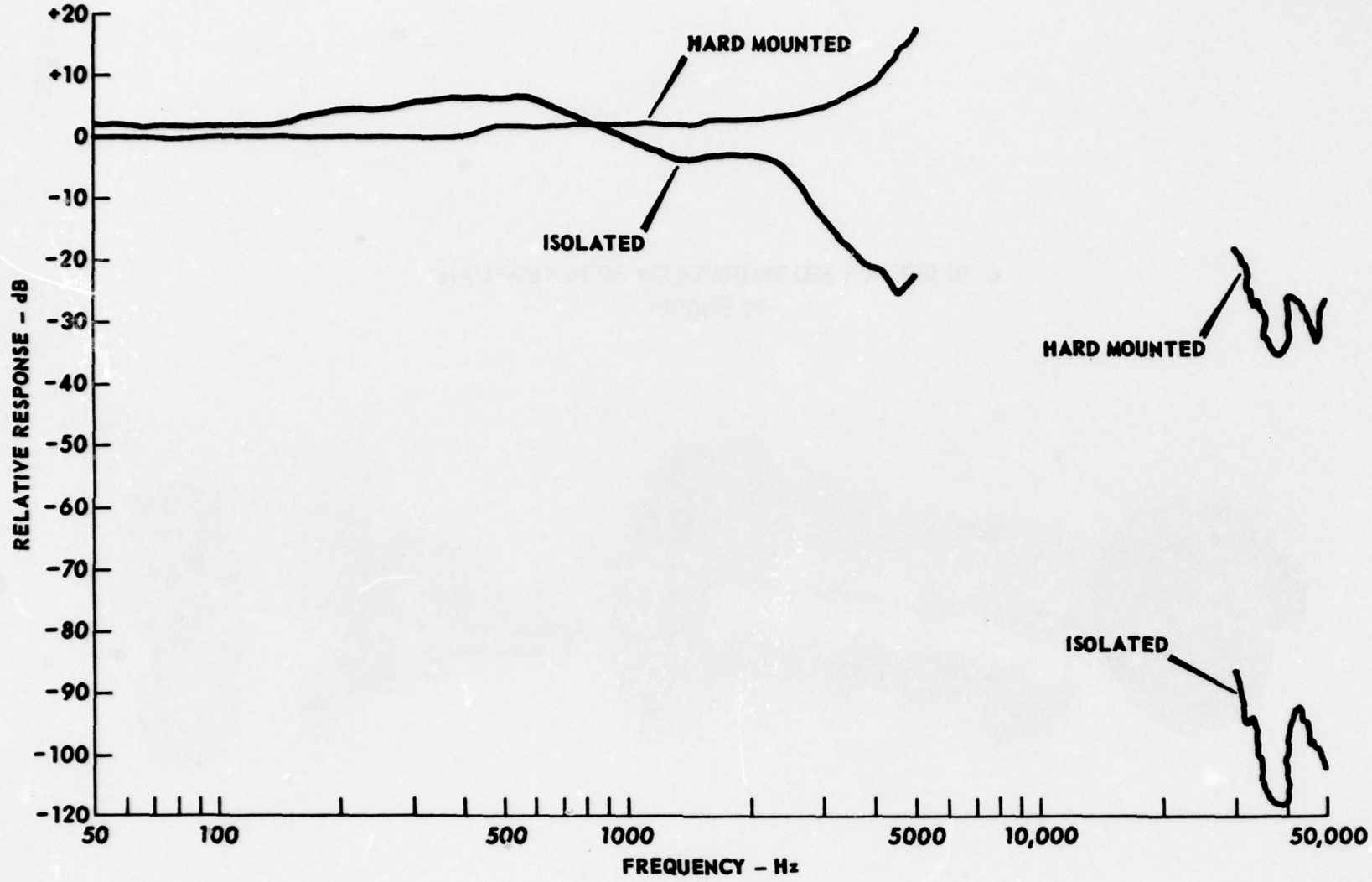

ARL - UT
AS-77-1233
VEM - GA
10 - 14 - 77

FIGURE 57
AMPLITUDE RESPONSE OF MOD 2 ACCELEROMETER SYSTEM
ISOLATED AND NONISOLATED

the system provided satisfactory performance since the background vibration level was still above the noise of the amplifier.

The housing for the new accelerometer is shown in Fig. 58. This housing is much more rigid than the first design and much smaller than the second design. It also has a raised circle in the base to give strain relief so that the accelerometer will respond only to motion perpendicular to the plane of the base. The original isolation material (Fig. 54) is used, which gives 30 dB of attenuation at 65 kHz. The output of this system, when mounted on the 19-element transducer, is almost identical to that of a bare accelerometer mounted in the same location (Fig. 59) at frequencies below the filter roll off. The accelerometer system was calibrated against a standard to produce the calibration curve shown in Fig. 60.

2. Acoustic Ambient Monitor

A calibrated, omnidirectional audio frequency hydrophone is required to adequately evaluate the experimental PARRAY. This hydrophone at the PARRAY location is used to monitor the low frequency signals and ambient noise. A standard hydrophone, NRL/USRD type F50, was used with a special purpose preamplifier and line receiver for this purpose. The F50 is supplied without a preamplifier and with 23 m of twinaxial cable. It is omnidirectional at audio frequencies and is calibrated for use from 1 Hz to 70 kHz.

Since the F50 hydrophone is located at the west tower, an additional 300 m of transducer cable is required to connect the F50 to the electronic consoles located at the LTTS main barge facility. The high output impedance of the F50 and the long cable run back to the barge require that a preamplifier and cable driver be located between the 23 m F50 cable and the 300 m shore cable. A block diagram of the acoustic ambient monitor system that was developed for the PARRAY system tests is shown in Fig. 61. As indicated in this figure, the preamplifier

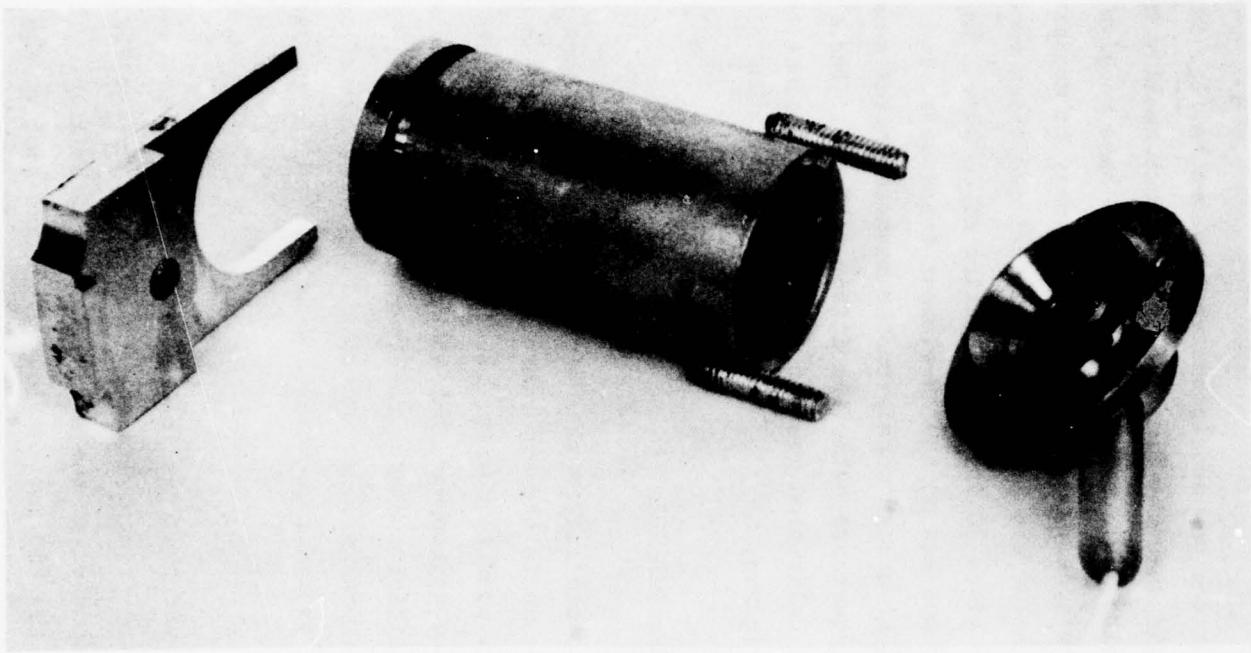

FIGURE 58

PHOTOGRAPH OF ACCELEROMETER HOUSING No. 3

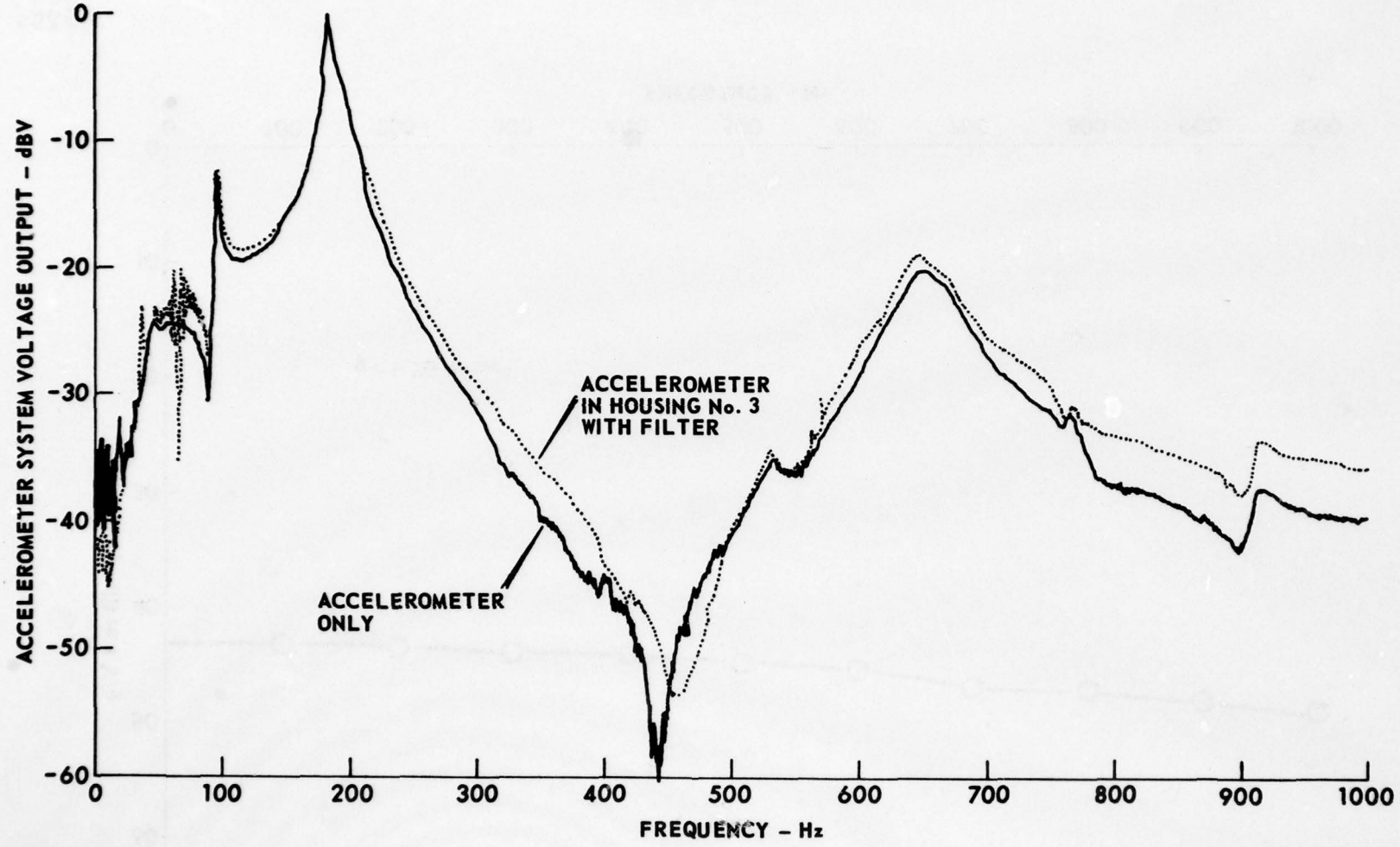

FIGURE 59
RESPONSE OF REAR OF HOUSING OF 19-ELEMENT TRANSDUCER DRIVEN BY SOLENOID SHAKER

ARL - UT
AS-77-1234
VEM - GA
10 - 14 - 77

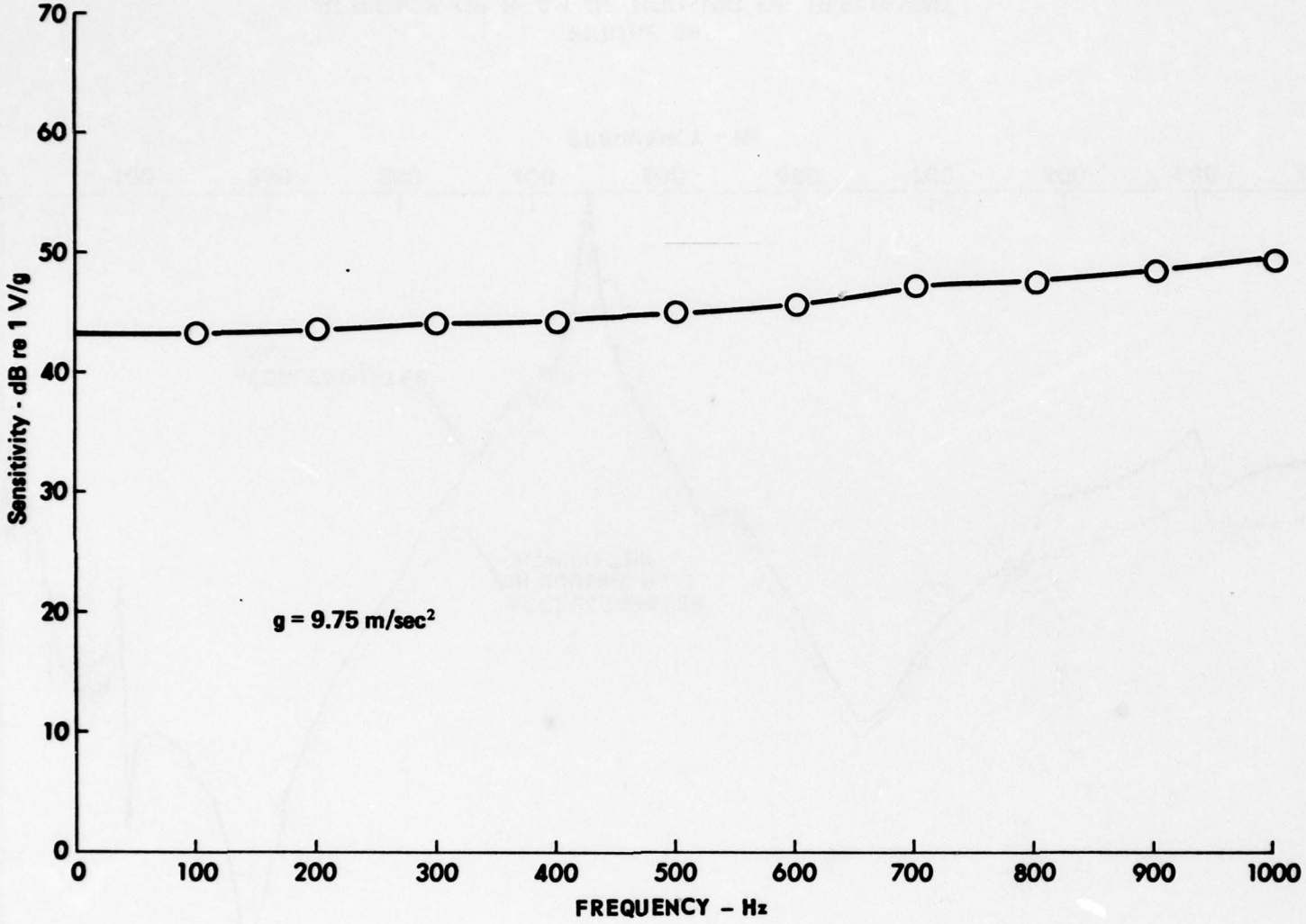

ARL - UT
AS-77-1243
VEM - GA
10 - 19 - 77

FIGURE 60
CALIBRATION CURVE FOR ACCELEROMETER SYSTEM No. 3

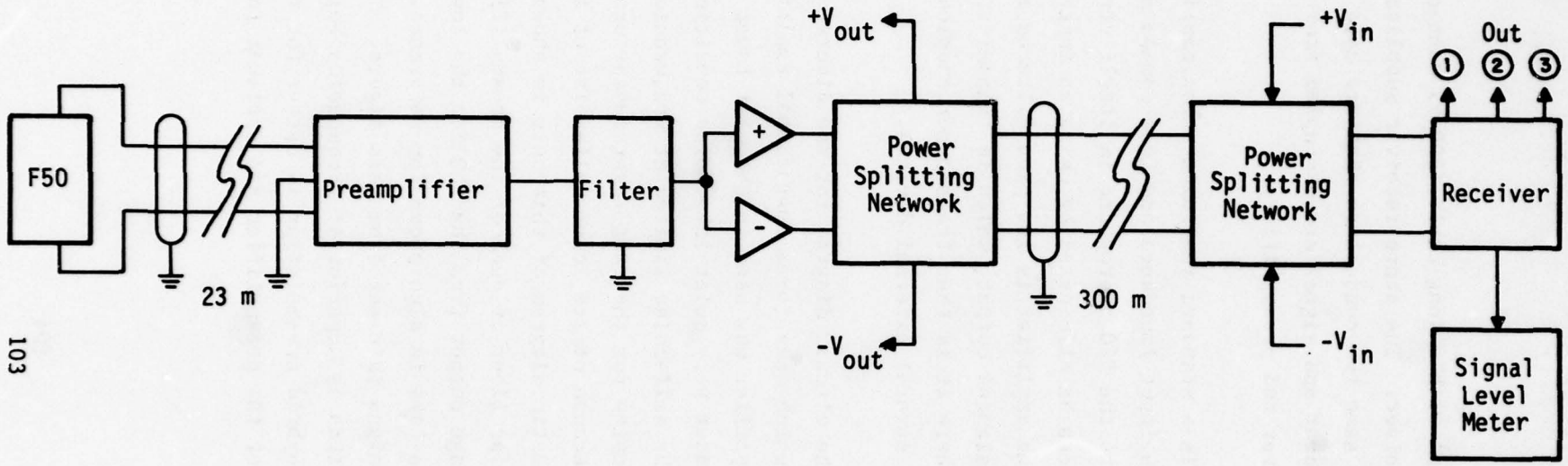

FIGURE 61
AMBIENT NOISE MONITORING SYSTEM

AS-77-2297
VEM 0231-O

is near the hydrophone (23 m) with a long cable (300 m) connecting the preamplifier to a shore receiver. The shore receiver supplies power to the preamplfifier on the same two conductors that are used to transmit the signal to shore. The power and signal are decoupled from each other by RC networks in the receiver and preamplifier.

The preamplifier is a standard instrumentation amplifier design which has a very high input impedance and good common mode rejection. The 23 m cable to the F50 hydrophone is itself very susceptible to 60 Hz pickup, which can be eliminated by using an instrumentation amplifier. The output of the amplifier is low pass filtered at 1.6 kHz and buffered to produce a balanced output, which is transmitted on a twinaxial cable to shore, where it is then transformer coupled into an amplifier and buffered into several external devices.

Figure 62 shows the circuit diagram for the discrete instrumentation amplifier, which uses three operational amplifiers; this discrete instrumentation amplifier was used in the west tower ambient noise sensor. Data taken under very quiet lake noise conditions indicate that this preamplifier may be self-noise limited at frequencies greater than 130 Hz. A different design for the east tower sensor uses a hybrid instrumentation amplifier because of its lower self-noise at frequencies greater than 50 Hz. A schematic diagram of this unit is shown in Fig. 63. The electronic noise floor of each of the preamplifiers is shown in Fig. 64. The voltage output from the F50 for the lowest ambient noise levels observed in the lake is also shown for reference. The tradeoff between the two designs is clear from this figure. The discrete circuit implementation is superior at frequencies below 50 Hz whereas performance of the hybrid preamplifier is better for frequencies above 50 Hz. A photograph of the preamplifier and canister for the F50 is shown in Fig. 65.

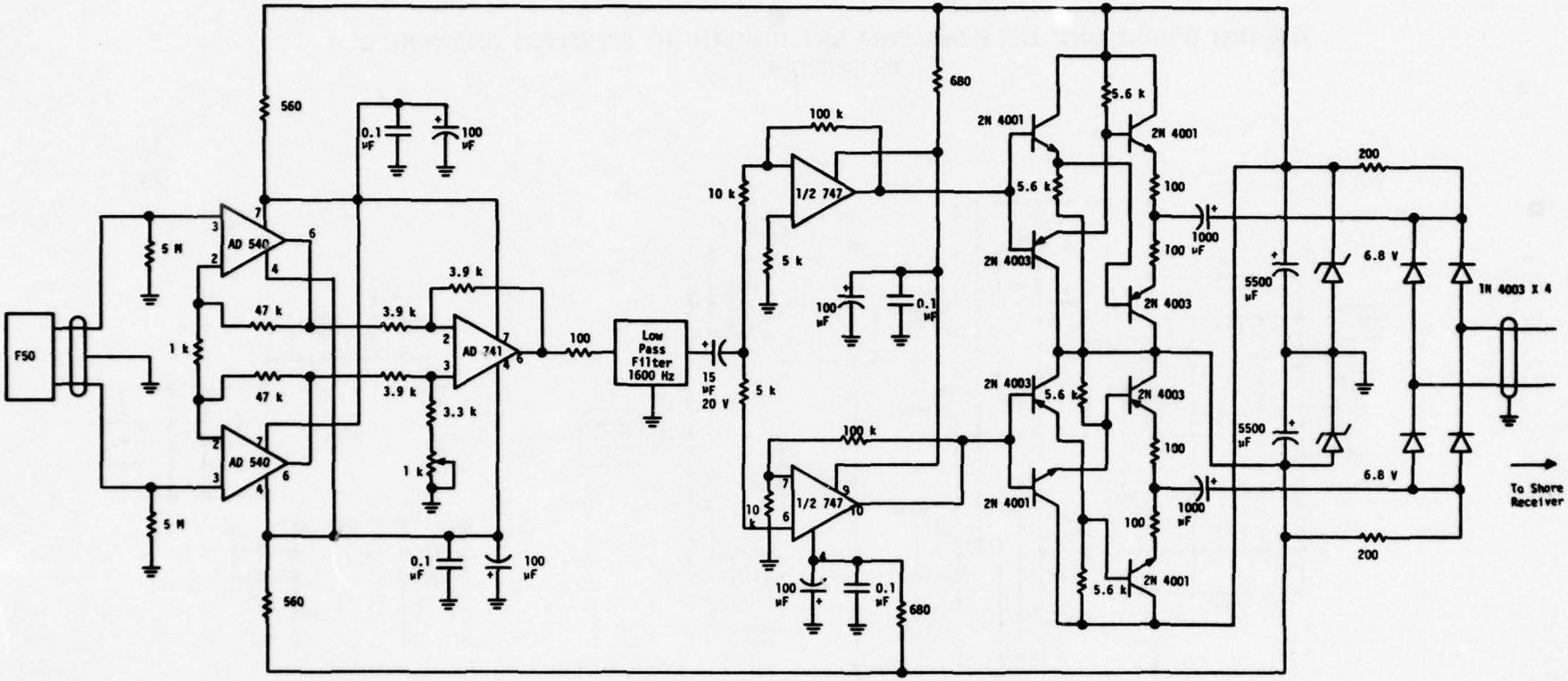

CS-77-2290
VEN 0231-0

105

FIGURE 62
SCHEMATIC DIAGRAM OF DISCRETE F50 PREAMPLIFIER AND CABLE DRIVER

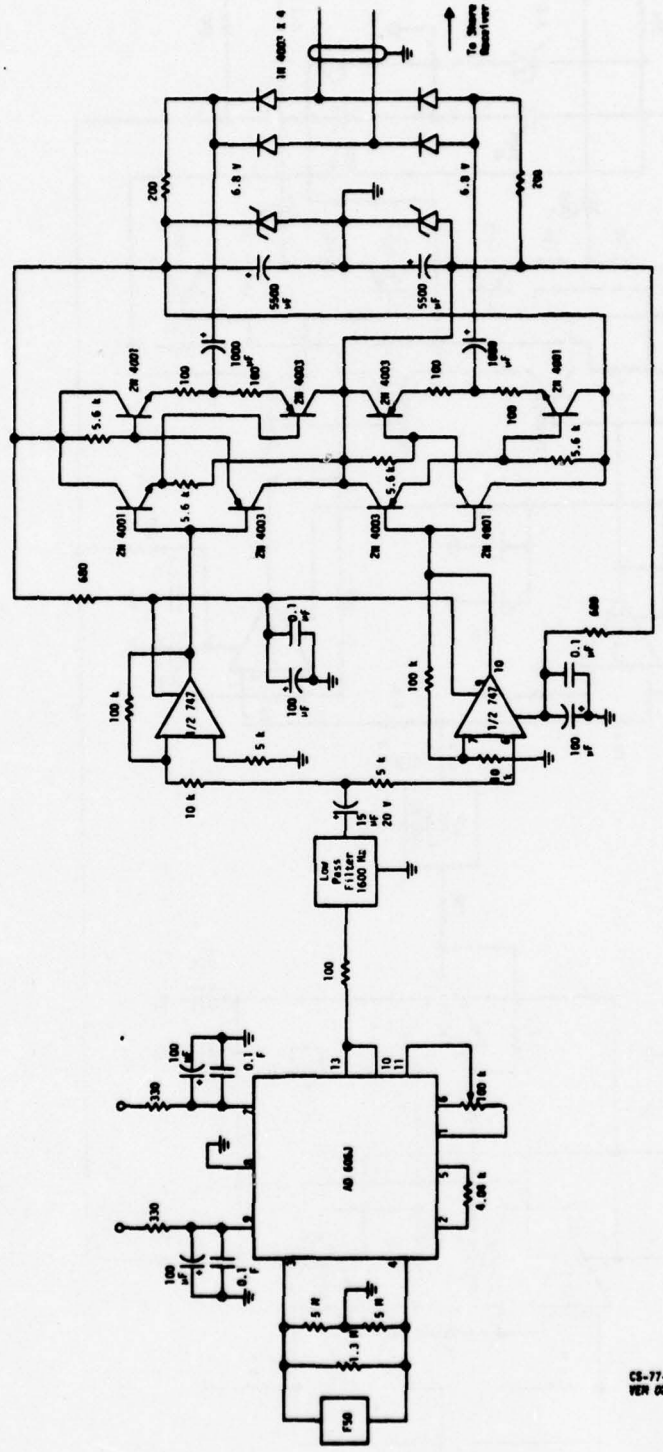

FIGURE 63
SCHEMATIC DIAGRAM OF HYBRID F50 PREAMPLIFIER AND CABLE DRIVER

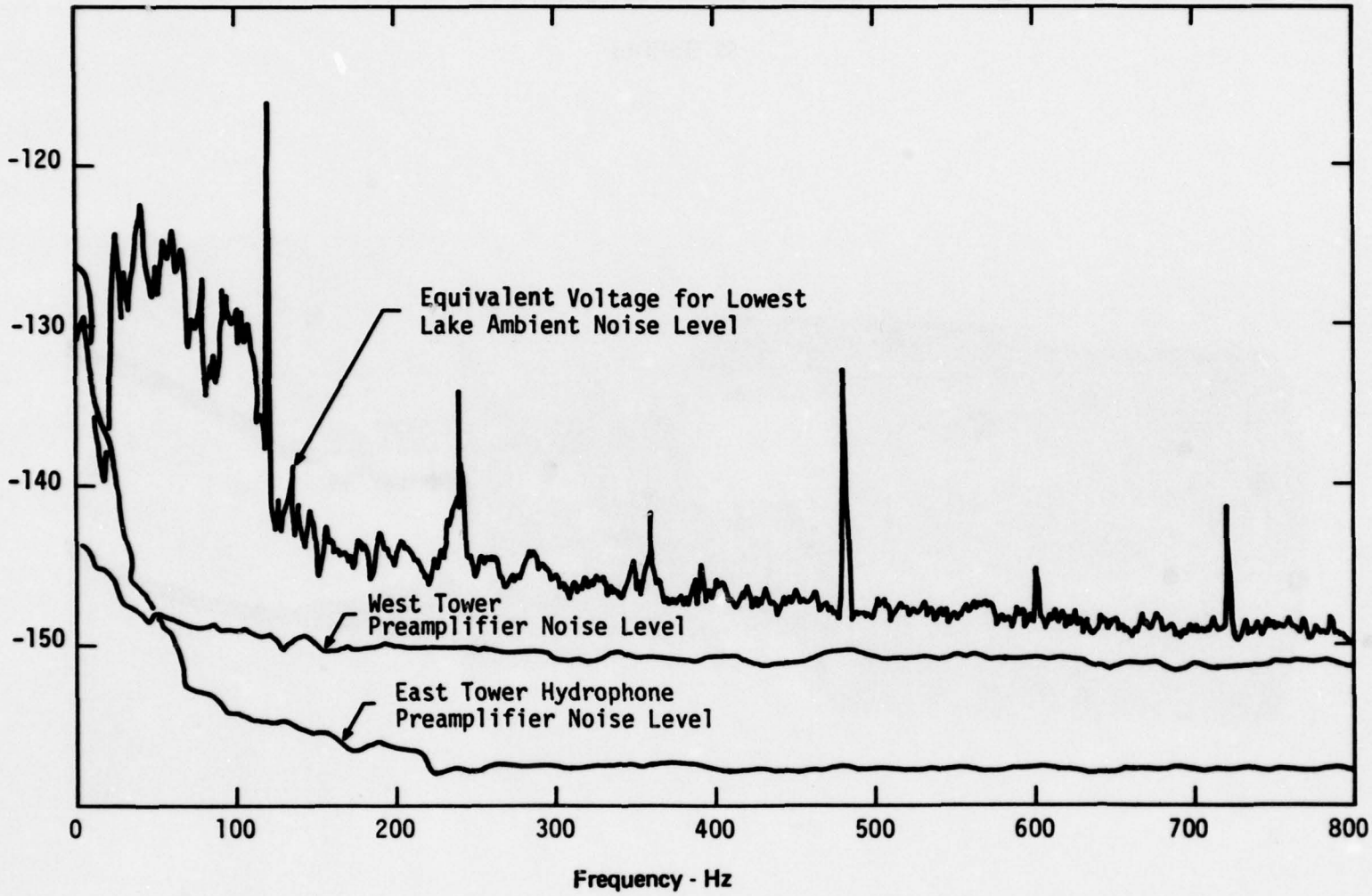

FIGURE 64
ELECTRONIC AND ACOUSTIC NOISE LEVELS OF AMBIENT NOISE MONITOR

AS-77-2298
VEM 0231-0

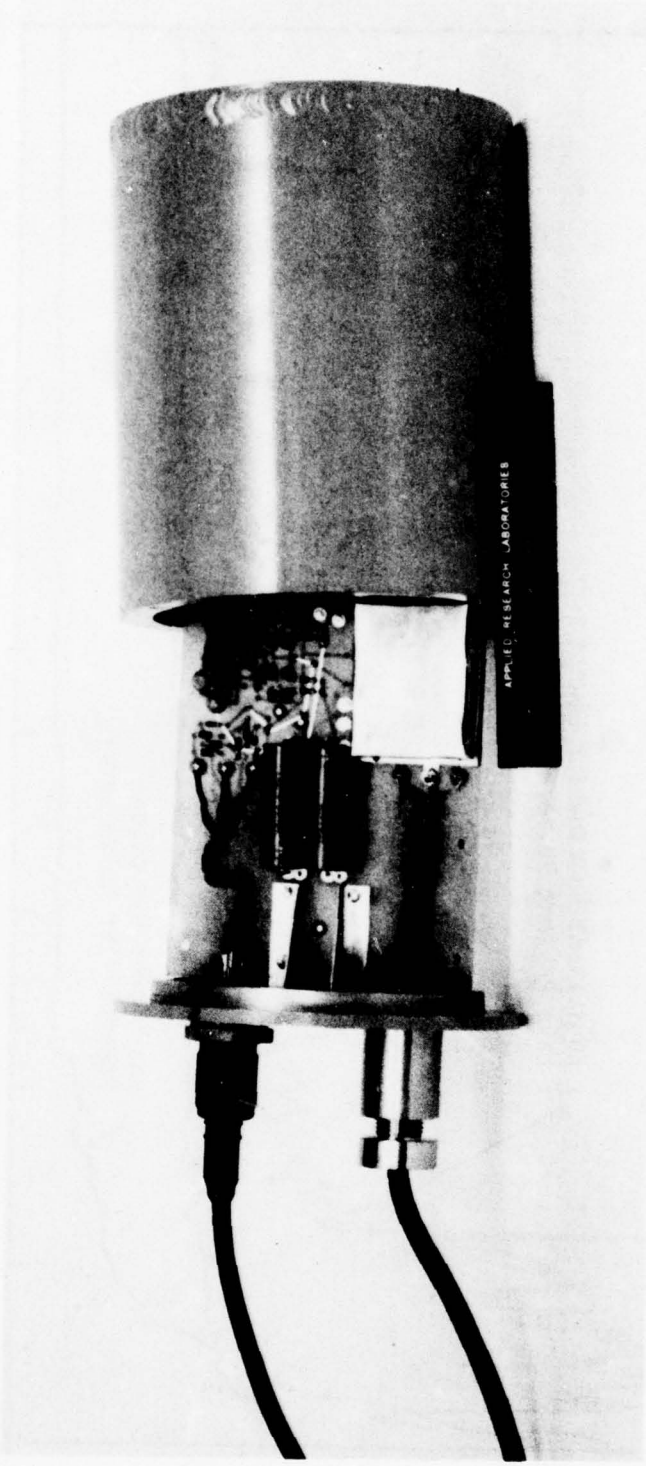

FIGURE 65
F50 PREAMPLIFIER AND CANISTER

The schematic diagram of the shore receivers, which are almost identical, is shown in Fig. 66. The supply voltage on the cable connecting the preamplifier to the shore receiver for the east tower sensor is greater because it operates on ±12 V, whereas the west tower sensor operates on ±6 V. This modification is made by the addition of two resistors in series with the power supply leads in the west tower receiver. Buffered outputs are provided for the spectrum analyzer, the DAPS, headphones, and a general purpose audio output.

A front view of the east tower shore receiver is shown in Fig. 67. The meter labeled "Lake Ambient" is calibrated in dB re 1 μPa for the 1/3 octave band centered at 80 Hz. This meter provides an immediate indication of the noise level emanating from Mansfield Dam.

The noise monitoring systems were calibrated using a J13 as a source and a calibrated NRL/USRD Type H23 hydrophone as a reference. The J13 was driven with bandlimited white noise and the resultant sound field was measured at a known location some distance from the J13. The F50 was then placed in exactly the same location previously occupied by the H23. By comparing the response of the H23 with the response of the F50, the response of the F50 was obtained. The sensitivity of the west tower sensor is shown in Fig. 68

3. Multiple Tone Signal Source

Measurements at LTTS with the 340 m PARRAY confirmed the desirability of simultaneously performing measurements at several frequencies. The variability of propagation of low frequency signals in the restricted waters at Lake Travis means that confidence in the measurements can be achieved only by sampling several frequencies for substantial periods of time. The time required to perform the measurements sequentially becomes excessive, and changes in propagation conditions, source location, etc., may still occur over the measurement period. Therefore, a multiple frequency signal source is required to perform meaningful experiments in a timely manner.

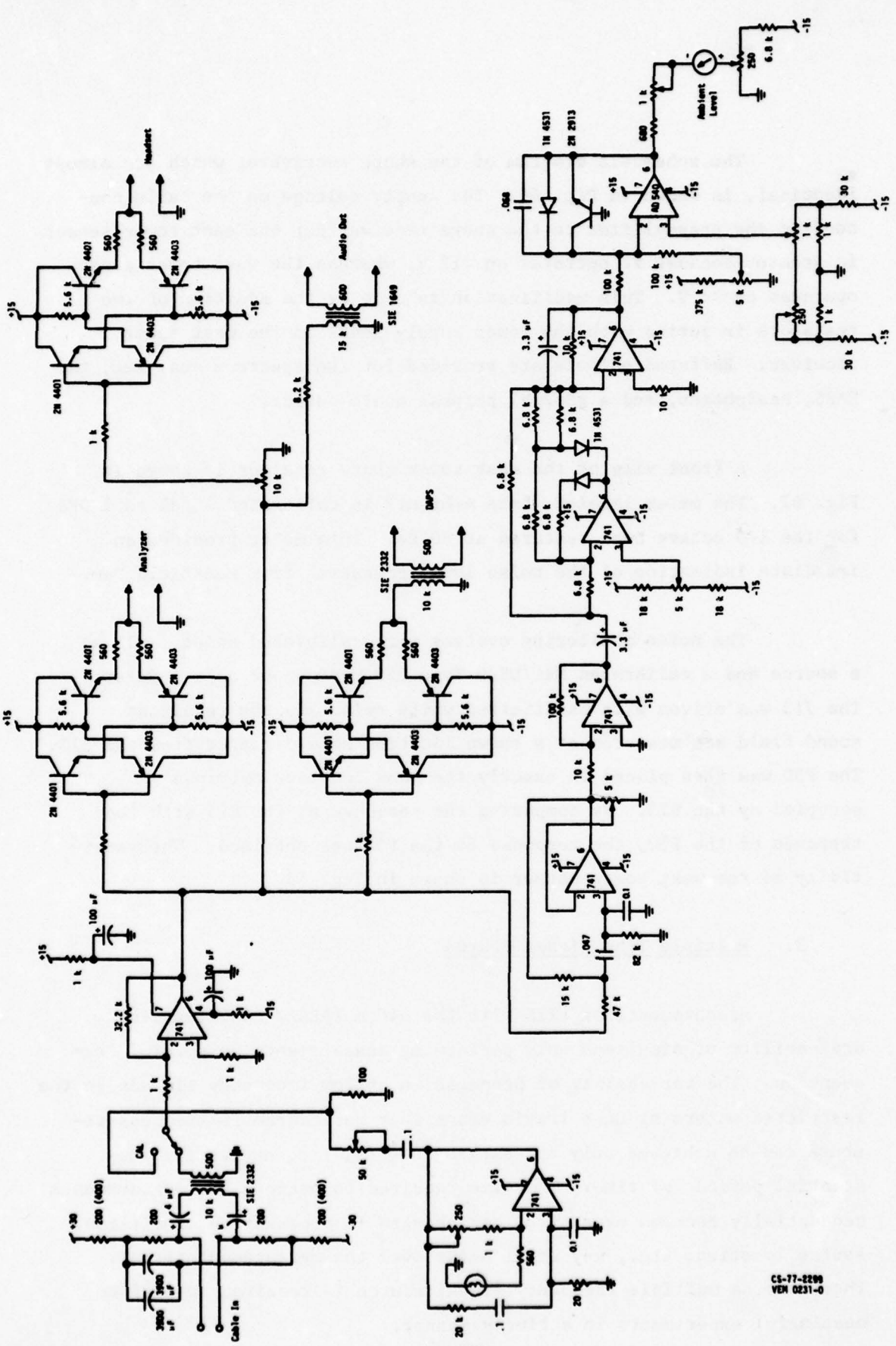

FIGURE 66
SCHEMATIC DIAGRAM OF AMBIENT NOISE MONITOR SHORE RECEIVER

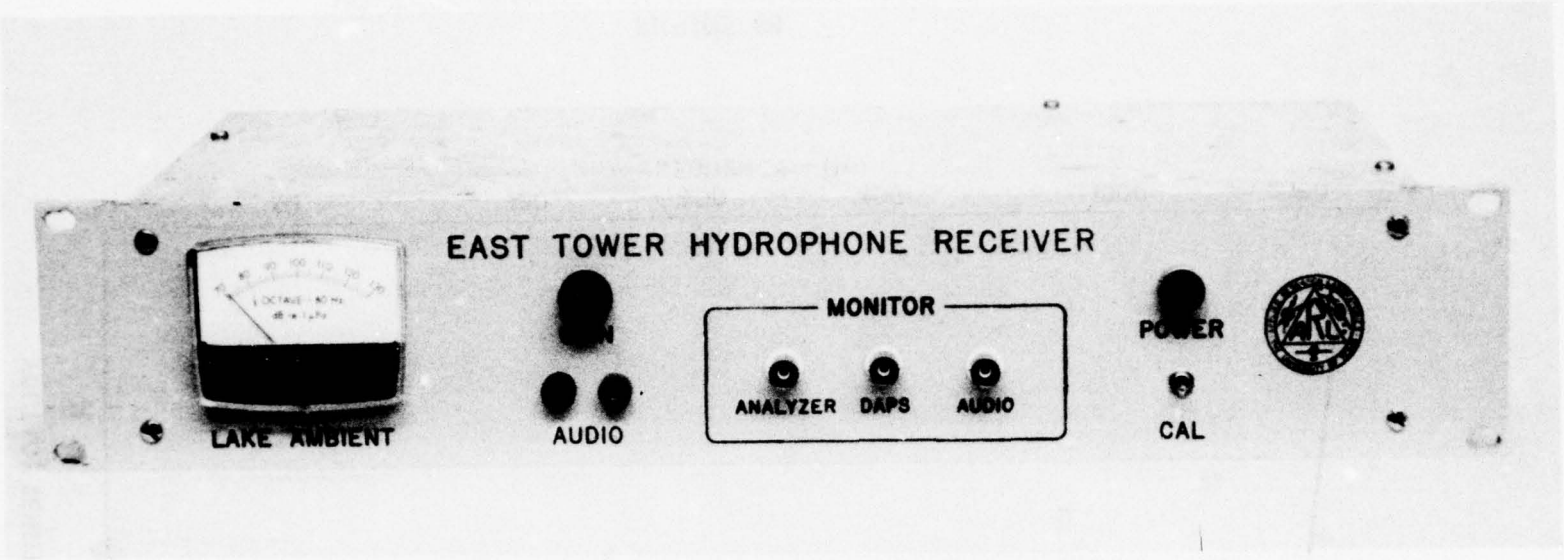

FIGURE 67

FRONT VIEW OF EAST TOWER SHORE RECEIVER FOR F50

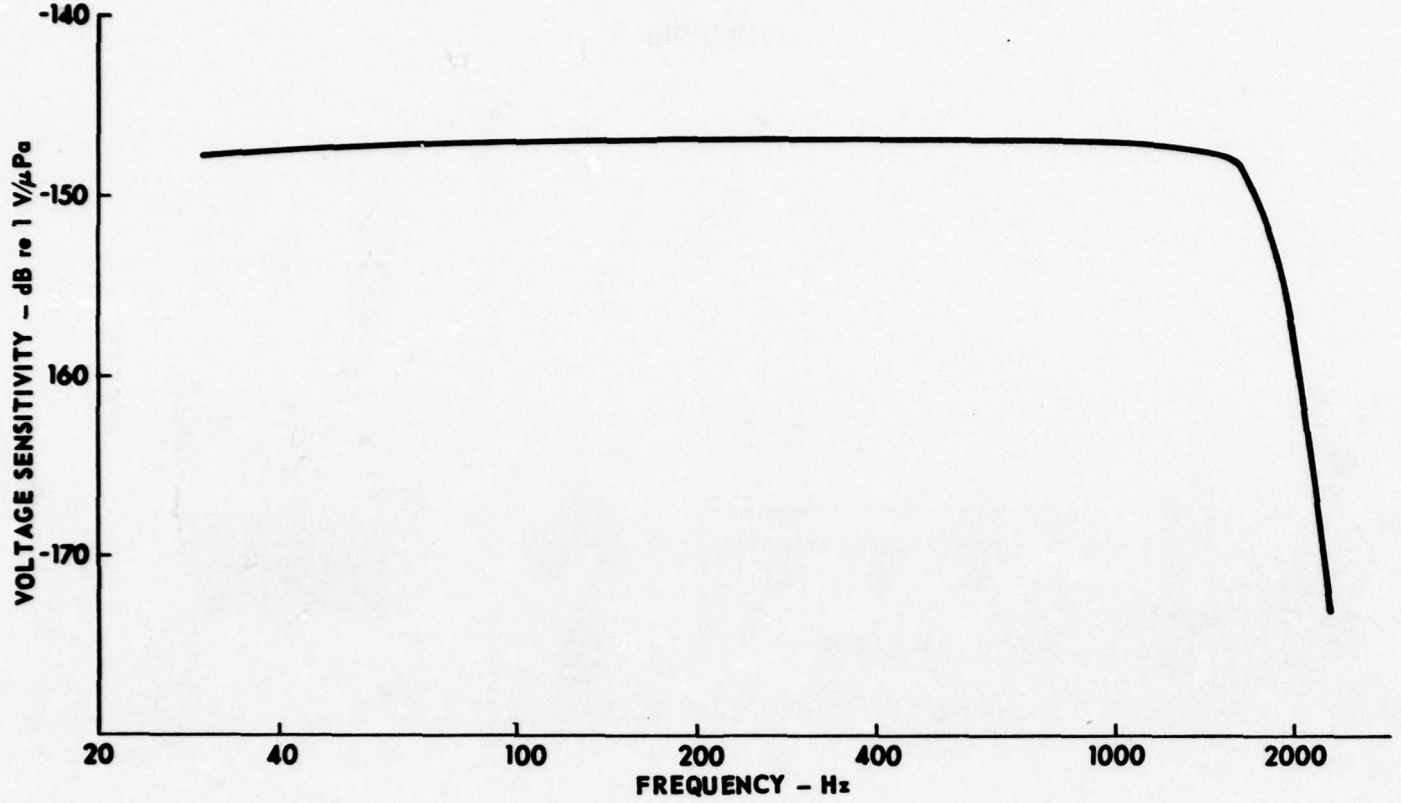

FIGURE 68
VOLTAGE SENSITIVITY OF AMBIENT NOISE MONITOR

The basic features required in a multiple frequency source are small size, accurate frequency, and individual amplitude and frequency controls. These features were used as guidelines for design and construction of the four-tone source shown in Fig. 69. This instrument contains four frequency synthesizers in a case that is small enough to be easily carried. This unit can operate in its transit case, as shown in Fig. 69, or it can be removed and mounted in a standard 48 cm (19 in.) rack. All of the controls and cable connections are on the front panel except for the power cord, which is at the rear of the case. The transit case lid is fastened over the front panel for protection whenever it is transported in the field.

A block diagram of the four-tone source is shown in Fig. 70. This diagram shows how all four sources are driven by the same reference oscillator to ensure overall, and relative, stability of the synthesizers. The synthesizers are of the phase locked loop variety and cover a frequency range of 1.000 Hz to 99.99 kHz, with four decimal digits of step resolution. The sine wave outputs of the synthesizers are connected through unit step attenuators (0 to 40 dB) for individual amplitude control before reaching the summation and output circuits.

The first elements of the summation circuitry shown in Fig. 70 are the OFF-ON switches. These switches allow any single source or any combination of sources to be summed together for final output. In addition to the summation output individual source monitor outputs are also available. An external input to the summing amplifier is available on the front panel so that more complex waveforms can be created if desired. The rest of the block diagram in Fig. 70 details the output circuitry, which is used only to prevent the operator from overdriving the output transducer. A window comparator circuit warns the operator through a panel light when the output voltage is at a dangerous level, and the active clipper circuit prevents this preset level from being exceeded. The output buffer is used for output isolation and final gain calibration adjustments.

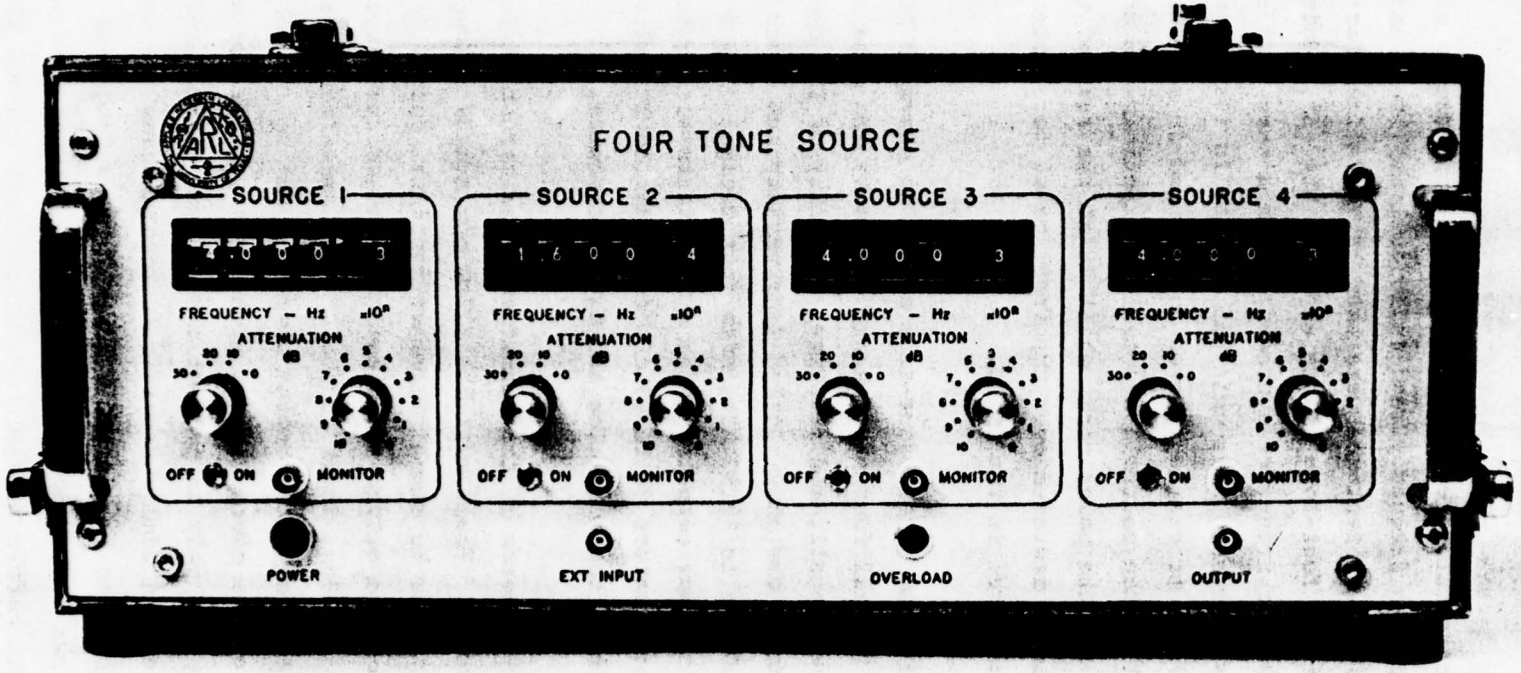

FIGURE 69
PHOTOGRAPH OF FRONT VIEW OF THE FOUR-TONE SOURCE

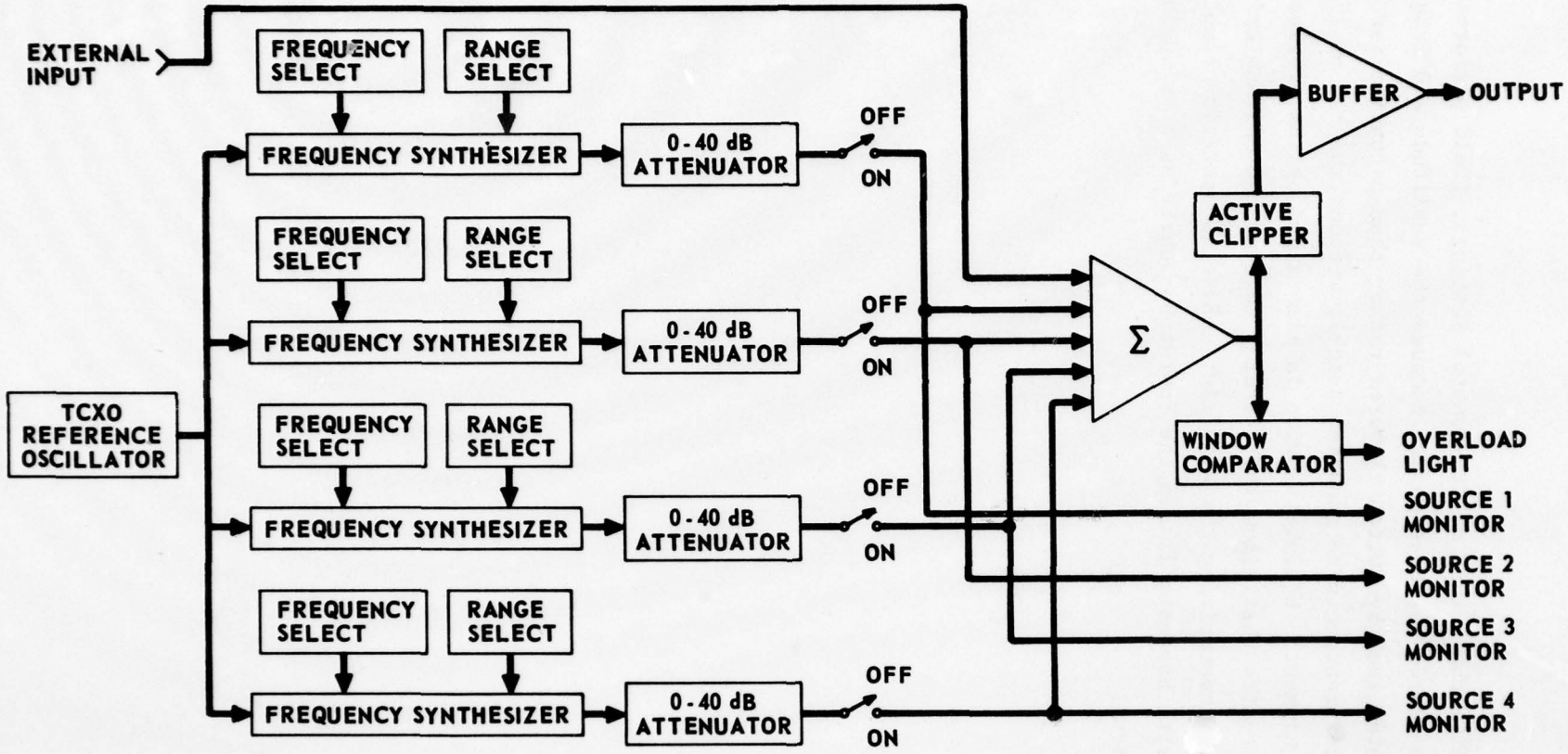

FIGURE 70
BLOCK DIAGRAM OF THE FOUR-TONE SOURCE

ARL:UT
AS-78-555
EPK-GA
3-23-78

Due to the nature of its control settings, field performance of the four-tone source has been good. Because the amplitude and frequency values are determined by switch closures rather than potentiometer settings, experiments can be repeated quickly without the use of monitoring equipment. Equipment setup is also aided by the overload protection circuits that allow the operator to find the maximum drive voltage without overdriving the amplifier. Ease of operation combined with portability has established the four-tone source as a valuable field instrument.

V. ANALYSIS, EXPERIMENTS, AND DESIGN SUPPORT STUDIES

A. Modulation Process in Nonlinear Interaction in Water

To develop an optimum design for the PARRAY receiver preprocessor, it is important to have a model of the parametric reception process expressed in familiar signal processing terms. Whereas some of the early models of the nonlinear interaction process in water clearly described the process to be equivalent to phase modulation, more recent models have been difficult to interpret in these familiar terms. Therefore, we undertook a program of investigation and experimentation with the following three objectives in mind:

(1) to interpret and compare the different models in signal processing terms,
(2) to experimentally assess the validity of the models, and
(3) to apply the resulting information in developing a simpler receiver preprocessor.

The remainder of this section presents the principal results of the investigation.

Four models were studied; these were developed by Date and Tozuka,[3] Zverev and Kalachev,[5] Berktay and Al-Temimi,[4] and Truchard.[11] The first three models consider interaction between two plane waves, one of which is a high frequency pump signal, and the other, a low frequency signal to be detected by the PARRAY. The Truchard model addresses the case of a spherically spreading pump wave and a plane low frequency wave. All of the models consider the case of a single point hydrophone.

To make the different models comparable, we have used special cases or have made slight changes in certain models. Because not all of the models include the effects of attenuation in the medium, we have used a value $\alpha=0$ for the Berktay and Al-Temimi model and for the Truchard model. In addition, the Truchard model assumes a spherically spreading pump wave. Because of this assumption, the principal difference between his model and the others is that the signals appearing at the PARRAY hydrophone are attenuated by spherical spreading. To make Truchard's model comparable to the others, we removed this effect by inserting a factor L (array length) into his expressions for both the interaction components and the pump signal received by the hydrophone. While we are confident that this is valid for studying the structure of the hydrophone signals from a signal processing point of view, it is not clear that this makes the different models exactly comparable with respect to the directional characteristics they predict for the PARRAY. We note in connection with this that Berktay and Shooter[9] present models that show identical directional characteristics for both plane and spherically spreading pump waves; however, we do not wish to imply that the principle can be applied to Truchard's model without exercising caution. We have also freely changed the notation used in the references.

The first model considered is the model of Date and Tozuka.[3] This model represents the nonlinear interaction between a high frequency pump signal and a low frequency signal as a phase modulation (PM) of the pump signal by the low frequency signal. For the case of sinusoidal pump and low frequency waves, the signal appearing at the output of the hydrophone is given by

$$s(t) = Hp_1 \cos\left[\omega_1 t - \frac{\omega_1 L}{c_o} + Q(\theta)\cos(\omega_2 t - M)\right] \quad , \qquad (10)$$

where

H = hydrophone sensitivity,

p_1 = peak pump pressure level,

ω_1 = pump radian frequency,

ω_2 = low frequency signal radian frequency,

L = pump-hydrophone separation,

c_o = sound speed,

θ = angle of arrival of low frequency signal with respect to pump-hydrophone axis,

$Q(\theta)$ = phase modulation index, and

$M = (\omega_2 L/2c_o)(1-\cos\theta)$.

The modulation index is designated $Q(\theta)$ to emphasize the dependence on the angle between the directions of propagation of the two waves. According to the Date and Tozuka model, the modulation index is

$$Q_1(\theta) = \frac{p_2\left(\frac{B}{2A} + 1\right)\omega_1 \cos\theta}{\left(\frac{B}{A} + 1\right)p_o c_o}\left(\frac{\sin M}{M}\right) \quad , \tag{11}$$

where

B/A = parameter of nonlinearity of the medium,

p_1 = peak pressure of low frequency signal, and

p_o = ambient pressure.

The second model to be considered is that of Zverev and Kalachev,[5] which represents the nonlinear interaction process as a PM of the high frequency pump wave by the low frequency signal as indicated by Eq. (10). According to this model, the modulation index of the process is

$$Q_2(\theta) = \frac{p_2\left(\frac{B}{2A} + \cos\theta\right)\omega_1 L}{\rho_o c_o^3}\left(\frac{\sin M}{M}\right) \quad , \tag{12}$$

where ρ_o is the density of the medium. Zverev and Kalachev also argue rather convincingly that there are errors in the derivation of the Date and Tozuka model. Even taking into account the supposed errors in Eq. (11), there are still unresolved differences in Eqs. (11) and (12) based on different mathematical models of the nonlinear media.

For both the Date and Tozuka model and the Zverev and Kalachev model, the signal appearing at the PARRAY hydrophone is a PM version of the pump signal. The modulating signal is the low frequency acoustic signal and the modulation index is given by Eq. (11) or Eq. (12). In most PARRAY applications, the modulation index will be a very small number, probably in the range 10^{-4} to 10^{-8}. Under these conditions the PM process is very nearly a linear modulation process; that is, the spectrum of the modulated signal contains only first order products of the carrier and modulating signal. The harmonics and crossproducts of the modulating signal spectral components produce negligibly small products in the modulated signal spectrum. The modulated signal spectrum consists of only the pump carrier and an upper and a lower sideband, where the sidebands are scaled and frequency shifted replicas of the low frequency signal. When they are viewed in this manner, these two models may be compared with two other models, which are discussed next.

By following a somewhat different development, Berktay and Al-Temimi[4] arrived at an expression for the sum and difference frequency components generated by the interaction of sinusoidal pump and low frequency signals. Their model says that the sum and difference sideband signals appearing at the PARRAY hydrophone are

$$s_3(t,\theta) = \frac{-Hp_1p_2\left(\frac{B}{2A} + \cos\theta\right)L}{2\rho_o c_o^3} \frac{\sin M}{M}$$

$$\times \left\{(\omega_1+\omega_2)\sin\left[(\omega_1+\omega_2)t - \frac{\omega_1 L}{c_o} - \frac{\omega_2 L}{2c_o}(1+\cos\theta)\right]\right. \tag{13}$$

$$\left. + (\omega_1-\omega_2)\sin\left[(\omega_1-\omega_2)t - \frac{\omega_1 L}{c_o} + \frac{\omega_2 L}{2c_o}(1+\cos\theta)\right]\right\} \quad .$$

In this expression, the first term in braces represents the upper sideband component, and the second term represents the lower sideband component. The carrier signal at the hydrophone is

$$c_3(t) = Hp_1\cos\left(\omega_1 t - \frac{\omega_1 L}{c_o}\right) \quad . \tag{14}$$

Taken together, Eqs. (13) and (14) give a complete picture of the modulated pump signal which appears at the output of the PARRAY hydrophone as predicted by this model. From a signal processing point of view, this model represents a form of quadrature amplitude modulation (QAM) of the pump signal by the low frequency signal. That is, the modulation sidebands are those which result from amplitude modulation (AM) of both the in-phase and quadrature components of the pump by the low frequency. The in-phase modulation index is

$$Q_{3i}(\theta) = \frac{p_2\left(\frac{B}{2A} + \cos\theta\right)\omega_2 L}{\rho_o c_o^3} \frac{\sin M}{M} \quad , \tag{15}$$

and the quadrature modulation index is

$$Q_{3q}(\theta) = \frac{p_2\left(\frac{B}{2A} + \cos\theta\right)\omega_1 L}{\rho_o c_o^3} \frac{\sin M}{M} \quad . \tag{16}$$

For most cases of interest to us, for which $\omega_1 >> \omega_2$, the modulation of the quadrature component is much larger than the modulation of the in-phase component, by the ratio ω_1/ω_2.

The last model investigated here is Truchard's model for a point source pump.[11] This model is not, strictly speaking, comparable to the other models discussed here because it assumes a spherically spreading pump wave, whereas the other models assume a plane pump wave. However, if we take the liberty to correct the pump and sideband signal amplitudes for the loss due to the spreading pump wave, we arrive at the following representation. Including a multiplier L to make up for the spreading loss, Truchard's model for the sideband signals at the hydrophone is

$$s_4(t,\theta) = \frac{-Hp_1p_2\left(\frac{B}{2A} + 1\right)L}{2\rho_o c_o^3} \frac{\sin M}{M}$$

$$\times \left\{ (\omega_1+\omega_2)\cos\left[(\omega_1+\omega_2)t - \frac{\omega_1 L}{c_o} - \frac{\omega_2 L}{2c_o}(1+\cos\theta)\right] \right. \qquad (17)$$

$$\left. + (\omega_1-\omega_2)\cos\left[(\omega_1-\omega_2)t - \frac{\omega_1 L}{c_o} + \frac{\omega_2 L}{2c_o}(1+\cos\theta)\right] \right\} .$$

The pump signal at the hydrophone is

$$c_4(t) = Hp_1 \sin\left(\omega_1 t - \frac{\omega_1 L}{c_o}\right) . \qquad (18)$$

This model also represents QAM. The modulation index for the in-phase component is

$$Q_{4i}(\theta) = \frac{p_2\left(\frac{B}{2A} + 1\right)\omega_2 L}{\rho_o c_o^3} \frac{\sin M}{M} , \qquad (19)$$

and the modulation index for the quadrature component is

$$Q_{4q}(\theta) = \frac{p_2\left(\frac{B}{2A} + 1\right)\omega_1 L}{\rho_o c_o^3} \frac{\sin M}{M} \quad . \tag{20}$$

This model differs from the model of Berktay and Al-Temimi (Eqs. (13) through (16)) in the phasing of the signals because a different reference was chosen for the pump phase. The only significant difference between the models expressed by Eqs. (13) through (16) and those expressed by Eqs. (17) through (20) is in the term involving B/A. This causes the Berktay and Al-Temimi model (Eqs. (13) through (16)) to predict slightly different PARRAY directional characteristics than the Truchard model (Eqs. (17) through (20)).

Now let us return briefly to the PM models to see how they can be compared with the QAM models. For simplicity, and because of the greater credibility of the Zverev and Kalachev model (Eqs. (10) and (12)), we will consider in detail only that one PM model. For small values of the modulation index, the Zverev and Kalachev model yields upper and lower sidebands which consist primarily of first order (linear) products of the pump and low frequency signals. The linear sideband components at the hydrophone are

$$p_2(t,\theta) = \frac{-Hp_1p_2\left(\frac{B}{2A} + \cos\theta\right)\omega_1 L}{2\rho_o c_o^3} \frac{\sin M}{M}$$

$$\times \left\{ \sin\left[(\omega_1+\omega_2)t - \frac{\omega_1 L}{c_o} - \frac{\omega_2 L}{2c_o}(1+\cos\theta)\right] \right. \tag{21}$$

$$\left. + \sin\left[(\omega_1-\omega_2)t - \frac{\omega_1 L}{c_o} + \frac{\omega_2 L}{2c_o}(1+\cos\theta)\right] \right\} \quad .$$

The carrier signal at the hydrophone is

$$c_2(t) = Hp_1\cos\left(\omega_1 t - \frac{\omega_1 L}{c_o}\right) \quad . \tag{22}$$

The modulation index for the quadrature modulation component is given by Eq. (12). This model predicts no in-phase component. Except for the absence of the in-phase term, the Zverev and Kalachev phase modulation model, as interpreted in Eqs. (12), (21), and (22), predicts results similar to the QAM models.

If we make the approximation (quite reasonable for our range of interest where $\omega_1 >> \omega_2$) that $\omega_1 \pm \omega_2 \approx \omega_1$, then the in-phase components vanish from the QAM models and the Berktay and Al-Temimi model agrees with the Zverev and Kalachev model. Furthermore, these models differ from the Truchard model in only one term. That term is

$$\left.\begin{array}{l}\text{Berktay and Al-Temimi (Eqs. (13) through (16))} \\ \text{and} \\ \text{Zverev and Kalachev (Eqs. (12), (21), and (22))}\end{array}\right\} \quad \frac{B}{2A} + \cos\theta \quad ,$$

$$\left.\begin{array}{l}\text{Truchard (Eqs. (17) through (20))}\end{array}\right\} \quad \frac{B}{2A} + 1 \quad .$$

This shows that the models predict slightly different directional characteristics for the PARRAY, with the greatest difference being in the far sidelobes and backlobes.

From a signal processing point of view, all three models are quite similar. Whether one uses a QAM or PM model, the structure of the hydrophone signal is very nearly the same. The in-phase AM component predicted by the QAM models will be so much smaller than the quadrature component that it will be of little practical value in the basic signal detection process. If only the quadrature AM components are considered, the sideband signals may be optimally detected by synchronously mixing the hydrophone signal with a 90° phase shifted version of the recovered carrier. This results in removal of the carrier and coherent addition of the sideband signals along with frequency translation of the sideband signals to baseband.

The validity of applying the synchronous quadrature demodulation technique depends on the correctness of the models with respect to the indicated phase relationships between the carrier and sidebands. To verify the accuracy of the models on this point, an experiment was performed.[29,16] Briefly, the experimental PARRAY receiver was used to receive the upper and lower sidebands independently so that the signal phases in the demodulated sidebands could be compared directly with each other. The results of the experiment confirmed the phase relationships indicated by the models. Also, of some lesser significance is the fact that the experimental results did not indicate any phase variation with changes in bearing, array length, source frequency, distance, and power level. This tends to indicate, for the parameter values used in the experiments at least, that the models are "complete" in this regard and that there is no inconsistency between model and experiment.

The practical significance of the experimental result is that it gives confidence in the models on this critical point for the development of signal processing techniques for the PARRAY. The phase locked loop PARRAY receiver described in a paper presented at the 92nd Meeting of the Acoustical Society of America should be a practical, optimum alternative to the more complex receiver currently being used.[29] A copy of this paper is included in an ARL:UT technical report.[16]

B. Analysis of the Effects of Vibration on the PARRAY

In every environment in which the PARRAY is employed, the transducers will be subject to some degree of physical motion relative to each other. In applications using a moving platform, the primary forces which cause the motion are the product of several rather obvious sources, principally vibration of the platform on which the transducers are mounted and turbulence caused by the passage of the transducers through the water. Even in a supposedly stationary environment, the transducers will still have some motion with respect to one another. If the transducers are mounted on the sea bottom, they are subject to forces caused

by seismic motion of the earth and by acoustic signals in the water. While these forces may be quite small, it is clear that they still produce some motion of the transducers. Because the effects of transducer motion on the operation of a PARRAY were not well understood, a study to develop a theory relating transducer motion to effects on PARRAY operation was initiated so that more accurate predictions about PARRAY performance in various environments may be made. The following is a brief summary of the study results.

First, consider the effects of sinusoidal motion of one of the transducers. Suppose that the velocity of the transducer along a line connecting the pump and hydrophone is modeled as

$$v_v(t) = k_v \cos\omega_v t \quad , \tag{23}$$

where ω_v is the radian frequency of the vibration and the peak velocity is k_v. The Doppler frequency shift caused by velocity $v_v(t)$ is

$$\delta(t) = \frac{\omega_o v_v(t)}{c} = \frac{\omega_o k_v \cos\omega_v t}{c} \quad , \tag{24}$$

where ω_o is the pump frequency and c is the sound speed. Then the signal received by the hydrophone is

$$s(t) = \sqrt{2}\, P \cos[(\omega_o + \delta(t))t] \tag{25}$$

$$s(t) = \sqrt{2}\, P \cos\left[\left(1 + \frac{k_v \cos\omega_v t}{c}\right)\omega_o t\right] \quad , \tag{26}$$

and the instantaneous frequency of this signal is

$$\omega(t) = \omega_o\left(1 + \frac{k_v \cos\omega_v t}{c}\right) \quad . \tag{27}$$

The instantaneous phase of this signal is

$$\phi(t) = \int \omega(t)dt = \int \omega_o\left(1 + \frac{k_v \cos\omega_v t}{c}\right)dt = \omega_o t + \frac{\omega_o k_v \sin\omega_v t}{\omega_v c} \quad . \quad (28)$$

Then the signal may be described in the form

$$s(t) = \sqrt{2}\ P \cos\left(\omega_o t + \frac{\omega_o k_v \sin\omega_v t}{\omega_v c}\right) \quad , \quad (29)$$

where we see that the signal is a carrier at frequency ω_o, which is phase modulated by the term $\omega_o k_v \sin\omega_v t/(\omega_v c)$. Expanding s(t) in terms of Bessel functions yields

$$s(t) = \sqrt{2}\ P \sum_{n=-\infty}^{\infty} J_n\left(\frac{\omega_o k_v}{\omega_v c}\right)\cos(\omega_o + n\omega_v)t \quad . \quad (30)$$

For small values of $(\omega_o k_v)/(\omega_v c)$ this reduces to

$$s(t) = \sqrt{2}\ P \cos(\omega_o t) + \frac{\sqrt{2}\ P\omega_o k_v}{2\omega_v c}\left[\cos(\omega_o+\omega_v)t - \cos(\omega_o-\omega_v)t\right] \quad . \quad (31)$$

The first term represents the received carrier and the second term represents the sidebands. Thus the carrier-to-sideband voltage ratio (pump excess) is

$$CSR = \frac{2\omega_v c}{\omega_o k_v} \quad . \quad (32)$$

In this expression ω_v is the radian frequency of the vibration, c is sound speed, ω_o is the radian pump frequency, and k_v is the peak velocity of the vibration along the pump-hydrophone axis.

This can also be put in terms of acceleration by substituting $a_v/\omega_v = k_v$, where a_v is the peak acceleration. Then

$$CSR = \frac{2\omega_v^2 c}{\omega_o a_v}$$

or

$$a_v = \frac{2\omega_v^2 c}{\omega_o CSR} \quad . \tag{33}$$

For example, if a carrier-to-sideband ratio of 160 dB at a frequency of 300 Hz with a 65 kHz pump frequency is required, then

$$a_v = \frac{2(2\pi\times300)^2(1500)}{(2\pi)(65\times10^3)(10^8)} = 260 \text{ μm/sec}^2 \text{ peak}$$

$$= 26 \text{ μg peak}$$

$$= 19 \text{ μg rms} \quad .$$

The acceleration of 19 μg rms at 300 Hz will generate a 300 Hz sideband signal with a carrier-to-sideband ratio of 160 dB.

Thus far only the motion of one transducer has been considered. If both transducers are in motion, the effects of the motions of both are directly additive where the relative phases of the displacements are included.

This analysis may readily be extended to the case of broadband excitation. If only one transducer is in motion along the pump-hydrophone axis,

$$S(\omega) = \frac{\omega_o A(\omega)}{\sqrt{2}\ \omega^2 c} P \quad , \tag{34}$$

where

ω_o = pump radian frequency,
$A(\omega)$ = acceleration spectrum,

c = sound speed,

P = received carrier level, and

$S(\omega)$ = received sideband signal spectrum (ω is measured with respect to the pump frequency).

Both upper and lower sidebands have spectrum $S(\omega)$. Usually the relative strength of the sideband with respect to the carrier, or the normalized sideband signal,

$$\frac{S(\omega)}{P} = \frac{\omega_o A(\omega)}{\sqrt{2}\ \omega^2 c} \quad , \tag{35}$$

is of interest. These formulas are appropriate for the low modulation index case, that is, when $S(\omega)/P \ll 1$. If both the pump and hydrophone are subject to accelerations which are independent but of the same level, then the received normalized sideband signal spectrum is

$$\frac{S(\omega)}{P} = \frac{\omega_o A(\omega)}{\omega^2 c} \quad . \tag{36}$$

The vibration sensitivity of the PARRAY is discussed in more detail in a paper presented at the 1978 IEEE International Conference on Acoustics, Speech, and Signal Processing.[16,31] In this paper, the vibrational response of the PARRAY is related to the acoustic response of the PARRAY and an equivalency between vibration and acoustic inputs to the PARRAY, which is useful for PARRAY system design, is developed.

C. PARRAY Applications Study

During this contract period, a study of applications of the PARRAY was conducted. One of the more interesting applications for the PARRAY is its use as an adjunct to existing arrays. The study, which is reported in detail in another report,[24] describes a particular method of combining a PARRAY with an existing line array, and develops a model

by means of which performance estimates for the resulting system are made. Deployment scenarios for such a system are broadly categorized on the basis of signal and noise environment, and the advantages and disadvantages of the system in each environment are discussed.

The motivation for the study stems from the fact that an end-fire array, in particular a PARRAY, has a beam pattern significantly different from that of a steered broadside line array. These two array types are almost complementary in their strengths and weaknesses. For instance, a broadside line array has a much narrower main lobe width in the horizontal dimension than a PARRAY of comparable dimensions. On the other hand, the broadside line array has no directionality in the vertical dimension, whereas the PARRAY has the same directionality in the vertical dimension that it has in the horizontal dimension. Because of this, the line array has a backlobe equal in amplitude to its forward lobe, whereas the PARRAY has a very high front-to-back ratio. Also, because of the discrete-element construction of most line arrays, grating lobes or high sidelobes may be troublesome at frequencies higher than the array design frequency. The PARRAY, which synthesizes a continuous array characteristic, is free from grating lobe formation even at high frequencies.

In the study, a technique for correlating the outputs of a line array and a PARRAY is developed. Figure 71 is a block diagram of the resulting system. The study shows that the characteristics of the correlation system are superior to the characteristics of the line array alone in several important respects. In particular, the correlation system is shown to resist interference from sources which are received in the sidelobes of the line array.

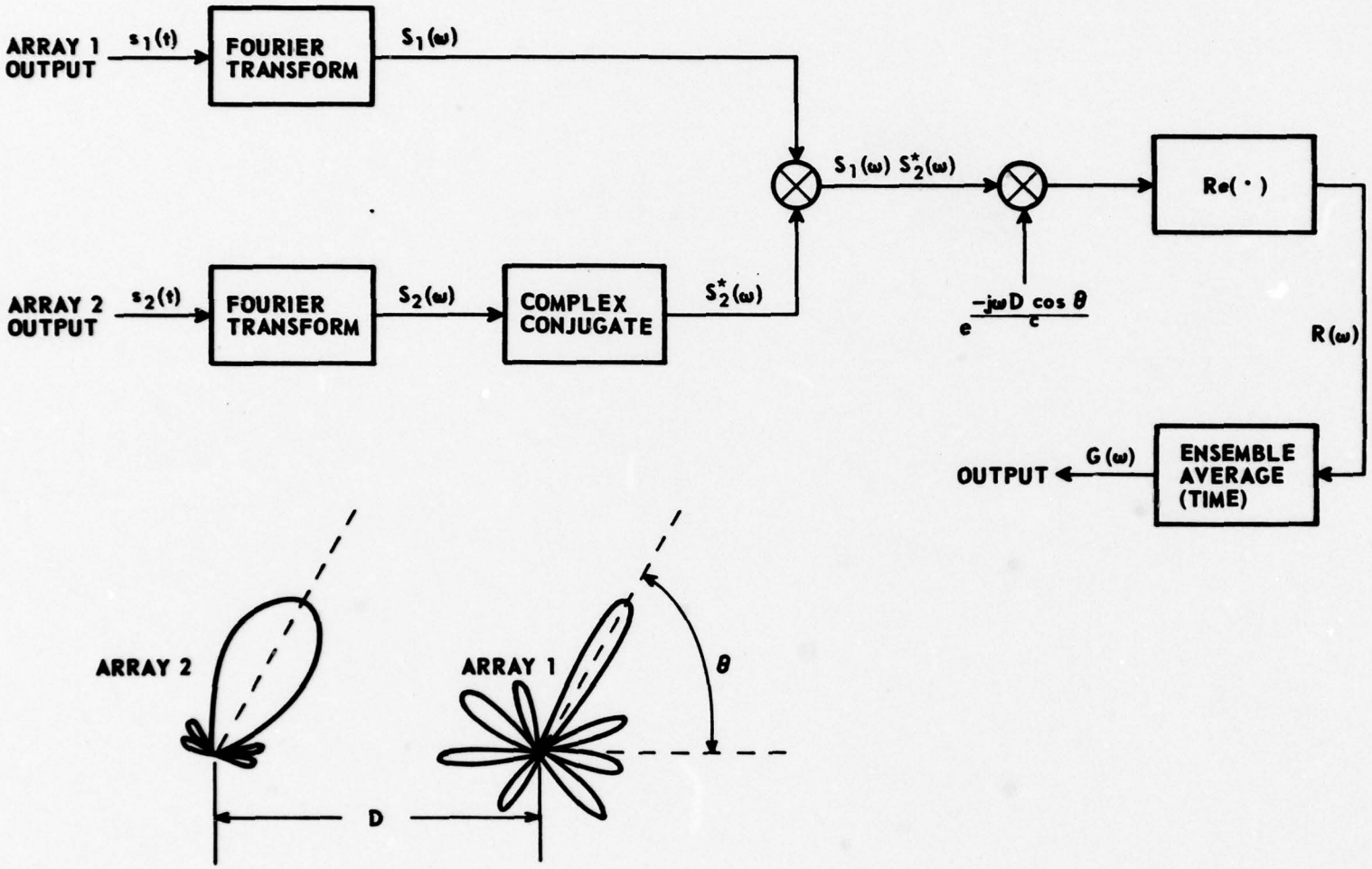

FIGURE 71
CROSSCORRELATION OF OUTPUTS OF TWO ARRAYS

VI. SUMMARY AND CONCLUSIONS

The parametric acoustic receiving array (PARRAY) can be characterized as a volumetric, virtual array synthesized in the water column between two small, high frequency transducers called the pump and the hydrophone. The directional response characteristics of the PARRAY are similar to those of a continuous end-fire array of length equivalent to the distance between the pump and hydrophone. At the beginning of the current program, it was known that the PARRAY can provide directional reception of low frequency acoustic waves with two small, high frequency transducers by exploiting the inherent nonlinearity of the water. However, the most crucial question was whether the self-noise of the PARRAY could be reduced to provide a sufficiently low system noise floor to make it useful in sonar and ocean acoustics research. A second crucial question was whether the directional response, and hence spatial processing gain, of a large aperture PARRAY could be achieved in the water. Affirmative answers to both questions were demonstrated in the freshwater environment of Lake Travis.

The program to develop an experimental large aperture PARRAY at ARL:UT was structured as an integrated program of analysis, experiments, hardware design, fabrication, lake testing, and sea testing to be conducted in three sequential stages. The first, or exploratory, phase of the program was accomplished in 1975 under Contract N00039-75-C-0207 with NAVELEX as technical agent for DARPA. During this exploratory phase, mission analysis and system definition studies were performed, subsystem requirements were developed, and technical risk area investigations were performed. Objectives of the first phase of the program were achieved on schedule and, consequently, the scope of the program was expanded to encompass the second phase of detailed design, fabrication, installation, and system tests at LTTS. Results of the second phase of

the development program are described in this report and summarized in the following paragraphs.

All objectives of the second phase of the program were achieved. State-of-the art advances were made in four major hardware areas: high spectral purity pump signal generation; commensurate power amplification; high efficiency, high power transducer element and array design; and detection of sideband signals with very small modulation indices. A large aperture, bottom mounted experimental PARRAY was designed, fabricated, bench tested, and installed at LTTS with the transducers located on bottom mounted towers separated by 340 m. The experimental PARRAY was tested and evaluated in Lake Travis. These tests verified that the predicted spatial processing gain is achieved and that the experimental PARRAY is ambient noise limited for ambient noise levels equivalent to light ("C") shipping and sea state 2. These were the lowest ambient noise conditions observed in Lake Travis over the period of the lake tests; hence, direct measurement of the actual noise floor of the experimental PARRAY will probably not be possible in this lake. These results demonstrated a greater than 40 dB reduction in the self-noise floor of the experimental PARRAY compared to any previous parametric acoustic receiver. This reduction in the self-noise floor was achieved through state-of-the art development of the electronic subsystems employed in the experimental PARRAY.

A summary of the hardware developments for the PARRAY is given in section A which follows. Significant results from the lake tests of the experimental PARRAY are summarized in section B.

A. Summary of Hardware Development

Spectral purity of the pump signal is one of the most critical parameters of the PARRAY. A crystal controlled pump signal source with spectrum level sideband noise 174 dB below the carrier level has been developed for the experimental PARRAY. This level of spectral purity represents an improvement of approximately 40 dB in the sideband noise

compared to that of oscillators available at the beginning of the PARRAY development program.

At the start of the PARRAY development program, a power amplifier for the pump signal was one of the biggest uncertainties. Manufacturers were not prepared to answer questions about the noise in the near sidebands of a high level signal. Starting with a basic design by Instruments, Inc., for a 250 W Class B power module, a pump power amplifier was developed that satisfies the baseline requirements of the PARRAY. Measurements with a 250 W amplifier have demonstrated that spectrum level sideband noise from the amplifier is 168 dB below the carrier level when the amplifier is delivering 250 W into a resistive load at the carrier frequency. Similar results have been obtained with the amplifier driving the PARRAY pump transducer.

The development of high efficiency transducers that can handle the high level cw carrier of the pump signal source has been one of the significant achievements of the PARRAY development program. These transducers, which were developed at ARL:UT, exhibit good sidelobe behavior and do not introduce spurious sideband noise at higher power levels. These transducers have been used for all of the recent PARRAY experiments and have given excellent results. The high electrical-to-acoustic conversion efficiency of these transducers is especially important in nonlinear acoustics applications. Transducers for a number of experimental programs have been constructed using the ARL:UT design, both at ARL:UT and at outside laboratories. These transducers may offer cost and performance advantages for use in acoustic torpedoes and high resolution minehunting sonars.

In the PARRAY system, signals extracted from the water include low level sideband information very near the high level carrier (pump). The receiver preprocessor developed at ARL:UT provides the capability of suppressing the high level carrier while simultaneously amplifying the low level signals. The unit separates the signals into upper and lower

sideband components for further processing. The self-noise of the receiver is sufficiently low so as to not contaminate the low level sideband information. The receiver preprocessor is capable of detecting signals approaching 180 dB below the carrier level.

B. Summary of Lake Tests of Experimental PARRAY

At the start of the PARRAY development program, the most crucial question involved the self-noise of the PARRAY. This question is a very complex one and involves a number of parameters, some of which can be controlled by the system designer and some of which are determined by environment. However, the bottom line was whether the PARRAY self-noise could be reduced to a level below the acoustic ambient noise at the output of the PARRAY. Tests were performed on the 340 m PARRAY at LTTS under a variety of conditions. These tests demonstrated that the 340 m PARRAY is ambient noise limited over the frequency range from 35 to 800 Hz under the quietest conditions observed at Lake Travis throughout the period of the tests. These conditions were equivalent to light ("C") shipping and sea state 2.

The second most crucial question at the start of the program was whether the medium was stable enough to support synthesis of the virtual end-fire array for pump-hydrophone separations of several hundred meters. This question related to the directional response function of the PARRAY, and hence to the spatial processing gain and F/B of the PARRAY. A closely related question was the temporal and phase stability of a signal received by the PARRAY, i.e., how narrowband can one analyze the signal at the output of the PARRAY.

The small size of the Lake Travis basin causes the lower portion of the lake to behave somewhat like a reverberation chamber, and for frequencies above 100 to 150 Hz the noise field in Lake Travis is relatively isotropic. Under these conditions, the spatial processing gain of the PARRAY should be the same as the directivity index, which can be

calculated from theoretical considerations. Measurements obtained with the 340 m PARRAY showed very good agreement between the spatial processing gain of the PARRAY (compared to an omnidirectional hydrophone) and the theoretical directivity index for the 340 m PARRAY. These measurements verified that in fact the directional response function of the experimental PARRAY closely approximated the theoretical function. These measurements were made with the pump and hydrophone near middepth of the 46 m deep channel of the lake. The pump and hydrophone were moved to locations approximately 8 m from the bottom of the lake and the measurements were repeated with results comparable to those at the mid-depth location.

Temporal and phase stability of signals received through the 340 m PARRAY were demonstrated by spectral analysis to 0.01 Hz resolution of a received 71 Hz signal. An improvement in S/N commensurate with the bandwidth reduction was obtained, and no spectral spreading of the 71 Hz signal was detected at this filter bandwidth. Subsequent processing to 0.004 Hz filter bandwidth did not provide additional signal-to-noise improvement with the receiving electronics used in the experiment.

A measure of the F/B of the 340 m PARRAY was obtained in the 70 to 80 Hz frequency range by utilizing the high amplitude noise in that band that was radiated from Mansfield Dam located directly behind the 340 m PARRAY. . A F/B of 44 dB was obtained from this measurement, which compares very well with the theoretical F/B of 48 dB in this frequency range.

The restricted waters of Lake Travis prevented direct measurement of the beam pattern of the 340 m PARRAY. Furthermore, the distance from the pump and hydrophone to the laboratory location on the LTTS barges makes the instrumentation of the pump and hydrophone more complex for some measurements. To alleviate these problems, two shorter PARRAYs were implemented. A PARRAY with a 5 m pump-hydrophone separation was installed on a column beneath the LTTS barge facility. The transducers

were later installed with a pump-hydrophone separation of 11 m on a moored, submerged rotator a short distance from the LTTS barges.

Beam patterns were obtained for selected frequencies from 300 to 2500 Hz with the 5 m and the 11 m PARRAYs. These beam patterns exhibited good agreement with theory for the forward hemisphere. Over the rear hemisphere spurious lobes, possibly due to reflections from the pump transducer, limited the measurements. It should be noted, however, that these spurious lobes are on the order of 30 dB below the level of the major lobe. This is quite good rejection of signals from the rear; however, the levels are still 4 to 10 dB higher than predicted. It should be noted that these latter measurements were obtained with the PARRAY transducers located 1 m above a reflecting plane. The reflecting plane consisted of a 0.6 m wide by 11 m long plate of 6.4 mm thick aluminum. Thus it is clear that for this type of reflecting plane there are no gross detrimental effects on the PARRAY beam pattern.

The PARRAY exhibits sensitivity to motion of its transducers in a manner significantly different from that of a conventional array. A theory relating motion of the PARRAY transducers to effects on the PARRAY output was developed and measurements were obtained with the 5 m PARRAY using accelerometers to measure the vibration of the PARRAY transducers while the PARRAY was receiving low frequency signals. The measured data agreed closely with predictions based on the analytical model.

C. Conclusions

State-of-the-art electronic and transducer hardware were developed and an experimental PARRAY with a 340 m pump-hydrophone separation was installed in Lake Travis. Tests performed on the 340 m PARRAY under a variety of conditions demonstrated that the self-noise of the experimental PARRAY was below ambient noise for the quietest conditions observed in Lake Travis throughout the tests. Further tests confirmed that the basic directional response characterisitcs of the experimental

PARRAY agree with analytical models and that the temporal and phase stability of the 340 m PARRAY will support narrowband processing to at least 0.01 Hz. It is to be demonstrated that these conclusions extend to an open ocean environment. This is to be addressed in the next phase of the development program.

REFERENCES

1. P. J. Westervelt, "Parametric acoustic array," J. Acoust. Soc. Am 35, 535-537 (1963).

2. H. O. Berktay, "Parametric amplification by the use of acoustic non-linearities and some possible applications," J. Sound Vib. 2, 462-470 (1965).

3. H. Date and Y. Tozuka, "Parametric Directional Microphones," The 6th International Congress on Acoustics, Tokyo, Japan, August 21-28, 1968.

4. H. O. Berktay and C. A. Al-Temimi, "Virtual arrays for underwater reception," J. Sound Vib. 9, 295-307 (1969).

5. V. A. Zverev and Z. I. Kalachev, "Modulation of sound by sound in the intersection of sound waves," Soviet Phys. Acoust. 16, 204-208 (1970).

6. W. L. Konrad, R. H. Mellen, and M. B. Moffett, "Parametric Sonar Receiving Experiments," Naval Underwater Systems Center TM No. PA4-304-71, 9 December 1971.

7. G. R. Barnard, J. G. Willette, J. J. Truchard, and J. A. Shooter, "Parametric acoustic receiving array," J. Acoust. Soc. Am. 52, 1437-1441 (1972).

8. H. O. Berktay and T. G. Muir, "Arrays of parametric receiving arrays," J. Acoust. Soc. Am. 53, 1377-1383 (1973).

9. H. O. Berktay and J. A. Shooter, "Parametric receivers with spherically spreading pump waves," J. Acoust. Soc. Am. 54, 1056-1061 (1973).

10. P. H. Rogers, A. L. Van Buren, A. O. Williams, Jr., and J. M. Barber, "Parametric detection of low frequency acoustic waves in the near-field of an arbitrary directional pump transducer," J. Acoust. Soc. Am. 55, 528-534 (1974).

11. J. J. Truchard, "Parametric acoustic receiving array. I. Theory," J. Acoust. Soc. Am. 58, 1141-1145 (1975).

12. J. J. Truchard, "Parametric acoustic receiving array. II. Experiment," J. Acoust. Soc. Am. 58, 1146-1150 (1975).

13. T. G. Goldsberry, "Investigation of the Feasibility of Mobile Parametric Receivers" (U), Applied Research Laboratories Technical Report No. 73-37, (ARL-TR-73-37), Applied Research Laboratories, The University of Texas at Austin, 6 August 1973. CONFIDENTIAL

14. T. G. Goldsberry, "Parameter selection criteria for parametric receivers," (paper presented at the 88th Meeting of the Acoustical Society of America, St. Louis, Missouri, 4-8 November 1974) [Abstract in J. Acoust. Soc. Am. 56, S41 (1974)].

15. T. G. Goldsberry, "Noise in parametric receivers," (paper presented at the 89th Meeting of the Acoustical Society of America, Austin, Texas, 8-11 April 1975.) [Abstract in J. Acoust. Soc. Am. 57, S74 (1975)].

16. T. G. Goldsberry, W. S. Olsen, C. R. Reeves, D. F. Rohde, and M. W. Widener, "PARRAY Technology Papers Presented at Scientific and Technical Meetings," Applied Research Laboratories Technical Report No. 79-4 (ARL-TR-79-4), Applied Research Laboratories, The University of Texas at Austin, to be published.

17. T. G. Goldsberry, W. S. Olsen, C. R. Reeves, D. F. Rohde, and M. W. Widener, "Investigation of the Parametric Acoustic Receiving Array (PARRAY)" (U), Applied Research Laboratories Technical Report No. 76-36 (ARL-TR-76-36), Applied Research Laboratories, The University of Texas at Austin, 31 December 1976. CONFIDENTIAL

18. T. G. Goldsberry et al., "Development and Evaluation of an Experimental Parametric Acoustic Receiving Array (PARRAY)," Quarterly Progress Report No. 1 under Contract N00039-76-C-0231, Applied Research Laboratories, The University of Texas at Austin, 13 December 1976.

19. T. G. Goldsberry et al., "Development and Evaluation of an Experimental Parametric Acoustic Receiving Array (PARRAY)," Quarterly Progress Report No. 2 under Contract N00039-76-C-0231, Applied Research Laboratories, The University of Texas at Austin, 29 August 1977.

20. T. G. Goldsberry et al., "Testing and Evaluation of an Experimental Parametric Acoustic Receiving Array (PARRAY)," Quarterly Progress Report No. 3 under Contract N00039-76-C-0231, Applied Research Laboratories, The University of Texas at Austin, 27 September 1977.

21. T. G. Goldsberry et al., "Testing and Performance Evaluation of an Experimental Parametric Acoustic Receiving Array (PARRAY)," Quarterly Progress Report No. 4 under Contract N00039-76-C-0231, Applied Research Laboratories, The University of Texas at Austin, 16 January 1978.

22. D. F. Rohde et al., "Examination of an Experimental Parametric Acoustic Receiving Array (PARRAY)," Quarterly Progress Report No. 5 under Contract N00039-76-C-0231, Applied Research Laboratories, The University of Texas at Austin, 5 May 1978.

23. C. R. Reeves and T. G. Goldsberry, "Test Plan for Interim Lake Tests of the Parametric Acoustic Receiving Array (PARRAY)," Applied Research Laboratories Technical Memorandum No. 77-21 (ARL-TM-77-21), Applied Research Laboratories, The University of Texas at Austin, 23 February 1977.

24. C. R. Reeves, T. G. Goldsberry, and D. F. Rohde, "Surveillance Applications of the PARRAY as a Line Array Adjunct" (U), Applied Research Laboratories Technical Report. No. 77-61 (ARL-TR-77-61), Applied Research Laboratories, The University of Texas at Austin, 31 December 1977. SECRET

25. D. F. Rohde et al., "Investigation of Platform Effects on an Experimental Parametric Acoustic Receiving Array (PARRAY)," Applied Research Laboratories Technical Report No. 78-24 (ARL-TR-78-24), Applied Research Laboratories, The University of Texas at Austin, 12 May 1978.

26. W. S. Olsen, T. G. Goldsberry, C. R. Reeves, and D. F. Rohde, "A crystal controlled pump signal source for an experimental parametric acoustic receiving array," (paper presented at the 92nd Meeting of the Acoustical Society of America, San Diego, California, 15-19 November 1976.) [Abstract in J. Acoust. Soc. Am. 60, S98 (1976)].

27. M. W. Widener, "The design of high efficiency transducer elements and arrays," (paper presented at the 92nd Meeting of the Acoustical Society of America, San Diego, California, 15-19 November 1976.) [Abstract in J. Acoust. Soc. Am. 60, S61 (1976)].

28. D. F. Rohde, T. G. Goldsberry, W. S. Olsen, and C. R. Reeves, "Band elimination processor for an experimental parametric acoustic receiving array," (paper presented at the 92nd Meeting of the Acoustical Society of America, San Diego, California, 15-19 November 1976.) [Abstract in J. Acoust. Soc. Am. 60, S98 (1976)].

29. C. R. Reeves, T. G. Goldsberry, W. S. Olsen, and D. F. Rohde, "Experimental measurement of the modulation process involved in non-linear interaction in water," (paper presented at the 92nd Meeting of the Acoustical Society of America, San Diego, California, 15-19 November 1976.) [Abstract in J. Acoust. Soc. Am. 60, S53 (1976)].

30. M. W. Widener, "The Design of High Frequency Transducer Elements and Arrays," Proceedings of Transducer Workshop, University of Birmingham, Birmingham, England, 15 December 1976.

31. C. R. Reeves, V. E. Maki, Jr., T. G. Goldsberry, and D. F. Rohde, "Vibration Sensitivity of the Parametric Acoustic Receiving Array," Applied Research Laboratories Technical Paper 77-42 (ARL-TP-77-42) and Proceedings of The International Conference on Acoustics, Speech, and Signal Processing, The Institute of Electrical and Electronic Engineers, Tulsa, Oklahoma, 10-12 April 1978.

32. R. T. Beyer, "Parameter of nonlinearity in fluids," J. Acoust. Soc. Am. 32, 719-721 (1960).

33. A. B. Coppens, Robert T. Beyer, M. B. Seiden, James Donohue, Frans Guepin, Richard H. Hodson, and Charles Townsend, "Parameter of nonlinearity in fluids, II," J. Acoust. Soc. Am. 38, 797-804 (1965).

15 February 1979

DISTRIBUTION LIST FOR
ARL-TR-79-5
UNDER CONTRACT N00039-76-C-0231
UNCLASSIFIED

Copy No.

Commander
Naval Electronic Systems Command
Department of the Navy
Washington, DC 20360

1 Attn: CAPT H. Cox, PME 124
2 CAPT D. B. Murton, PME 124-60
3 CAPT R. B. Gilchrist, Code 03
4 CDR D. J. Griffiths, Code 320
5 Dr. G. Hetland, PME 124-62
6 Dr. J. A. Sinsky, Code 320A
7 Ms. Joan C. Bertrand, Code 3202

Defense Advanced Research Projects Agency
1400 Wilson Boulevard
Arlington, VA 22209

8 Attn: CDR V. P. Simmons (TTO)
9 Dr. T. Kooij

Commander
Naval Sea Systems Command
Department of the Navy
Washington, DC 20362

10 Attn: CAPT A. H. Gilmore, Code 63X
11 Mr. C. D. Smith, Code 06R/63R
12 Mr. D. E. Porter, Code 63R
13 Mr. D. L. Baird, Code 63X3
14 Mr. C. E. Fox, Code 6322
15 CDR D. F. Bolka, Code 63G1
16 Mr. D. M. Early, Code 63D
17 CAPT W. A. White, Code 633X
18 Mr. John Neely, Code 63X3

Chief of Naval Material
Department of the Navy
Washington, DC 20360

19 Attn: RADM D. M. Jackson, Code ASW-00
20 Mr. Lou Griffith, Code 031

Distribution list for ARL-TR-79-5 under Contract N00039-76-C-0231 (Cont'd)

Copy No.

Office of Assistant Secretary
of the Navy (R,E&S)
The Pentagon
Washington, DC 20350
21 Attn: Dr. Richard F. Hoglund
Special Deputy for Technology

Director
Naval Research Laboratory
Department of the Navy
Washington, DC 20375
22 Attn: Code 8150
23 Dr. M. Potosky, Code 8109
24 Dr. J. Jarzynski, Code 8131

Naval Research Laboratory
Underwater Sound Reference Division
P. O. Box 8337
Orlando, FL 32806
25 Attn: Dr. Lee Van Buren
26 Dr. Peter H. Rogers

Commanding Officer
Naval Ocean Systems Center
Department of the Navy
San Diego, CA 92152
27 Attn: Dr. H. Schenck, Code 71
28 Dr. M. Akers, Code 714
29 Dr. H. P. Bucher

Office of the Chief of Naval Operations
The Pentagon
Washington, DC 20350
30 Attn: CAPT J. W. Van Metre, Code 224
31 CDR R. H. Scales, Code 224 F

Officer-in-Charge
New London Laboratory
Naval Underwater Systems Center
Department of the Navy
New London, CT 06320
32 Attn: M. B. Moffett, Code TD 124
33 W. L. Konrad

Distribution list for ARL-TR-79-5 under Contract N00039-76-C-0231 (Cont'd)

Copy No.

Chief of Naval Research
Department of the Navy
Arlington, VA 22217
34 Attn: R. F. Obrochta, Code 212
35 Dr. L. E. Hargrove, Code 421

Commander
Naval Ocean Research and Development Activity
NSTL Station, MS 39529
36 Attn: Dr. A. L. Anderson
37 Dr. S. W. Marshall

Commanding Officer
USCG Research and Development Center
Avery Point
Groton, CT 06340
38 Attn: CAPT M. Y. Suzich

39 - 50 Commanding Officer and Director
Defense Documentation Center
Defense Services Administration
Cameron Station, Building 5
5010 Duke Street
Alexandria, VA 22314

51 Battelle Columbus Laboratories
505 King Avenue
Columbus, OH 43201
Attn: TACTEC

52 Dr. F. H. Fenlon
Applied Research Laboratory
The Pennsylvania State University
State College, PA 16801

53 Mr. A. Nelkin
Westinghouse Electric Corporation
P. O. Box 1488, MS9R40
Annapolis, MD 21404

54 Mr. J. F. Bartram
Raytheon Company
P. O. Box 360
Portsmouth, RI 02871

55 Mr. E. P. Aurand
19 Hanapepe Place
Honolulu, HI 96825

Distribution list for ARL-TR-79-5 under Contract N00039-76-C-0231 (Cont'd)

Copy No.

56 Dr. P. M. Schultheiss
Yale University
Department of Engineering and
Applied Science
New Haven, CT 06520

57 Mr. V. J. Lujetic
RAMCOR, Inc.
800 Follin Lane
Vienna, VA 22180

58 Mr. Jack Fagan
Systems Planning Corporation
1500 Wilson Blvd., Suite 1500
Arlington, VA 22209

59 Dr. F. J. Jackson
Bolt, Beranek, and Newman, Inc.
1701 North Fort Myer Drive
Arlington, VA 22209

60 Dr. J. E. Barger
Bolt, Beranek, and Newman, Inc.
50 Moulton Street
Cambridge, MA 02138

61 Dr. William S. Hodgkiss
Marine Physical Laboratory of
The Scripps Institution of Oceanography
San Diego, CA 92152

62 Mr. J. Dow
TRACOR, Inc.
6500 Tracor Lane
Austin, TX 78721

63 Mr. J. L. Bardin
Radian Corporation
8500 Shoal Creek Blvd.
Austin, TX 78758

64 Office of Naval Research
Resident Representative
Room 582, Federal Building
Austin, TX 78701

Distribution list for ARL-TR-79-5 under Contract N00039-76-C-0231 (Cont'd)

Copy No.

65	Physical Acoustics Group, ARL:UT
66	Garland R. Barnard, ARL:UT
67	Tommy G. Goldsberry, ARL:UT
68	Robert A. Lamb, ARL:UT
69	Thomas G. Muir, ARL:UT
70	Wiley S. Olsen, ARL:UT
71	C. Richard Reeves, ARL:UT
72	David F. Rohde, ARL:UT
73	M. Ward Widener, ARL:UT
74	Reuben H. Wallace, ARL:UT
75	Library, ARL:UT
76 - 105	ARL:UT Reserve